Numerical Analysis of Dynamical Systems with Codimension two Singularities

Dissertation
zur Erlangung des Doktorgrades
der Fakultät für Mathematik der Universität Bielefeld

vorgelegt von
Joseph Nikolai Páez Chávez

Bielefeld, im Dezember 2008

1. Gutachter: Prof. Dr. Wolf-Jürgen Beyn

2. Gutachter: Prof. Dr. Barnabas Garay

Datum der mündlichen Prüfung: 23. März 2009

Im Zuge der Veröffentlichung wurde die vorliegende Dissertation redaktionell korrigiert. Bielefeld, im März 2009

Agradecimientos

Deseo aprovechar esta oportunidad para expresar mi profunda gratitud a las personas y entidades que de una u otra forma hicieron posible la elaboración del presente trabajo.

Agradezco al Dr. Gottfried Strobl y a la Dr. Martina Möller, docentes del Oberstufen-Kolleg de la Universidad de Bielefeld, por su valiosa ayuda y apoyo para que este proyecto sea posible. De igual forma al Ing. Pedro Vargas, director del Departamento de Relaciones Externas de la Escuela Superior Politécnica del Litoral (ESPOL), y al M.Sc. Washington Armas, director del Instituto de Ciencias Matemáticas de la ESPOL, cuyas gestiones hicieron posible la obtención del apoyo económico e institucional por parte de la ESPOL para la realización de este proyecto.

Mi especial agradecimiento al Prof. Dr. Wolf-Jürgen Beyn, por haber aceptado dirigir el presente trabajo, y por las numerosas conversaciones y amables consejos recibidos, sin los cuales no habría sido posible escribir esta tesis. En este sentido, deseo también agradecer al Dr. Thorsten Hüls, quien estuvo en todo momento dispuesto a brindarme su valiosa ayuda en la etapa de preparación y elaboración de este trabajo. Deseo asimismo expresar mi gratitud en general al Grupo de Investigación de Análisis Numérico de Sistemas Dinámicos de la Universidad de Bielefeld, por su amistoso apoyo y colaboración. Agradezco también al Prof. Dr. Barnabas Garay por su generosa hospitalidad durante mi visita a Budapest y Veszprém y por sus comentarios y recomendaciones acerca del presente trabajo.

Finalmente, deseo expresar mi gratitud al Estado Alemán, en cuya red social de apoyo para estudiantes fui acogido. De igual forma al Estado Ecuatoriano, que a través de la ESPOL, finació mi estadía en la República Federal de Alemania.

Danksagung

Ich möchte diese Gelegenheit wahrnehmen, um meine tiefe Dankbarkeit den Personen und Institutionen gegenüber auszudrücken, die auf die eine oder andere Weise die Verwirklichung der vorliegenden Arbeit möglich gemacht haben.

Ich danke Herrn Dr. Gottfried Strobl und Frau Dr. Martina Möller, Lehrende am Oberstufen-Kolleg der Universität Bielefeld, für ihre wertvolle Hilfe und Unterstützung, die dieses Projekt ermöglicht haben. Ebenso danke ich Herrn Ing. Pedro Vargas, Direktor des Dezernats für internationale Zusammenarbeit der Polytechnischen Hochschule in Guayaquil (ESPOL), und Herrn Washington Armas M.Sc., Direktor des Mathematischen Instituts der ESPOL, deren Anstrengungen mir den Bezug finanzieller und institutioneller Unterstützung für dieses Projekt von Seiten der ESPOL möglich gemacht haben.

Mein spezieller Dank gilt Herrn Prof. Dr. Wolf-Jürgen Beyn, für seine Bereitschaft, die vorliegende Arbeit zu betreuen, für zahlreiche Unterredungen und seinen freundlichen Rat, ohne den es nicht möglich gewesen wäre, diese Doktorarbeit zu schreiben. In diesem Sinne möchte ich ebenfalls Herrn Dr. Thorsten Hüls danken, der stets bereit war, mir seine wertvolle Hilfe für die Vorbereitung und Ausarbeitung dieser Arbeit zu geben. Darüber hinaus möchte ich meine generelle Dankbarkeit gegenüber der Arbeitsgemeinschaft Numerische Analysis Dynamischer Systeme der Universität Bielefeld ausdrücken, für deren freundschaftliche Unterstützung und Zusammenarbeit. Ich danke auch Herrn Prof. Dr. Barnabas Garay, für seine großzügige Gastfreundschaft während meines Aufenthaltes in Budapest und Vezprém und für seine Kommentare und Ratschläge bezüglich der vorliegenden Arbeit.

Schließlich möchte ich meine Dankbarkeit gegenüber dem Deutschen Staat ausdrücken, in dessen sozialem Netz für Studierende ich aufgenommen wurde. Gleichermaßen danke ich dem Ecuadorianischen Staat, der mir durch die ESPOL meinen Aufenthalt in der Bundesrepublik Deutschland finanziert hat.

A Wiltrud, con amor.

Contents

List of Figures

Introduction

One of the major tasks of scientists is to comprehend the physical environment where we live, which is also the scenario of many fascinating and complex phenomena. As a whole, it is very complicated to understand and explain how the components of our environment interact, therefore one needs to divide it into various (sub) systems. Once we have isolated a specific system, the problem a scientist usually addresses is to uncover the laws governing its evolution. If these laws are deterministic, i.e. the system does not change its state "spontaneously" and if the laws governing the system do not change in time, then the system is referred to as autonomous. On the other hand, (non) autonomous systems can be classified into two groups. If all possible states of the system are characterized by points of a set of finite (resp. infinite) dimension, then the system is said to be finite-dimensional (resp. infinite-dimensional). Another classification can be given in terms of the time with respect to which a system changes its state. If the time takes values along the real line $\mathbb{R}$, then the system is referred to as continuous-time system. Contrariwise, if the time takes values only on $\mathbb{Z}$, then the system is called discrete-time system. In this thesis, we will restrict our attention to finite-dimensional, discrete- and continuous-time dynamical systems.

One of the main approaches for studying a dynamical system is building a mathematical model which represents the laws governing the evolution of the system. This task of course is an art itself; models should be, mathematically speaking, simple enough, in such a way that the model can be handled, but it should not be too simple either, such that the real behavior of the system is not reasonably explained by the model. In the present work, we deal with two different kind of models, i.e.

$$\dot{x}(t) = F(x(t)), \tag{0.1}$$

$$x \mapsto G(x), \tag{0.2}$$

which represent an N-dimensional, continuous-time and discrete-time dynamical system, respectively, where $F : \mathbb{R}^N \to \mathbb{R}^N$, $G : \mathbb{R}^N \to \mathbb{R}^N$ are sufficiently smooth functions. An interesting fact is that most of the systems

that appear in applications can be satisfactorily modeled only in terms of nonlinear equations, which have proven to be very difficult to solve. This fact has motivated great efforts of mathematicians to develop fascinating techniques for addressing this problem. One method for dealing e.g. with systems of the type of (0.1) is numerical time-integration, which allows us to explore the dynamics of the system by solving an initial value problem. For this purpose, we may employ one-step methods, which in their simplest form can be written as

$$x_{n+1} = x_n + hF(x_n), \quad n = 0, 1, \ldots, \tag{0.3}$$

with initial value $x_0 := \xi \in \mathbb{R}^N$ and step-size $h > 0$. This schema is the well-known Euler's method. By the similarity between systems (0.2) and (0.3), it becomes evident that we can view numerical methods as discrete-time systems. By doing this, we can appeal to the already developed machinery for the study of discrete systems, in such a way that we can achieve a deeper insight into the connection between the dynamics of system (0.1) and its discretization (0.3). This approach gave rise to the born of the so-called Numerical Dynamics. Moreover, if we want to know the effect of external, or control parameters on the dynamics of system (0.1), then additional techniques must be employed. This task is widely addressed by Bifurcation Theory, which, combined with Numerical Dynamics, will be the cornerstone of the present work.

The first part of this thesis addresses the problem of explaining the effect of discretization methods on the local bifurcation diagram of a two-parametric, continuous-time dynamical system with a codimension two singularity (a complete list and the corresponding analysis of the possible codimension two singularities can be found in [44]). Two main questions are outlined and, at some extent, answered, i.e., does a one-step method applied to the continuous-time system reproduce by a "discrete version" the codimension two singularity? If this is so, does the discrete point remain at the same position in both, state space, as well as parameter space? The second major question is a natural consequence of a positive answer to the first one, namely, is the bifurcation picture also reproduced (and maybe shifted) by the discretization method? In the present work, we restrict our attention to two concrete cases: Bogdanov-Takens and fold-Hopf singularities. For the Bogdanov-Takens case, we consider a quite general family of one-step methods: implicit Runge-Kutta methods. On the other hand, for the fold-Hopf case we consider general one-step methods, without assuming any particular structure.

In the second part of the thesis, we concentrate on discrete, global phenomena that occur near a codimension two point. In Chapter 1, we will

see that a Bogdanov-Takens bifurcation is turned into a $1:1$ resonance by Runge-Kutta methods. Thus, a natural question that arises is what can be said about the effect of discretization methods on the emanating homoclinic curve? Answering this question is beyond the scope of this thesis, however, we will provide a numerical approach which allows, at least quantitatively, tackling this issue. That is, we will develop a theory-based numerical method for starting the continuation of tangential homoclinic orbits near a $1:1$ resonance. This method will allow us to carry out several interesting experiments (cf. Section 2.3), since homoclinic orbits are one of the most fascinating objects of study in the theory of dynamical systems, because their presence leads to nontrivial dynamics.

Chapter 1

Discretizing dynamical systems with singularities

"What we know is a drop. What we don't know is an ocean"
Isaac Newton

Consider $f, g \in C^k(\Omega \times \Lambda, \mathbb{R}^N)$ with open sets $0 \in \Omega \subset \mathbb{R}^N$, $0 \in \Lambda \subset \mathbb{R}^2$, $k \geq 1$ sufficiently large, and

$$\dot{x}(t) = f(x(t), \alpha), \tag{1.1}$$

$$x \mapsto g(x, \alpha), \tag{1.2}$$

thereby defining a continuous-time and a discrete-time dynamical system, respectively. Throughout this chapter, we often assume (1.2) to come from a one-step discretization of (1.1). The main topic of this chapter is to analyze how "well" a one-step method applied to (1.1) reproduces the bifurcation diagram of the continuous-time system near a codimension two singularity.

In particular, we deal with systems having Bogdanov-Takens and fold-Hopf bifurcations. The cusp case is addressed in [48], and for the remaining codimension two singularities a similar analysis seems not to be available. One of our main concerns will be the analysis of the discretized emanating path of Hopf points, which is originated at the codimension two singularities we will deal with.

By [48], it is known that a fold point persists at the same position under general Runge-Kutta methods, thus the emanating path of fold points is

not affected by those one-step methods and hence a further analysis in this direction is not necessary. On the other hand, the analysis of the path of discretized Hopf points requires more attention. Discretization of systems with Hopf points has been addressed to a large extent (cf. [4, 12, 23, 37, 42, 49, 53]). It has been proven that Hopf points are $O(h^p)$-shifted and turned into Neimark-Sacker points by general one-step methods of order $p \geq 1$. Nevertheless, these results strictly apply when dealing with one-parameter systems, so the analysis of the discretized Hopf curve has to be carried out in a codimension two context.

This chapter is organized in the following way. In the first two sections, we will present the basic setup for our analysis. In the subsequent sections, we determine how Bogdanov-Takens and fold-Hopf points are affected by one-step methods. Then, we take up the analysis of the discretized Hopf curve and also the behavior of the eigenvalues along the discretized path is discussed. The theoretical part of the chapter ends with the analysis of the intersection of the discretized fold and Hopf curves. Finally, we illustrate the obtained results by a numerical example.

1.1 Codimension two singularities of continuous-time systems

1.1.1 Bogdanov-Takens bifurcation

Definition 1.1. *A point $(x_0, \alpha_0) \in \Omega \times \Lambda$ is referred to as a nondegenerate Bogdanov-Takens singularity of codimension two (in short BT_2 point) of* (1.1) *if:*

1c $f(x_0, \alpha_0) = 0$,

2c *The only Jordan block of $f_x(x_0, \alpha_0)$ corresponding to the eigenvalue* 0 *is* $\begin{pmatrix} 0 & 1 \\ 0 & 0 \end{pmatrix}$, *and there is no more eigenvalues on the imaginary axis,*

3c $ab \neq 0$, *where* $a := \frac{1}{2} p_0^T B_f(v_0, v_0)$ *and* $b := p_1^T B_f(v_0, v_0) + p_0^T B_f(v_0, v_1)$. *The bilinear form $B_f(\cdot, \cdot)$ is given by*

$$B_f(v, w) := f_{xx}(x_0, \alpha_0)[v, w] = \sum_{i=1}^{N} \sum_{j=1}^{N} \frac{\partial f(x_0, \alpha_0)}{\partial x_j \partial x_i} v_i w_j,$$

$v, w \in \mathbb{R}^N$ and the vectors $v_0, v_1, p_0, p_1 \in \mathbb{R}^N$ satisfy the set of equations:

$$\begin{array}{rclcrcl} f_x(x_0,\alpha_0)v_0 & = & 0, & & f_x(x_0,\alpha_0)v_1 & = & v_0, \\ f_x^T(x_0,\alpha_0)p_0 & = & 0, & & f_x^T(x_0,\alpha_0)p_1 & = & p_0, \end{array} \tag{1.3}$$

with $v_0^T p_1 = v_1^T p_0 = 1$ and $v_0^T p_0 = v_1^T p_1 = 0$ (biorthogonality).

Suppose that system (1.1) has a BT_2 point at the origin. Then, the restriction of the system at $\alpha = 0$ to its center manifold is locally topologically equivalent to (cf. [44])

$$\begin{cases} \dot{w}_1 = w_2, \\ \dot{w}_2 = a w_1^2 + b w_1 w_2 + O(||w||^3), \end{cases}$$

where a, b are given as in Definition 1.1. This system is referred to as the critical normal form of the Bogdanov-Takens bifurcation. The general unfolding, which consists of a generic parametric perturbation of the above system, is (cf. [44])

$$\begin{cases} \dot{w}_1 = w_2, \\ \dot{w}_2 = \beta_1 + \beta_2 w_1 + a w_1^2 + b w_1 w_2 + O(||w||^3), \end{cases}$$

which is referred to as the topological normal form of the Bogdanov-Takens bifurcation. A straightforward analysis of the above system shows that paths of fold and Hopf points meet tangentially at the origin in parameter space. This fact is illustrated in Figure 1.1. In this picture, we show the bifurcation diagram of the normal form for $a = 1$, $b = -1$. The curves labeled by F, H correspond to the path of fold and Hopf points, respectively. More precisely, the $\beta_2 < 0$-branch of H represents real Hopf points whereas the $\beta_2 > 0$-branch of H represents imaginary Hopf points, also known as neutral saddles. Throughout this chapter, we will not consider global bifurcations.

Once we have formally introduced the concept of a BT_2 point, it is important, from a numerical and practical viewpoint, to know how to locate such points. This task has been addressed by many authors, for instance see [5, 18, 19, 28, 51]. In those articles, a BT_2 point is calculated by computing the zeroes of certain systems for which the BT_2 point is a regular solution. Another approach consists in computing codimension two points by following a hierarchy in codimension, that is, to find firstly codimension one bifurcations and then to continue these points with respect to a second parameter. Along these curves one monitors the zeroes of certain test functions, and thus codimension two singularities are detected. This method is implemented in the continuation software CONTENT [45] and MATCONT [21], among others. A more detailed discussion about this hierarchy-based approach and a thorough survey of continuation packages can be found in [43, Chapter 2].

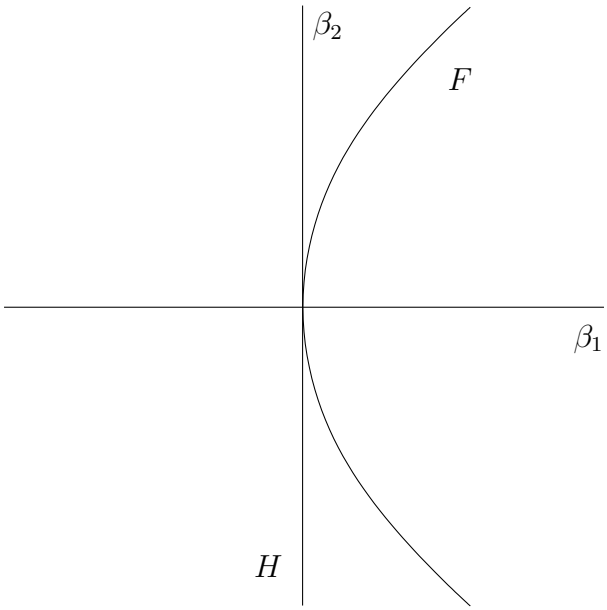

Fig. 1.1: Local bifurcation diagram near a BT_2 point.

For our purposes, it will be useful to introduce defining systems for the continuation of fold and Hopf points. Any generic fold, Hopf point of (1.1) is a regular solution of (cf. [6, Theorem 5.1])

$$\begin{cases} f(x,\alpha) &= 0, \\ \det(f_x(x,\alpha)) &= 0, \end{cases} \tag{1.4}$$

$$\begin{cases} f(x,\alpha) &= 0, \\ \det(2f_x(x,\alpha)\odot I_N) &= 0, \end{cases} \tag{1.5}$$

respectively, where $\odot$ stands for the bialternate product of matrices (cf. [29, 35, 44]). Finally, this allows us to formalize the notion of genericity of a BT_2 point. A BT_2 point (x_0,α_0) of (1.1) is said to be generic if the system

$$\begin{cases} f(x,\alpha) &= 0, \\ \det(2f_x(x,\alpha)\odot I_N) &= 0, \\ \det(f_x(x,\alpha)) &= 0, \end{cases} \tag{1.6}$$

is regular at (x_0,α_0). It is clear that the genericity of a BT_2 point implies the regularity of systems (1.4) and (1.5) at (x_0,α_0) and hence the existence of emanating paths of fold and Hopf singularities is guaranteed.

1.1.2 Fold-Hopf bifurcation

Definition 1.2. *A point* $(x_0, \alpha_0) \in \Omega \times \Lambda$ *is referred to as a fold-Hopf point (in short FH point*[1]*) of* (1.1) *if:*

1c $f(x_0, \alpha_0) = 0$,

2c $f_x(x_0, \alpha_0)$ *has the only critical simple eigenvalues* $\{0, \pm i\omega_0\}$, $0 < \omega_0 \in \mathbb{R}$.

Suppose that system (1.1) has an FH point at the origin. Then, under certain nondegeneracy conditions, the restriction of the system at $\alpha = 0$ to its center manifold is locally topologically equivalent to (cf. [44])

$$\begin{cases} \dot{\xi} = \xi^2 + s\,|\zeta|^2 + O(||(\xi, \zeta, \bar{\zeta})||^4), \\ \dot{\zeta} = i\omega_1\zeta + (\theta + i\vartheta)\xi\zeta + \xi^2\zeta + O(||(\xi, \zeta, \bar{\zeta})||^4), \end{cases}$$

where $\xi \in \mathbb{R}$, $\zeta \in \mathbb{C}$, $0 \neq \omega_1, \theta \in \mathbb{R}$, $\vartheta \in \mathbb{R}$ $s \in \{-1, 1\}$. By introducing perturbation parameters and neglecting the $O(||\cdot||^4)$-terms, the above system can be written in cylindrical coordinates (ξ, ρ, φ) as

$$\begin{cases} \dot{\xi} = \beta_1 + \xi^2 + s\rho^2, \\ \dot{\rho} = \rho(\beta_2 + \theta\xi + \xi^2), \\ \dot{\varphi} = \omega_1 + \vartheta\xi, \end{cases} \tag{1.7}$$

where $\zeta = \rho e^{i\varphi}$. In contrast to the Bogdanov-Takens case, the higher order terms do affect the topology of the bifurcation diagram near the FH point. In general, system (1.7) is not a normal form. However, this truncated system exhibits the same local bifurcations as the nontruncated one. For our purposes, this information is enough, namely, for the study of the paths of fold and Hopf points. Moreover, the shape that system (1.7) takes is basically a matter of choice, namely, the higher order terms we consider may vary. Systems equivalent to (1.7), but with different higher order terms, can be found in [32, 33].

As in the Bogdanov-Takens case, we have that the emanating paths of fold and Hopf singularities meet tangentially in parameter space at the FH point. In Figure 1.2, we show the local bifurcation diagram. The curves labeled by F and H correspond to paths of fold and Hopf points, respectively. We do not consider further local and global phenomena that take place near an FH point.

The methods outlined in the previous section for detecting codimension two bifurcations and for the continuation of curves of fold and Hopf points

[1] Also called zero-Hopf, zero-pair, Hopf-saddle-node, Hopf-steady-state, Gavrilov-Guckenheimer, among others.

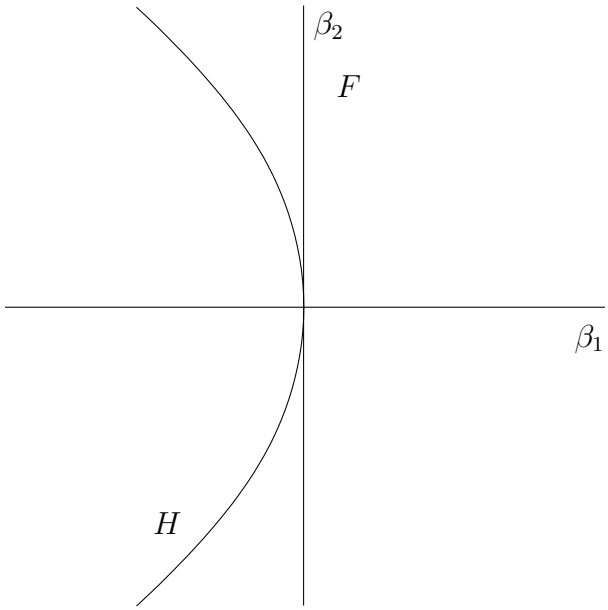

Fig. 1.2: Local bifurcation diagram near an FH point.

apply in this case, too. In the spirit of the previous section, we say that an FH point (x_0, α_0) of (1.1) is generic, if the system

$$\begin{cases} f(x,\alpha) &= 0, \\ \det(2f_x(x,\alpha) \odot I_N) &= 0, \\ \det(f_x(x,\alpha)) &= 0, \end{cases}$$

is regular at (x_0, α_0).

1.2 Codimension two singularities of discrete-time systems

1.2.1 $1:1$ Resonance

Definition 1.3. *A point $(x_0, \alpha_0) \in \Omega \times \Lambda$ is referred to as a nondegenerate $1:1$ resonance of codimension two (in short $R1_2$ point) of* (1.2) *if:*

1d $g(x_0, \alpha_0) - x_0 = 0$,

2d *The only Jordan block of $g_x(x_0, \alpha_0)$ corresponding to the eigenvalue* 1 *is* $\begin{pmatrix} 1 & 1 \\ 0 & 1 \end{pmatrix}$, *and there is no more eigenvalues on the unit circle,*

3d $\tilde{a}\tilde{b} \neq 0$, *where* $\tilde{a} := \frac{1}{2}\tilde{p}_0^T B_g(\tilde{v}_0, \tilde{v}_0)$ *and* $\tilde{b} := \tilde{p}_1^T B_g(\tilde{v}_0, \tilde{v}_0) + \tilde{p}_0^T B_g(\tilde{v}_0, \tilde{v}_1)$. *The bilinear form* $B_g(\cdot, \cdot)$ *is given by*

$$B_g(v, w) := g_{xx}(x_0, \alpha_0)[v, w] = \sum_{i=1}^{N} \sum_{j=1}^{N} \frac{\partial g(x_0, \alpha_0)}{\partial x_j \partial x_i} v_i w_j,$$

$v, w \in \mathbb{R}^N$ *and the vectors* $\tilde{v}_0, \tilde{v}_1, \tilde{p}_0, \tilde{p}_1 \in \mathbb{R}^N$ *satisfy the set of equations:*

$$\begin{array}{rclcrcl} (g_x(x_0, \alpha_0) - I_N)\tilde{v}_0 & = & 0, & & (g_x(x_0, \alpha_0) - I_N)\tilde{v}_1 & = & \tilde{v}_0, \\ (g_x(x_0, \alpha_0) - I_N)^T\tilde{p}_0 & = & 0, & & (g_x(x_0, \alpha_0) - I_N)^T\tilde{p}_1 & = & \tilde{p}_0, \end{array} \tag{1.8}$$

with $\tilde{v}_0^T\tilde{p}_1 = \tilde{v}_1^T\tilde{p}_0 = 1$ *and* $\tilde{v}_0^T\tilde{p}_0 = \tilde{v}_1^T\tilde{p}_1 = 0$ *(biorthogonality).*

Suppose that system (1.2) has an $R1_2$ point at the origin. Then, the restriction of the system at $\alpha = 0$ to its center manifold is locally topologically equivalent to (cf. [44])

$$\begin{pmatrix} w_1 \\ w_2 \end{pmatrix} \mapsto \begin{pmatrix} w_1 + w_2 \\ w_2 + aw_1^2 + bw_1w_2 \end{pmatrix} + O(||w||^3),$$

where a, b are given as in Definition 1.3. This system is referred to as the critical normal form of the $1:1$ resonance. From this singularity, it has been shown that paths of fold and Neimark-Sacker points emanate. Moreover, global bifurcations are also known to exist near an $R1_2$ point, however, the theoretical prediction of such phenomena is rather complicated, if we work with the discrete system. The technique of interpolating a discrete map by a flow (cf. [17, Takens's Theorem]) is used. The idea is to approximate a discrete system up to a certain order by a 1-flow of a differential equation, and then the already known information about the local bifurcation diagram of the vector field is used for predicting both local, as well as global phenomena that occur in the original map. This technique has been applied for the analysis of strong resonances (see eg. [44, 55]).

Assume system (1.2) to be planar, i.e. $N = 2$, and that it undergoes an $R1_2$ bifurcation at the origin. Then, under certain transversality conditions, there exists a smooth invertible change of coordinates, smoothly depending on parameters, that transforms (1.2) for all sufficiently small $||\alpha||$ into (cf. [44, Lemma 9.7])

$$\begin{pmatrix} \xi_1 \\ \xi_2 \end{pmatrix} \mapsto N_\nu(\xi) := \begin{pmatrix} \xi_1 + \xi_2 \\ \xi_2 + \nu_1 + \nu_2\xi_2 + A(\nu)\xi_1^2 + B(\nu)\xi_1\xi_2 \end{pmatrix} + O(||\xi||^3), \tag{1.9}$$

where $A(\cdot)$, $B(\cdot)$ depend smoothly on ν, and $A(0) = a$, $B(0) = b$. The above map is the normal form of the $1:1$ resonance. The next step is to approximate N_ν by a flow. This is done in the following lemma (cf. [44, Lemma 9.8]):

Lemma 1.4. *The map* (1.9) *can be represented for all sufficiently small* $||\nu||$ *in the form*

$$N_\nu(\xi) = \varphi_\nu^1(\xi) + O(||\nu||^2) + O(||\xi||^2||\nu||) + O(||\xi||^3),$$

where φ_ν^t *is the flow of a smooth planar system*

$$\dot{\xi} = F(\xi, \nu),$$

with $F(\xi,\nu) := F_0(\nu) + F_1(\xi,\nu) + F_2(\xi)$*, where:*

$$F_0(\nu) := \begin{pmatrix} -\frac{1}{2}\nu_1 \\ \nu_1 \end{pmatrix},$$

$$F_1(\xi,\nu) := \begin{pmatrix} \xi_2 + \left(\frac{1}{3}b - \frac{1}{2}a\right)\nu_1\xi_1 + \left(\left(\frac{1}{5}a - \frac{5}{12}b\right)\nu_1 - \frac{1}{2}\nu_2\right)\xi_2 \\ \left(\frac{2}{3}a - \frac{1}{2}b\right)\nu_1\xi_1 + \left(\left(\frac{1}{2}b - \frac{1}{6}a\right)\nu_1 + \nu_2\right)\xi_2 \end{pmatrix},$$

and

$$F_2(\xi) := \begin{pmatrix} -\frac{1}{2}a\xi_1^2 + \left(\frac{2}{3}a - \frac{1}{2}b\right)\xi_1\xi_2 + \left(\frac{1}{3}b - \frac{1}{6}a\right)\xi_2^2 \\ a\xi_1^2 + (b-a)\xi_1\xi_2 + \left(\frac{1}{6}a - \frac{1}{2}b\right)\xi_2^2 \end{pmatrix}.$$

The dynamics of the above vector field are described by the Bogdanov-Takens theory. Thus, the bifurcation diagram, concerning local phenomena, of system (1.9) can be deduced from Figure 1.1, i.e., there exist paths of fold and Neimark-Sacker points that emanate from the $R1_2$ singularity and meet tangentially at this point, in parameter space.

As in Section 1.1.1, standard minimally augmented systems can be introduced for the continuation of fold and Neimark-Sacker curves for systems of arbitrary dimension. Such defining systems may given by (cf. [44])

$$\begin{cases} g(x,\alpha) - x &= 0, \\ \det(g_x(x,\alpha) - I_N) &= 0, \end{cases} \tag{1.10}$$

$$\begin{cases} g(x,\alpha) - x &= 0, \\ \det(g_x(x,\alpha) \odot g_x(x,\alpha) - I_m) &= 0, \end{cases} \tag{1.11}$$

whose solutions correspond to fold and Neimark-Sacker points, respectively, and $m = \frac{1}{2}N(N-1)$. Along these curves, one monitors certain test functions and thus codimension two singularities are located.

1.2.2 Fold-Neimark-Sacker bifurcation

Definition 1.5. *A point* $(x_0, \alpha_0) \in \Omega \times \Lambda$ *is referred to as a fold-Neimark-Sacker point (in short FN point) of* (1.2) *if:*

1d $g(x_0, \alpha_0) - x_0 = 0$,

2d $g_x(x_0, \alpha_0)$ *has the only critical simple eigenvalues* $\{1, e^{\pm i\theta_0}\}$, $0 < \theta_0 \in \mathbb{R}$, $e^{ik\theta_0} \neq 1$, $k = 1, 2, 3, 4$.

In this case, the critical normal form is given by (cf. [50])

$$\begin{pmatrix} w \\ z \end{pmatrix} \mapsto \begin{pmatrix} w + sz\bar{z} + w^2 + cw^3 \\ e^{i\theta_0} z + awz + bzw^2 \end{pmatrix} + O(||(w, z)||^4),$$

where $(w, z) \in \mathbb{R} \times \mathbb{C}$, and s, c, a, b are real coefficients that determine the dynamics of the system near the origin. The analysis of the bifurcation picture near this singularity is far from being simple. Interpolation techniques (cf. previous section) are also applied in this case. Results in this direction are more recent (cf. [14, 15, 52]), and so complicated global phenomena are predicted near this bifurcation. It is of course clear that paths of fold and Neimark-Sacker points emanate from an FN point. These curves can also be continued by means of (1.10) and (1.11).

1.3 BT$_2$ singularities under Runge-Kutta methods

In this section, we tackle one of the main questions of this chapter, namely, the effect of one-step discretizations methods applied to systems having a BT$_2$ point. It is worth doing a brief review of what has been done in this direction. When dealing with systems having a hyperbolic equilibrium, it has been shown that one-step methods reproduces "correctly" the phase portrait near the equilibrium, and furthermore the discretized stable and unstable manifolds converge to their continue counterpart (cf. [3, 27]). The dynamics of the continuous-time system and its discretization are dominated, in this case, by their linear part. If the continuous-time system possesses a non-hyperbolic equilibrium, then the analysis is more complicated. Taking into account the linear part of the systems is not sufficient, thus higher order terms have to be considered.

The codimension one cases: fold, transcritical, and pitchfork singularities are studied in detail in [48]. The study of fold, and cusp bifurcations under general implicit Runge-Kutta methods is also considered there. The analysis

we are to present in the next section will closely follow the approach of the above cited work concerning fold points under Runge-Kutta methods. In fact, due to the similar conditions that define fold and BT_2 singularities, some preliminary results can be extended to the latter case at almost no extra cost.

Before we present the main result of this section, we will briefly introduce the general Runge-Kutta method we will deal with.

1.3.1 General implicit Runge-Kutta methods

Consider a one-step discretization method applied to (1.1) of the form

$$x \mapsto \psi^h(x, \alpha) := x + h\Phi(h, x, \alpha), \tag{1.12}$$

with step-size $h > 0$, and $\psi, \Phi : \mathbb{R}^+ \times \Omega \times \Lambda \to \mathbb{R}^N$ sufficiently smooth. The one-step method (1.12) is referred to as a s-stage implicit Runge-Kutta method, $s \geq 1$ if

$$\Phi(h, x, \alpha) := \sum_{i=1}^{s} \gamma_i k_i(h, x, \alpha), \tag{1.13}$$

where the function $(k_i)_{i=1,\dots,s}$ is a solution of the system

$$k_i(h, x, \alpha) = f(W_i(h, x, \alpha), \alpha), \quad i = 1, \dots, s, \tag{1.14}$$

with

$$W_i(h, x, \alpha) := x + h \sum_{j=1}^{s} \tau_{ij} k_j(h, x, \alpha), \quad i = 1, \dots, s, \tag{1.15}$$

and γ_i, τ_{ij}, $i, j = 1, \dots, s$ are real constants that determine the order of the method. Of course, this schema may represent, strictly speaking, not only implicit methods, but also explicit (ERK), diagonal implicit (DIRK), and singly diagonal implicit (SDIRK) Runge-Kutta methods, depending on the values of τ_{ij} (cf. [36]). In what follows, we will assume $\sum_{i=1}^{s} \gamma_i = 1$, which is a necessary condition for the method to be at least of order one.

1.3.2 Persistence theorem

Throughout this section, we suppose we are given a continuous-time dynamical system (1.1), which undergoes a BT_2 bifurcation at the origin. We assume that this system is discretized via implicit Runge-Kutta methods, as described in the previous section. We will show that the BT_2 point persists at the same position as an $R1_2$ point for the one-step method, for all sufficiently small step-size. Namely, we have the following:

Theorem 1.6. *Let system* (1.1) *have a* BT_2 *singularity at the origin* $(x_0, \alpha_0) = (0, 0)$. *Consider a general s-stage implicit Runge-Kutta method with step-size* $h > 0$ *and given by* (1.12)–(1.15). *Then, there exists a positive constant* ρ, *such that* (1.12) *has an* $R1_2$ *singularity at the origin for all* $h \in (0, \rho)$.

For the sake of simplicity, we will firstly introduce several preliminary lemmata. At the end, we will combine them in order to prove Theorem 1.6. In this way, the proof can be presented in a more readable manner.

Lemma 1.7. *Let the assumptions of Theorem 1.6 be fulfilled. Then, there exists a positive constant* ρ_1, *such that condition* ***1d*** *of Definition 1.3 (with* $g := \psi^h(\cdot, \cdot)$*) holds for all* $h \in (0, \rho_1)$.

Proof. Let $\Omega' \times \Lambda' \subset \Omega \times \Lambda$ be a compact neighborhood of the origin and

$$L := \sup_{(x,\alpha)\in\Omega'\times\Lambda'} ||f_x(x, \alpha)||$$

be a local Lipschitz constant of f in $\Omega' \times \Lambda'$. Then, by [36, Theorem 7.2], it follows that system (1.14) has a unique, smooth solution $(k_i)_{i=1,\dots,s}$ defined in some small neighborhood of the origin, provided

$$h < \frac{1}{L \max_{i=1,\dots,s} \sum_{j=1}^{s} |\tau_{ij}|} =: \rho_1.$$

In particular, we have that for $(x, \alpha) = (0, 0)$ system (1.14) reads

$$k_i^0(h) = f\left(h \sum_{j=1}^{s} \tau_{ij} k_j^0(h), 0\right), \quad i = 1, \dots, s,$$

where the superscript '0' denotes evaluation of functions at the origin. The above system has the solution $k_i^0(h) = 0$, $i = 1, \dots, s$, thereby we obtain

$$\psi^h(x_0, \alpha_0) - x_0 = \psi^0(h) - 0 = h \sum_{i=1}^{s} \gamma_i k_i^0(h) = 0,$$

for all $h \in (0, \rho_1)$. □

Lemma 1.8. *Let the assumptions of Theorem 1.6 be fulfilled. Then, there exists a positive constant* ρ_2, *such that* $\mathrm{null}(f_x^0) = \mathrm{null}(\psi_x^0(h) - I_N)$ *for all* $h \in (0, \rho_2)$.

Proof. Choose any $0 \neq v \in \text{null}(f_x^0)$. We will firstly show that $v \in \text{null}(k_{ix}^0(h))$, $i = 1, \ldots, s$, and for all h in some interval. Consider $h \in (0, \rho_1)$, ρ_1 as in the previous lemma. Then, by differentiating (1.14) with respect to x, for all $i = 1, \ldots, s$ and (x, α) in some small neighborhood of the origin, we obtain:

$$\begin{aligned} k_{ix}(h, x, \alpha) &= (f(W_i(h, x, \alpha), \alpha))_x, \\ &= f_x(W_i(h, x, \alpha), \alpha) W_{ix}(h, x, \alpha), \\ &= f_x(W_i(h, x, \alpha), \alpha) \left(I_N + h \sum_{j=1}^{s} \tau_{ij} k_{jx}(h, x, \alpha) \right), \end{aligned}$$

thereby $k_{ix}^0(h)$ reads

$$k_{ix}^0(h) = f_x^0 \left(I_N + h \sum_{j=1}^{s} \tau_{ij} k_{jx}^0(h) \right). \tag{1.16}$$

Define $z_i(h) := k_{ix}^0(h)v$, $i = 1, \ldots, s$. By multiplying both sides of (1.16) by v, we obtain the following system

$$z_i(h) - h \sum_{j=1}^{s} \tau_{ij} f_x^0 z_j(h) = 0, \quad i = 1, \ldots, s,$$

which can be represented by the matrix equation

$$(I_{sN} - h\tau \otimes f_x^0) \begin{pmatrix} z_1(h) \\ \vdots \\ z_s(h) \end{pmatrix} = 0 \in \mathbb{R}^{sN},$$

where $\otimes$ stands for the Kronecker product of matrices and $\tau := (\tau_{ij})_{i,j=1,\ldots,s} \in \mathbb{R}^{s,s}$. For all $h \in (0, \rho_2')$, $\rho_2' := \min\left(\rho_1, \frac{1}{||\tau \otimes f_x^0||}\right)$, Theorem A.1 guarantees the invertibility of $I_{sN} - h\tau \otimes f_x^0$, therefore we have that $z_i(h) = k_{ix}^0(h)v = 0$, so $v \in \text{null}(k_{ix}^0(h))$, $i = 1, \ldots, s$, and for all $h \in (0, \rho_2')$. This allows us to conclude that $v \in \text{null}(\psi_x^0(h) - I_N)$, because

$$(\psi_x^0(h) - I_N)v = \left(I_N + h \sum_{i=1}^{s} \gamma_i k_{ix}^0(h) - I_N \right) v = h \sum_{i=1}^{s} \gamma_i k_{ix}^0(h)v = 0.$$

Conversely, for any $h \in (0, \rho_2')$ choose an arbitrary $0 \neq w \in \text{null}(\psi_x^0(h) - I_N)$. We will show that $w \in \text{null}(f_x^0)$, and hence it will immediately follow

$\text{null}(f_x^0) = \text{null}(\psi_x^0(h) - I_N)$. By (1.16), we can write $\psi_x^0(h) - I_N$ as

$$\begin{aligned}\psi_x^0(h) - I_N &= h\sum_{i=1}^{s}\gamma_i k_{ix}^0(h),\\ &= h\sum_{i=1}^{s}\gamma_i f_x^0\left(I_N + h\sum_{j=1}^{s}\tau_{ij}k_{jx}^0(h)\right),\\ &= hf_x^0\left(I_N + h\sum_{i=1}^{s}\sum_{j=1}^{s}\gamma_i\tau_{ij}k_{jx}^0(h)\right),\\ &= hf_x^0 A(h), \end{aligned} \tag{1.17}$$

where

$$A(h) := I_N + h\sum_{i=1}^{s}\sum_{j=1}^{s}\gamma_i\tau_{ij}k_{jx}^0(h).$$

Since $w \in \text{null}(\psi_x^0(h) - I_N)$, we have that

$$hf_x^0 A(h)w = 0,$$

so $A(h)w \in \text{null}(f_x^0) \subseteq \text{null}(k_{ix}^0(h))$, $i = 1, \ldots, s$. This implies that

$$A(h)A(h)w = A(h)w + h\sum_{i=1}^{s}\sum_{j=1}^{s}\gamma_i\tau_{ij}k_{jx}^0(h)A(h)w = A(h)w. \tag{1.18}$$

Take $h \in (0, \rho_2'')$, where

$$\rho_2'' := \min\left(\rho_2', \frac{1}{\sup_{h\in(0,\rho_2')}||\sum_{i=1}^{s}\sum_{j=1}^{s}\gamma_i\tau_{ij}k_{jx}^0(h)||}\right),$$

then Lemma A.1 ensures the invertibility of $A(h)$, thus from (1.18) we can deduce that

$$A(h)w = w,$$

which implies that $w \in \text{null}(f_x^0)$. Finally take $\rho_2 := \rho_2''$. □

Lemma 1.9. *Let the assumptions of Theorem 1.6 be fulfilled. Then, for every $h \in (0, \rho_2)$ the following assertions hold:*

(i) $\exists\tilde{v}_1(h) \in \mathbb{R}^N : (\psi_x^0(h) - I_N)\tilde{v}_1(h) = v_0$,

(ii) $\nexists\tilde{v}_2(h) \in \mathbb{R}^N : (\psi_x^0(h) - I_N)\tilde{v}_2(h) = \tilde{v}_1(h)$.

Proof. Let us firstly prove (i). Define $\tilde{v}_1(h) := \frac{1}{h}(A(h))^{-1}v_1$, $h \in (0, \rho_2)$. Then, by (1.3), it follows

$$(\psi_x^0(h) - I_N)\tilde{v}_1(h) = hf_x^0 A(h)\left(\frac{1}{h}(A(h))^{-1}v_1\right) = f_x^0 v_1 = v_0.$$

As for (ii), suppose that for some $h \in (0, \rho_2)$ there exists a $\tilde{v}_2(h) \in \mathbb{R}^N$, such that $(\psi_x^0(h) - I_N)\tilde{v}_2(h) = \tilde{v}_1(h)$. We will see that this assumption leads us to a contradiction. Note that

$$p_0^T k_{ix}^0(h) = p_0^T f_x^0\left(I_N + h\sum_{j=1}^{s}\tau_{ij}k_{jx}^0(h)\right) = 0, \tag{1.19}$$

for all $i = 1, \ldots, s$, and hence we obtain that

$$p_0^T A(h) = p_0^T\left(I_N + h\sum_{i=1}^{s}\sum_{j=1}^{s}\gamma_i\tau_{ij}k_{jx}^0(h)\right) = p_0^T. \tag{1.20}$$

By the existence of $\tilde{v}_2(h)$, we can express v_1 in terms of $\tilde{v}_2(h)$ as follows

$$v_1 = hA(h)\tilde{v}_1(h) = hA(h)(hf_x^0 A(h)\tilde{v}_2(h)) = h^2 A(h)f_x^0 A(h)\tilde{v}_2(h).$$

However, by (1.20) and the biorthogonality imposed to the vectors v_0, v_1, p_0, p_1, we obtain

$$1 = p_0^T v_1 = h^2 p_0^T A(h)f_x^0 A(h)\tilde{v}_2(h) = h^2 p_0^T f_x^0 A(h)\tilde{v}_2(h) = 0,$$

which is a contradiction. □

Lemma 1.10. *Let the assumptions of Theorem 1.6 be fulfilled. Then, there exists a positive constant $\rho_3 \leq \rho_2$, such that for all $h \in (0, \rho_3)$ the following assertions hold:*

(i) $\text{null}(f_x^{0T}) = \text{null}((\psi_x^0(h) - I_N)^T)$,

(ii) $\frac{1}{h}p_1^T(\psi_x^0(h) - I_N) = p_0^T$,

(iii) $\sum_{i=1}^{s}\gamma_i W_{ix}^0(h)\tilde{v}_1(h) = \frac{1}{h}v_1$,

(iv) $p_0^T\sum_{i=1}^{s}\gamma_i W_{ixx}^0(h)[v_0, v_0] = 2h\omega a$, $\omega := \sum_{i=1}^{s}\sum_{j=1}^{s}\gamma_i\tau_{ij}$,

(v) $\lim_{h\to 0^+} c(h) = 0$, $c(h) := v_1^T((A(h))^{-1})^T p_1$,

(vi) $2(h\omega - c(h))a + b \neq 0$.

Proof. Assume $h \in (0, \rho_2)$. Let us show (i). Choose any $0 \neq v \in \text{null}(f_x^{0T})$, then by (1.17), it follows

$$v^T(\psi_x^0(h) - I_N) = hv^T f_x^0 A(h) = 0,$$

so $v \in \text{null}((\psi_x^0(h) - I_N)^T)$. Contrariwise, take $0 \neq w \in \text{null}((\psi_x^0(h) - I_N)^T)$, hence

$$w^T f_x^0 = w^T(hf_x^0 A(h))(hA(h))^{-1} = w^T(\psi_x^0(h) - I_N)(hA(h))^{-1} = 0,$$

thereby $w \in \text{null}(f_x^{0T})$. As for (ii), we use (1.3) and (1.20) in order to obtain

$$\frac{1}{h}p_1^T(\psi_x^0(h) - I_N) = \frac{1}{h}p_1^T(hf_x^0 A(h)) = p_0^T A(h) = p_0^T.$$

Next, we show (iii):

$$\begin{aligned}
\sum_{i=1}^{s} \gamma_i W_{ix}^0(h)\tilde{v}_1(h) &= \sum_{i=1}^{s} \gamma_i \left(I_N + h \sum_{j=1}^{s} \tau_{ij} k_{jx}^0(h) \right) \left(\frac{1}{h}(A(h))^{-1} v_1 \right), \\
&= \frac{1}{h} \left(I_N + h \sum_{i=1}^{s} \sum_{j=1}^{s} \gamma_i \tau_{ij} k_{jx}^0(h) \right) (A(h))^{-1} v_1, \\
&= \frac{1}{h} A(h)(A(h))^{-1} v_1, \\
&= \frac{1}{h} v_1.
\end{aligned}$$

Before taking up (iv), let us compute $k_{lxx}(h, x, \alpha)[v, w]$, for $v, w \in \mathbb{R}^N$, $h \in (0, \rho_2)$, (x, α) in a small neighborhood of the origin, $l = 1, \ldots, s$:

$$\begin{aligned}
k_{lxx}(h, x, \alpha)[v, w] &= (f(W_l(h, x, \alpha), \alpha))_{xx}[v, w], \\
&= (f_x(W_l(h, x, \alpha), \alpha) W_{lx}(h, x, \alpha))_x [v, w], \\
&= f_{xx}(W_l(h, x, \alpha), \alpha)[W_{lx}(h, x, \alpha)v, W_{lx}(h, x, \alpha)w] \\
&\quad + f_x(W_l(h, x, \alpha), \alpha) W_{lxx}(h, x, \alpha)[v, w]. \qquad (1.21)
\end{aligned}$$

By evaluating this expression at $(x, \alpha) = (0, 0)$, $v = w = v_0$, and recalling that $v_0 \in \text{null}(k_{lx}^0(h))$, $l = 1, \ldots, s$, we arrive at

$$k_{lxx}^0(h)[v_0, v_0] = f_{xx}^0[v_0, v_0] + f_x^0 W_{lxx}^0(h)[v_0, v_0]. \qquad (1.22)$$

Consequently, we obtain:

$$\begin{aligned} p_0^T \sum_{i=1}^{s} \gamma_i W_{ixx}^0(h)[v_0, v_0] &= h p_0^T \sum_{i=1}^{s}\sum_{l=1}^{s} \gamma_i \tau_{il} k_{lxx}^0(h)[v_0, v_0], \\ &= h p_0^T \sum_{i=1}^{s}\sum_{l=1}^{s} \gamma_i \tau_{il} (f_{xx}^0[v_0, v_0] + f_x^0 W_{lxx}^0(h)[v_0, v_0]), \\ &= h\omega p_0^T f_{xx}^0[v_0, v_0] = 2h\omega \left(\frac{1}{2} p_0^T B_f(v_0, v_0)\right), \\ &= 2h\omega a. \end{aligned}$$

Let us take up (v). By Lemma A.1, we can write $(A(h))^{-1}$ as follows:

$$\begin{aligned} (A(h))^{-1} &= \sum_{l=0}^{\infty} (-1)^l \left(h \sum_{i=1}^{s}\sum_{j=1}^{s} \gamma_i \tau_{ij} k_{jx}^0(h) \right)^l, \\ &= I_N + hB(h), \end{aligned}$$

where

$$B(h) := \sum_{l=1}^{\infty} (-1)^l (h)^{l-1} \left(\sum_{i=1}^{s}\sum_{j=1}^{s} \gamma_i \tau_{ij} k_{jx}^0(h) \right)^l,$$

thus $c(h)$ reads

$$c(h) = v_1^T ((A(h))^{-1})^T p_1 = v_1^T (I_N + hB(h))^T p_1 = h v_1^T B^T(h) p_1,$$

hence (v) follows. It is left to show (vi). By (v), we can choose some positive ρ_3' so that $|c(h)| < \frac{|b|}{6|a|}$, for all $h \in (0, \rho_3')$. Then, take $\rho_3 := \min\left(\rho_2, \rho_3', \frac{|b|}{6|a||\omega|}\right)$, thereby it holds

$$|2(h\omega - c(h))a| \leq 2h|a||\omega| + 2|a||c(h)| < \frac{|b|}{3} + \frac{|b|}{3} = \frac{2|b|}{3},$$

therefore, (vi) follows. □

Lemma 1.11. *Let the assumptions of Theorem 1.6 be fulfilled. Then, for all $h \in (0, \rho_2)$ the vectors $\tilde{v}_0(h), \tilde{v}_1(h), \tilde{p}_0(h), \tilde{p}_1(h)$ satisfy the set of equations* (1.8) *of Definition 1.3 (with $g := \psi^h(\cdot, \cdot)$), where:*

$$\begin{aligned} \tilde{v}_0(h) &:= v_0, & \tilde{v}_1(h) &:= \tfrac{1}{h}(A(h))^{-1} v_1, \\ \tilde{p}_0(h) &:= h p_0, & \tilde{p}_1(h) &:= p_1 - c(h) p_0. \end{aligned}$$

Furthermore, this set of vectors is biorthogonal.

Proof. Assume $h \in (0, \rho_2)$. That $\tilde{v}_0(h), \tilde{v}_1(h)$ satisfy the first two equations of (1.8) follows immediately from Lemma 1.8, and (i) of Lemma 1.9. As for the remaining two equations, it holds by (i) of Lemma 1.10 that

$$\tilde{p}_0^T(h)(\psi_x^0(h) - I_N) = hp_0^T(\psi_x^0(h) - I_N) = 0.$$

Finally, by (i), and (ii) of Lemma 1.10, it is seen

$$\tilde{p}_1^T(h)(\psi_x^0(h) - I_N) = h\left(\frac{1}{h}p_1^T(\psi_x^0(h) - I_N)\right) = hp_0^T = \tilde{p}_0^T(h).$$

It is left to show biorthogonality. By (1.8), it holds

$$\tilde{v}_0^T(h)\tilde{p}_0(h) = \tilde{v}_1^T(h)(\psi_x^0(h) - I_N)^T\tilde{p}_0(h) = 0.$$

On the other hand, by the biorthogonality of v_0, v_1, p_0, p_1, we have

$$\tilde{v}_0^T(h)\tilde{p}_1(h) = v_0^T p_1 - c(h)v_0^T p_0 = 1.$$

Hence, it also follows

$$\tilde{v}_1^T(h)\tilde{p}_0(h) = \tilde{v}_1^T(h)(\psi_x^0(h) - I_N)^T\tilde{p}_1(h) = \tilde{v}_0^T(h)\tilde{p}_1(h) = 1.$$

Lastly, we see that

$$\begin{aligned}
\tilde{p}_1^T(h)\tilde{v}_1(h) &= (p_1 - c(h)p_0)^T\left(\frac{1}{h}(A(h))^{-1}v_1\right), \\
&= \frac{1}{h}(p_1^T(A(h))^{-1}v_1 - c(h)p_0^T(A(h))^{-1}v_1), \\
&= \frac{1}{h}\left(c(h) - c(h)(hp_0^T)\left(\frac{1}{h}(A(h))^{-1}v_1\right)\right), \\
&= \frac{c(h)}{h}(1 - \tilde{p}_0^T(h)\tilde{v}_1(h)), \\
&= 0. \quad \square
\end{aligned}$$

With these preliminary results, we are ready to present:

Proof of Theorem 1.6. We have to show that conditions **1d**–**3d** of Definition 1.3 (with $g := \psi^h(\cdot,\cdot)$) hold for all $h \in (0, \rho)$, ρ some positive constant. Indeed, take $\rho := \min(\rho_1, \rho_2, \rho_3)$. Then, Lemma 1.7 proves **1d**. Likewise, Lemma 1.8 shows that $\psi_x^0(h)$ has an eigenvalue equal to 1, with geometric multiplicity equal to 1. This means that the only Jordan Block associated to this eigenvalue is of dimension ≥ 1. Nevertheless, Lemma 1.9 tells us that there exists one, and only one generalized eigenvector corresponding to

this eigenvalue, hence **2d** follows. As for **3d**, some extra work needs to be done. Firstly, we have to compute the normal form coefficients in order to check nondegeneracy. These coefficients will be denoted by $\tilde{a}(h), \tilde{b}(h)$. For the computations, Lemma 1.11 provides us with the required eigenvectors. Let us then compute $\tilde{a}(h)$. With the help of (1.22), we obtain:

$$\begin{aligned}
\tilde{a}(h) &= \frac{1}{2}\tilde{p}_0^T(h)B_\psi(\tilde{v}_0(h),\tilde{v}_0(h)),\\
&= \frac{1}{2}hp_0^T\psi_{xx}^0(h)[v_0,v_0],\\
&= \frac{1}{2}h^2p_0^T\sum_{i=1}^{s}\gamma_i(f_{xx}^0[v_0,v_0]+f_x^0W_{ixx}^0(h)[v_0,v_0]),\\
&= \frac{1}{2}h^2p_0^TB_f(v_0,v_0),\\
&= h^2a. \qquad (1.23)
\end{aligned}$$

Next, we compute $\tilde{b}(h)$ as follows:

$$\begin{aligned}
\tilde{b}(h) &= \tilde{p}_1^T(h)B_\psi(\tilde{v}_0(h),\tilde{v}_0(h))+\tilde{p}_0^T(h)B_\psi(\tilde{v}_0(h),\tilde{v}_1(h)),\\
&= (p_1^T-c(h)p_0^T)\psi_{xx}^0(h)[v_0,v_0]+hp_0^T\psi_{xx}^0(h)[v_0,\tilde{v}_1(h)].
\end{aligned}$$

By (1.21) and (1.22), we obtain:

$$\begin{aligned}
\tilde{b}(h) &= h(p_1^T-c(h)p_0^T)\sum_{i=1}^{s}\gamma_i(f_{xx}^0[v_0,v_0]+f_x^0W_{ixx}^0(h)[v_0,v_0])\\
&\quad +h^2p_0^T\sum_{i=1}^{s}\gamma_i(f_{xx}^0[v_0,W_{ix}^0(h)\tilde{v}_1(h)]+f_x^0W_{ixx}^0(h)[v_0,\tilde{v}_1(h)]),\\
&= hp_1^Tf_{xx}^0[v_0,v_0]+hp_0^T\sum_{i=1}^{s}\gamma_iW_{ixx}^0(h)[v_0,v_0]-hc(h)p_0^Tf_{xx}^0[v_0,v_0]\\
&\quad +h^2p_0^Tf_{xx}^0\left[v_0,\sum_{i=1}^{s}\gamma_iW_{ix}^0(h)\tilde{v}_1(h)\right].
\end{aligned}$$

Finally, by taking into account (iii), and (iv) of Lemma 1.10, we arrive at:

$$\begin{aligned}
\tilde{b}(h) &= 2h^2\omega a-2hc(h)a+hp_1^TB_f(v_0,v_0)+hp_0^TB_f(v_0,v_1),\\
&= 2h(h\omega-c(h))a+hb. \qquad (1.24)
\end{aligned}$$

Lastly, it is left to show nondegeneracy. Indeed, we have that $\tilde{a}(h)\tilde{b}(h)\neq 0$ for all $h\in(0,\rho)$. For if we assume $\tilde{a}(h_*)\tilde{b}(h_*)=0$ for some $h_*\in(0,\rho)$, this would imply

$$\tilde{a}(h_*)\tilde{b}(h_*)=h_*^2a(2h_*(h_*\omega-c(h_*))a+h_*b)=2h_*^3(h_*\omega-c(h_*))a^2+h_*^3ab=0.$$

Since $a, h_* \neq 0$, it follows

$$2(h_*\omega - c(h_*))a + b = 0,$$

which clearly contradicts (vi) of Lemma 1.10. □

1.3.3 Discretized eigenvectors and critical coefficients

Analyzing the dynamics of a given system near a singularity demands the utilization of a more elaborated approach than that used in the hyperbolic case (cf. Section 1.3). Topological equivalence and reduction techniques play a central role in this analysis. Indeed, Shoshitaishvili's Theorem and the Reduction Principle (cf. [16, 44]) essentially tells us that the relevant dynamics (i.e., that which can not be described by looking at the linear part of the system) occur on the center manifold, and are captured by the restriction of the system to this manifold. This allows us to reduce the dimension of the system to be studied, and thus, one focuses on finding a simplified (not necessarily the simplest) dynamical system that qualitatively describes the behavior of the reduced system. This simplified system is referred to as a normal form.

For this reason, normal form analysis has proven to be a powerful technique for the investigation of the behavior of a dynamical system in a small neighborhood of a bifurcation. Thus, a natural question would be to know how the normal form of a specific one-step method applied to a continuous-time system looks like, and whether this discretized normal form is related to the normal form of the original system. This is the question we are to take up along this section.

Let the assumptions of Theorem 1.6 be satisfied. Suppose that the restriction of system (1.1) at $\alpha = 0$ to its center manifold takes the form (cf. Section 1.1.1)

$$\begin{cases} \dot{w}_1 = w_2, \\ \dot{w}_2 = aw_1^2 + bw_1w_2 + O(||w||^3), \end{cases}$$

Therefore, by Theorem 1.6, and in particular by (1.23) and (1.24), the restriction of system (1.12) at $\alpha = 0$ to its center manifold can take the form (cf. Section 1.2.1)

$$\begin{pmatrix} w_1 \\ w_2 \end{pmatrix} \mapsto \begin{pmatrix} w_1 + w_2 \\ w_2 + (h^2a)w_1^2 + (2h(h\omega - c(h))a + hb)w_1w_2 \end{pmatrix} + O(||w||^3).$$

This by-product result of the previous section clearly answers the above outlined question, and furthermore this shows that the local dynamics of the

one-step map at $\alpha = 0$ depends only on the normal form coefficients of the original system and on the structure of the Runge-Kutta method.

Moreover, recall that the tangent space at $x = 0$ of the center manifold of system 1.1 at $\alpha = 0$ is spanned by

$$\{v_0, v_1\}.$$

Likewise, as a by-product, we showed that the center manifold of system 1.12 at $\alpha = 0$ intersects the center manifold of the continuous-time system at $x = 0$ (for the BT_2 point persist at $x = 0$), and its tangent space at this point is spanned by (cf. Lemma 1.11)

$$\left\{ v_0, \frac{1}{h}(A(h))^{-1} v_1 \right\},$$

which implies that the manifolds intersect of course in a nontransversal manner at $x = 0$. It is worth recalling that the center manifold of the one-step map must not be thought of as it approximates or discretizes its continuous counter part. In fact, discretizations of center manifolds of continuous-time systems may lead to stable or unstable invariant manifolds of one-step methods (cf. [4, 8]). Similarly, the discrete normal form coefficients and generalized eigenvectors do not approximate their continuous counterpart.

Finally, we want to summarize this section by presenting a set of formulae which allows computation of normal form coefficients and generalized eigenvectors of general Runge-Kutta methods applied to a continuous-time system that undergoes a BT_2 singularity:

$$\begin{array}{rclrcl} \tilde{v}_0(h) & = & v_0, & \tilde{v}_1(h) & = & \frac{1}{h}(A(h))^{-1} v_1, \\ \tilde{p}_0(h) & = & h p_0, & \tilde{p}_1(h) & = & p_1 - c(h) p_0, \\ \tilde{a}(h) & = & h^2 a, & \tilde{b}(h) & = & 2h(h\omega - c(h))a + hb. \end{array}$$

These formulae follow from Lemma 1.11, and the proof of Theorem 1.6.

1.4 FH singularities under general one-step methods

In the spirit of Section 1.3, we will now study the effect of one-step discretizations methods applied to systems having an FH point. More precisely, we will suppose we are given a continuous-time dynamical system (1.1), which undergoes an FH singularity at the origin. We assume that this system is discretized via general p-th order one-step methods. Under these conditions,

it will be shown that the FH point is $O(h^p)$-shifted and turned into an FN point by the one-step map, for all sufficiently small step-size.

Few remarks concerning the choice of the discretization method to be studied seem to be in order. As we saw in the previous section, a BT_2 point persists under general Runge-Kutta methods. This fact allowed us to derive explicit formulae that relate original and discretized eigenvectors and normal form coefficients. However, when dealing with systems having an FH singularity, the situation is quite different. Due to the presence of a simple pair of purely imaginary eigenvalues (i.e. Hopf eigenvalues), it is not possible that an FH point persists at the same position as a BT_2 point does. For this reason, such a set of formulae, as presented in the previous section, is not achievable. The best one might obtain is an $O(h^k)$-approximation, $k \geq 1$ of those objects. Therefore, we consider that in this section a more general approach is suitable, which also will help us to tackle the forthcoming questions we will deal with.

Before we present the main result of this section, let us introduce the notion of a standard one-step method.

Definition 1.12. *Consider a general one-step method of order $p \geq 1$ applied to* (1.1)*, and given by*

$$x \mapsto \psi^h(x, \alpha) := x + h\Phi(h, x, \alpha), \tag{1.25}$$

with $\psi, \Phi : [-h_0, h_0] \times \bar{\Omega} \times \bar{\Lambda} \to \mathbb{R}^N$ sufficiently smooth, $h_0 > 0$, and $0 \in \bar{\Omega} \subset \Omega$, $0 \in \bar{\Lambda} \subset \Lambda$ are compact sets. Then, (1.25) *is said to be standard, if there exist smooth functions $\Upsilon, \Xi : [-h_0, h_0] \times \bar{\Omega} \times \bar{\Lambda} \to \mathbb{R}^N$ such that:*

$$\begin{aligned}
\psi^h(x, \alpha) &= \varphi^h(x, \alpha) + \Upsilon(h, x, \alpha)h^{p+1}, \\
\psi^h_w(x, \alpha) &= \varphi^h_w(x, \alpha) + \Upsilon_w(h, x, \alpha)h^{p+1}, \\
\Phi(h, x, \alpha) &= f(x, \alpha) + \Xi(h, x, \alpha)h, \\
\Phi_w(h, x, \alpha) &= f_w(x, \alpha) + \Xi_w(h, x, \alpha)h,
\end{aligned}$$

hold for all $(h, x, \alpha) \in [-h_0, h_0] \times \bar{\Omega} \times \bar{\Lambda}$, where w stands for any of the variables of $f(\cdot, \cdot)$, and $\varphi^t(\cdot, \alpha)$ for the t-flow of (1.1) *at α.*

The main result of this section is then formulated as follows:

Theorem 1.13. *Let a general one-step discretization method of order $p \geq 1$ applied to* (1.1) *be given by* (1.25)*. Assume:*

(i) (1.25) *is standard,*

(ii) system (1.1) *has a generic FH point (x_{FH}, α_{FH}) at the origin,*

then, there exists a positive constant $\rho \leq h_0$*, such that* (1.25) *possesses a unique FN point* $(x_{FN}(h), \alpha_{FN}(h))$*, which depends smoothly on* h*, for all* $h \in (-\rho, \rho)$*. Furthermore, the following estimate holds*

$$||(x_{FN}(h), \alpha_{FN}(h)) - (x_{FH}, \alpha_{FH})|| \leq C|h|^p,$$

$C > 0$*,* $h \in (-\rho, \rho)$*.*

Before proving this theorem, some comments are in order. As we explained before, in this section we consider general one-step methods, in contrast to the previous section in which we dealt with general Runge-Kutta methods. The approach in this section is consequently different; the structure of the discretization method cannot be exploited as before, thus a more general technique has to be employed.

Generic FH points can be seen as regular zeroes of a defining system (see Section 1.1.2). Likewise, defining systems can be constructed, so that an FN point is a regular zero of them. The basic idea is to suitably construct such systems, and then to establish closeness properties between them. Once this is done, the closeness estimate between the FH and FN points, and the smooth dependence of the latter on h follow from application of Vainikko's Lemma (see Appendix A), and the Implicit Function Theorem. This technique has been applied in several contexts, e.g., for finding $O(h^p)$-close hyperbolic equilibria of discretized continuous-time systems (cf. [4]), and in a much more elaborated context in [9], where the authors study the effect of one-step methods applied to systems possessing connecting orbits. With these remarks, we are ready to present:

Proof of Theorem 1.13. A generic FH point of (1.1) is a regular zero of (see Section 1.1.2)

$$\tilde{F}(x, \alpha) := \begin{pmatrix} f(x, \alpha) \\ \det(2f_x(x, \alpha) \odot I_N) \\ \det(f_x(x, \alpha)) \end{pmatrix} = 0. \tag{1.26}$$

We will try to rewrite the above equation in terms of the h-flow $\varphi^h(\cdot, \alpha)$ of (1.1). By a straightforward analysis of the variational equation of (1.1) at an equilibrium (x_0, α_0), the following relation follows (cf. [34, Section 1.3]):

$$\Delta(\varphi_x^h(x_0, \alpha_0)) = e^{h\Delta(f_x(x_0, \alpha_0))}, \tag{1.27}$$

where $\Delta(A)$ denotes the spectrum of a matrix $A \in \mathbb{R}^{N,N}$. Thus, we can conclude that $\varphi_x^h(x_0, \alpha_0)$ has a pair of eigenvalues on the unit circle (resp. an eigenvalue equal to 1), if and only if $f_x(x_0, \alpha_0)$ has a pair of purely imaginary

eigenvalues (resp. an eigenvalue equal to 0), for $h \neq 0$. Therefore, (1.26) can be written, with help of (1.10) and (1.11), in terms of the h-flow $\varphi^h(\cdot, \alpha)$ as follows

$$\left\{ \begin{array}{rcl} \varphi^h(x,\alpha) - x & = & 0, \\ \det(\varphi^h_x(x,\alpha) \odot \varphi^h_x(x,\alpha) - I_m) & = & 0, \\ \det(\varphi^h_x(x,\alpha) - I_N) & = & 0. \end{array} \right.$$

However, note that this system becomes trivial at $h = 0$, which is inconvenient for our approach, since we want to perform our analysis for h small. Therefore, we will rather consider the following system

$$F(h,x,\alpha) := \left(\begin{array}{c} \frac{1}{h}(\varphi^h(x,\alpha) - x) \\ \det\left(\frac{1}{h}(\varphi^h_x(x,\alpha) \odot \varphi^h_x(x,\alpha) - I_m)\right) \\ \det\left(\frac{1}{h}(\varphi^h_x(x,\alpha) - I_N)\right) \end{array} \right) = 0,$$

which will be later shown not to be trivial at $h = 0$. Similarly, a FN point of (1.25) is a solution of (cf. (1.10), (1.11))

$$\left\{ \begin{array}{rcl} \psi^h(x,\alpha) - x & = & 0, \\ \det(\psi^h_x(x,\alpha) \odot \psi^h_x(x,\alpha) - I_m) & = & 0, \\ \det(\psi^h_x(x,\alpha) - I_N) & = & 0, \end{array} \right.$$

but, as before, this system becomes trivial at $h = 0$, so we will use the following system (see above)

$$G(h,x,\alpha) := \left(\begin{array}{c} \frac{1}{h}(\psi^h(x,\alpha) - x) \\ \det\left(\frac{1}{h}(\psi^h_x(x,\alpha) \odot \psi^h_x(x,\alpha) - I_m)\right) \\ \det\left(\frac{1}{h}(\psi^h_x(x,\alpha) - I_N)\right) \end{array} \right) = 0. \tag{1.28}$$

The next step is to establish relations between $\tilde{F}$, F, and G, which will be crucial for our analysis. Let us begin with G, and $\tilde{F}$. The following expansions hold locally (cf. Definition 1.12):

$$\begin{array}{rcl} \Phi(h,x,\alpha) & = & f(x,\alpha) + \Xi(h,x,\alpha)h, \\ \Phi_w(h,x,\alpha) & = & f_w(x,\alpha) + \Xi_w(h,x,\alpha)h, \end{array}$$

thereby we obtain:

$$\begin{aligned} G(h,x,\alpha) &= \begin{pmatrix} \frac{1}{h}(\psi^h(x,\alpha)-x) \\ \det\left(\frac{1}{h}(\psi^h_x(x,\alpha)\odot\psi^h_x(x,\alpha)-I_m)\right) \\ \det\left(\frac{1}{h}(\psi^h_x(x,\alpha)-I_N)\right) \end{pmatrix}, \\ &= \begin{pmatrix} \Phi(h,x,\alpha) \\ \det(2\Phi_x(h,x,\alpha)\odot I_N+\Phi_x(h,x,\alpha)\odot\Phi_x(h,x,\alpha)h) \\ \det(\Phi_x(h,x,\alpha)) \end{pmatrix}, \\ &= \begin{pmatrix} f(x,\alpha)+\Xi(h,x,\alpha)h \\ \det(2f_x(x,\alpha)\odot I_N+\Theta_1(h,x,\alpha)h) \\ \det(f_x(x,\alpha)+\Xi_x(h,x,\alpha)h) \end{pmatrix}, \\ &= \tilde{F}(x,\alpha)+\Theta(h,x,\alpha)h, \end{aligned} \tag{1.29}$$

where $\Theta_1(h,x,\alpha) := \Phi_x(h,x,\alpha)\odot\Phi_x(h,x,\alpha)+2\Xi_x(h,x,\alpha)\odot I_N$, and Θ is some smooth function[2]. As for F and G, the following expansions will be needed (cf. Definition 1.12):

$$\begin{aligned} \psi^h(x,\alpha) &= \varphi^h(x,\alpha)+\Upsilon(h,x,\alpha)h^{p+1}, \\ \psi^h_w(x,\alpha) &= \varphi^h_w(x,\alpha)+\Upsilon_w(h,x,\alpha)h^{p+1}, \end{aligned}$$

which hold locally, too. So, we obtain:

$$\begin{aligned} G(h,x,\alpha) &= \begin{pmatrix} \frac{1}{h}(\psi^h(x,\alpha)-x) \\ \det\left(\frac{1}{h}(\psi^h_x(x,\alpha)\odot\psi^h_x(x,\alpha)-I_m)\right) \\ \det\left(\frac{1}{h}(\psi^h_x(x,\alpha)-I_N)\right) \end{pmatrix}, \\ &= \begin{pmatrix} \frac{1}{h}(\varphi^h(x,\alpha)-x)+\Upsilon(h,x,\alpha)h^p \\ \det\left(\frac{1}{h}(\varphi^h_x(x,\alpha)\odot\varphi^h_x(x,\alpha)-I_m)+\Psi_1(h,x,\alpha)h^p\right) \\ \det\left(\frac{1}{h}(\varphi^h_x(x,\alpha)-I_N)+\Upsilon_x(h,x,\alpha)h^p\right) \end{pmatrix}, \\ &= F(h,x,\alpha)+\Psi(h,x,\alpha)h^p, \end{aligned} \tag{1.30}$$

where $\Psi_1(h,x,\alpha) := 2\varphi^h_x(x,\alpha)\odot\Upsilon_x(h,x,\alpha)+\Upsilon_x(h,x,\alpha)\odot\Upsilon_x(h,x,\alpha)h^{p+1}$, and Ψ is some smooth function. The next step is to apply Lemma A.2 to $H := G(h,\cdot,\cdot)$, for all h in some interval. Consequently, we need firstly to show that the assumptions of that lemma are fulfilled for small h. Let us then define $y := (x,\alpha)$, and take $y_0 := (x_{FH},\alpha_{FH}) = (0,0)$. We will show that $G_y(h,y_0)$ is nonsingular for all h in some interval. Indeed, assume $h\in(-h_0,h_0)$, then by (1.29), and recalling the genericity of the FH point, it holds

$$G_y(h,y_0) = \tilde{F}_y(y_0)+\Theta_y(h,y_0)h = \tilde{F}_y(y_0)(I_N+(\tilde{F}_y(y_0))^{-1}\Theta_y(h,y_0)h).$$

[2]In what follows, by the term "(some smooth function) $\cdot\, w^k$", $k\geq 1$, w some real variable, we mean the integral remainder of a Taylor series.

Choose $0 < \rho_1 < h_0$, so that

$$||(\tilde{F}_y(y_0))^{-1}\Theta_y(h,y_0)h|| < ||(\tilde{F}_y(y_0))^{-1}|| \left(\sup_{h\in(-h_0,h_0)} ||\Theta_y(h,y_0)|| \right) |h| < 1,$$

for all $h \in (-\rho_1, \rho_1)$. Then, Lemma A.1 ensures the invertibility of $G_y(h, y_0)$ in $(-\rho_1, \rho_1)$, and furthermore the following estimate holds

$$||(G_y(h,y_0))^{-1}|| < \frac{||(\tilde{F}_y(y_0))^{-1}||}{1 - ||(\tilde{F}_y(y_0))^{-1}|| \sup_{h\in(-h_0,h_0)} ||\Theta_y(h,y_0)||\rho_1} =: \frac{1}{\sigma}.$$

Take $\kappa := \frac{1}{2}\sigma$. Then, by the continuity of G_y, we can find a closed ball $B_\delta(y_0)$, $\delta > 0$, and a positive constant ρ_1', such that

$$||G_y(h,y) - G_y(h,y_0)|| \leq \kappa,$$

for all $y \in B_\delta(y_0)$, $h \in [-\rho_1', \rho_1']$. Likewise, by the continuity of G, and noticing that $G(0, y_0) = 0$ (see (1.29)), we can find a positive constant ρ_1'', such that

$$||G(h,y_0)|| \leq (\sigma - \kappa)\delta,$$

for all $h \in [-\rho_1'', \rho_1'']$. Finally, take $\rho_2 := \min(\rho_1, \rho_1', \rho_1'')$, consequently the assumptions of Lemma A.2 hold for $H := G(h, \cdot)$, for all $h \in (-\rho_2, \rho_2)$. Moreover, for $G(0, y_0) = 0$ and $G_y(0, y_0) = \tilde{F}_y(y_0)$ is nonsingular, the Implicit Function Theorem guarantees the existence of a function $y_{FN} := (x_{FN}, \alpha_{FN}) : (-\rho_2', \rho_2') \to \mathbb{R}^{N+2}$, such that

$$G(h, y_{FN}(h)) = 0, \quad y_{FN}(0) = (x_{FN}(0), \alpha_{FN}(0)) = (0,0),$$

$h \in (-\rho_2', \rho_2')$. This shows the existence, uniqueness, and smooth dependence on h of an FN point of (1.25). It is left to show the closeness between the FH and FN points. To achieve this, choose $0 < \rho_2'' \leq \rho_2'$, so that $y_{FN}(h) \in B_\delta(y_0)$ for all $h \in (-\rho_2'', \rho_2'')$. Define $\rho_3 := \min(\rho_2, \rho_2'')$, then Lemma A.2 applied to $G(h, \cdot)$, $h \in (-\rho_3, \rho_3)$, combined with (1.30) yields:

$$\begin{aligned} ||(x_{FN}(h), \alpha_{FN}(h)) - (x_{FH}, \alpha_{FH})|| &\leq \frac{1}{\sigma - \kappa} ||G(h, y_{FN}(h)) - G(h,0)||, \\ &= \frac{2}{\sigma} ||\Psi(h,0)|| |h^p|, \\ &< \frac{2}{\sigma} \left(\sup_{h\in(-\rho_3,\rho_3)} ||\Psi(h,0)|| \right) |h|^p. \end{aligned}$$

To conclude, choose $0 < \rho < \rho_3$, and $C := \frac{2}{\sigma} \left(\sup_{h\in(-\rho_3,\rho_3)} ||\Psi(h,0)|| \right)$. □

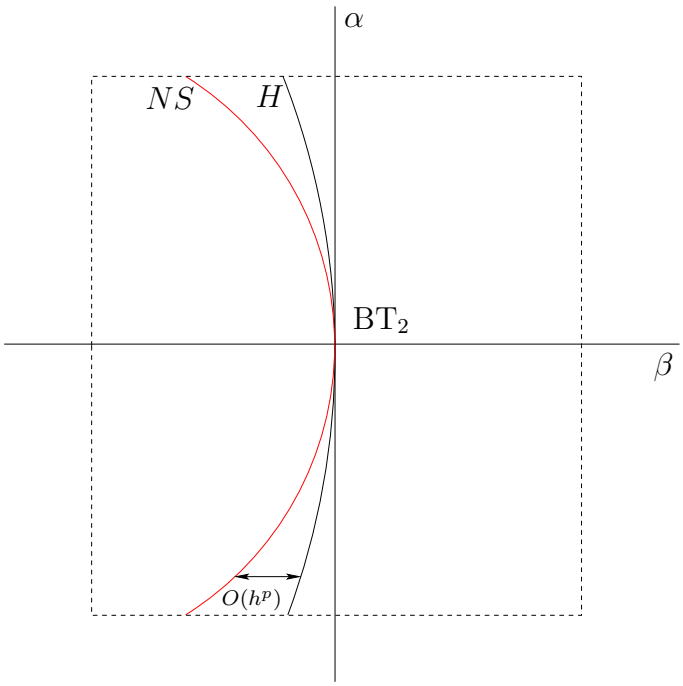

Fig. 1.3: Discretized path of Hopf points near a BT_2 singularity.

1.5 Analysis of the discretized path of Hopf points

In Sections 1.3 and 1.4, we saw that one-step methods reproduce "correctly" BT_2, and FH points. As we mentioned at the beginning of the chapter, we are interested to know whether the local bifurcation diagram near these codimension two singularities are "well" reproduced by one-step methods. In this sense, the first part of this task has been achieved, namely, the organizing centers were shown to persist under one-step methods.

In this section, we tackle the problem of analyzing the discretized path of Hopf points that emanates from the discretized codimension two bifurcations. As we already pointed out in the introduction of the chapter, this analysis must be done in a codimension two context. The main result of this section is illustrated in Figure 1.3. The curves labeled by H, NS represent paths of Hopf, Neimark-Sacker points, respectively. Throughout this section, we assume $(\beta, \alpha) \in \mathbb{R}^2$ to be the parameters of system (1.1). In the next section, we will see that it is possible to find a sufficiently small, step-size-independent neighborhood (the dashed square in Figure 1.3) of a BT_2 (resp. FH) point,

such that the discretized path of Hopf points approximates the original curve accordingly to the order of the method.

1.5.1 Closeness theorem

Throughout this section, we suppose we are given a continuous-time dynamical system (1.1), which undergoes a BT_2 or an FH bifurcation at the origin. We assume that this system is discretized via general one-step methods, as in Section 1.4. The aim is as previously described, namely, to study the emanating path of Hopf points under discretizations. For this purpose, we do not reduce the systems, e.g. via center manifold theory, but we rather work with them in full dimension. To do so, the approach employed for the study of FH points under discretizations will prove to be convenient and straightforward for this section, too. As before, we will suitably define systems whose solutions correspond to the objects we deal with. Then, closeness properties between the systems combined with Vainikko's Lemma will yield the desired result. The outlined question leads us then to the following:

Theorem 1.14. *Let a general one-step discretization method of order $p \geq 1$ applied to* (1.1) *be given by* (1.25). *Assume:*

(i) (1.25) *is standard,*

(ii) system (1.1) *has a generic BT_2 or FH point at the origin,*

then, there exist positive constants $\rho \leq h_0$, δ, and curves of Hopf and Neimark-Sacker points defined by:

$$\begin{array}{rclrcl} C_H(\alpha) & := & (x_H(\alpha), \beta_H(\alpha), \alpha), & C_H(0) & = & (0,0,0), \\ C_{NS}(h,\alpha) & := & (x_{NS}(h,\alpha), \beta_{NS}(h,\alpha), \alpha), & C_{NS}(0,0) & = & (0,0,0), \end{array}$$

with $x_H : (-\delta,\delta) \to \mathbb{R}^N$, $x_{NS} : (-\rho,\rho)\times(-\delta,\delta) \to \mathbb{R}^N$, $\beta_H : (-\delta,\delta) \to \mathbb{R}$, $\beta_{NS} : (-\rho,\rho)\times(-\delta,\delta) \to \mathbb{R}$ smooth[3]*. Furthermore, the following estimate holds for all $(h,\alpha) \in (-\rho,\rho)\times(-\delta,\delta)$, and uniformly in α*

$$||d_{NS}(h,\alpha) - d_H(\alpha)|| \leq C|h|^p, \tag{1.31}$$

where $d_H(\cdot) := (x_H(\cdot), \beta_H(\cdot))$, and $d_{NS}(\cdot,\cdot) := (x_{NS}(\cdot,\cdot), \beta_{NS}(\cdot,\cdot))$, $C > 0$.

[3]By the term "Neimark-Sacker curve", we mean the image of the function $C_{NS}(h_*,\cdot)$, for $h_* \in (-\rho,\rho)$ fixed.

Proof. A generic FH or BT_2 point of (1.1) is a regular zero of (see Section 1.1.1 and 1.1.2)

$$\left\{\begin{array}{rcl} f(x,\beta,\alpha) & = & 0,\\ \det(2f_x(x,\beta,\alpha)\odot I_N) & = & 0,\\ \det(f_x(x,\beta,\alpha)) & = & 0,\end{array}\right.$$

which implies that the system (cf. Section 1.1.1)

$$\tilde{F}(x,\beta,\alpha) := \left(\begin{array}{c} f(x,\beta,\alpha)\\ \det(2f_x(x,\beta,\alpha)\odot I_N)\end{array}\right) = 0, \tag{1.32}$$

is regular at the origin. Define $y := (x,\beta)$. Then, without loss of generality, we assume that $\tilde{F}_y(0,0)$ is nonsingular. Therefore, the Implicit Function Theorem guarantees the existence of a smooth function $d_H := (x_H,\beta_H) : (-\delta_1,\delta_1) \to \mathbb{R}^N\times\mathbb{R}$, such that

$$\tilde{F}(d_H(\alpha),\alpha) = 0, \quad d_H(0) = (x_H(0),\beta_H(0)) = (0,0),$$

$\alpha\in(-\delta_1,\delta_1)$. As in the proof of Theorem 1.13, we will rewrite (1.32) in terms of the h-flow $\varphi^h(\cdot,\beta,\alpha)$ of (1.1). Thus, system (1.32) can then be replaced by

$$F(h,x,\beta,\alpha) := \left(\begin{array}{c} \frac{1}{h}(\varphi^h(x,\beta,\alpha)-x)\\ \det\left(\frac{1}{h}(\varphi^h_x(x,\beta,\alpha)\odot\varphi^h_x(x,\beta,\alpha)-I_m)\right)\end{array}\right) = 0,$$

and it holds (see (1.27))

$$F(h,d_H(\alpha),\alpha) = 0,$$

for all $(h,\alpha)\in(-h_0,h_0)\times(-\delta_1,\delta_1)$. In this sense, a system whose solutions describe a curve of Neimark-Sacker points of (1.25) is given by (see (1.11), (1.28))

$$G(h,x,\beta,\alpha) := \left(\begin{array}{c} \frac{1}{h}(\psi^h(x,\beta,\alpha)-x)\\ \det\left(\frac{1}{h}(\psi^h_x(x,\beta,\alpha)\odot\psi^h_x(x,\beta,\alpha)-I_m)\right)\end{array}\right) = 0.$$

Hence, we will see that a curve of Neimark-Sacker points actually exists. For this purpose, we will use the following relation

$$G(h,x,\beta,\alpha) = \tilde{F}(x,\beta,\alpha) + \Theta(h,x,\beta,\alpha)h, \tag{1.33}$$

which holds locally, and Θ is some smooth function. This is readily seen, by truncation of (1.29). So, for $\tilde{F}_y(0,0)$ is nonsingular, we have that $G_y(0,0,0) = \tilde{F}_y(0,0)$ (see above) is nonsingular, thereby the Implicit Function Theorem

guarantees the existence of a smooth function $d_{NS} := (x_{NS}, \beta_{NS}) : (-\rho_1', \rho_1') \times (-\delta_1', \delta_1') \to \mathbb{R}^N \times \mathbb{R}$, such that

$$G(h, d_{NS}(h, \alpha), \alpha) = 0, \quad d_{NS}(0,0) = (x_{NS}(0,0), \beta_{NS}(0,0)) = (0,0),$$

$(h, \alpha) \in (-\rho_1', \rho_1') \times (-\delta_1', \delta_1')$. We have thus shown the existence and smoothness of the curves C_H, C_{NS}. Now we will show the $O(h^p)$-closeness part. To accomplish this, we will use the following relation

$$G(h, x, \beta, \alpha) = F(h, x, \beta, \alpha) + \Psi(h, x, \beta, \alpha) h^p, \tag{1.34}$$

which holds locally, and Ψ is some smooth function. As before, this follows by truncation of (1.30). The next step is to apply Vainikko's Lemma to $H := G(h, \cdot, \alpha)$. Therefore, we need to show that the assumptions of the lemma are fulfilled for all (h, α) in some neighborhood. Let us firstly show that $G_y(h, y_0, \alpha)$ is locally nonsingular. Assume $(h, \alpha) \in (-\rho_2, \rho_2) \times (-\delta_2, \delta_2)$, with $0 < \rho_2 < \min(h_0, \rho_1')$ and $0 < \delta_2 < \min(\delta_1, \delta_1')$ thus chosen, that (1.33) holds and $\tilde{F}_y(y_0, \alpha)$ is nonsingular. This is possible, for $\tilde{F}_y(y_0, 0)$ is nonsingular. Thus we have that

$$\begin{aligned} G_y(h, y_0, \alpha) &= \tilde{F}_y(y_0, \alpha) + \Theta_y(h, y_0, \alpha) h, \\ &= \tilde{F}_y(y_0, \alpha)(I_N + (\tilde{F}_y(y_0, \alpha))^{-1} \Theta_y(h, y_0, \alpha) h). \end{aligned}$$

Choose $0 < \rho_3 < \rho_2$, so that

$$\begin{aligned} ||(\tilde{F}_y(y_0, \alpha))^{-1} \Theta_y(h, y_0, \alpha) h|| &< \sup_{\alpha \in (-\delta_2, \delta_2)} ||(\tilde{F}_y(y_0, \alpha))^{-1}|| \\ &\quad \left(\sup_{(h,\alpha) \in (-\rho_2, \rho_2) \times (-\delta_2, \delta_2)} ||\Theta_y(h, y_0, \alpha)|| \right) |h|, \\ &< 1, \end{aligned}$$

for all $h \in (-\rho_3, \rho_3)$. Then, Lemma A.1 ensures the invertibility of $G_y(h, y_0, \alpha)$ for all $(h, \alpha) \in (-\rho_3, \rho_3) \times (-\delta_2, \delta_2)$, and furthermore the following estimate holds

$$||(G_y(h, y_0, \alpha))^{-1}|| < \frac{K}{1 - K \sup_{(h,\alpha) \in (-\rho_2, \rho_2) \times (-\delta_2, \delta_2)} ||\Theta_y(h, y_0, \alpha)|| \rho_3} =: \frac{1}{\sigma},$$

where $K := \sup_{\alpha \in (-\delta_2, \delta_2)} ||(\tilde{F}_y(y_0, \alpha))^{-1}||$. Take $\kappa := \frac{1}{2}\sigma$. Then, by the continuity of G_y, we can find a closed ball $B_\epsilon(y_0)$, $\epsilon > 0$, and positive constants ρ_3', δ_2', such that

$$||G_y(h, y, \alpha) - G_y(h, y_0, \alpha)|| \leq \kappa,$$

for all $y \in B_\epsilon(y_0)$, $(h,\alpha) \in [-\rho_3', \rho_3'] \times [-\delta_2', \delta_2']$. Likewise, by the continuity of G, and noticing that $G(0, y_0, 0) = 0$ (see (1.33)), we can find positive constants ρ_3'', δ_2'', such that

$$||G(h, y_0, \alpha)|| \leq (\sigma - \kappa)\epsilon,$$

for all $(h,\alpha) \in [-\rho_3'', \rho_3''] \times [-\delta_2'', \delta_2'']$. Finally, take $\rho_4 := \min(\rho_3, \rho_3', \rho_3'')$, $\delta_3 := \min(\delta_2, \delta_2', \delta_2'')$, consequently the assumptions of Vainikko's Lemma hold for $H := G(h, \cdot, \alpha)$, and for all $(h,\alpha) \in (-\rho_4, \rho_4) \times (-\delta_3, \delta_3)$. Moreover, since $d_H(0) = d_{NS}(0,0) = 0$, we can choose positive constants $\rho_5 \leq \rho_4$, $\delta_4 \leq \delta_3$, such that

$$d_H(\alpha), d_{NS}(h,\alpha) \in B_\epsilon(y_0),$$

for all $(h,\alpha) \in (-\rho_5, \rho_5) \times (-\delta_4, \delta_4)$. Thus, Vainikko's Lemma combined with (1.34) yields:

$$\begin{aligned} ||d_{NS}(h,\alpha) - d_H(\alpha)|| &\leq \frac{1}{\sigma - \kappa} ||G(h, d_{NS}(h,\alpha), \alpha) - G(h, d_H(\alpha), \alpha)||, \\ &= \frac{2}{\sigma} ||\Psi(h, d_H(\alpha), \alpha)|| |h^p|, \qquad (1.35) \\ &< \frac{2}{\sigma} \left(\sup_{(h,\alpha) \in (-\rho_5, \rho_5) \times (-\delta_4, \delta_4)} ||\Psi(h, d_H(\alpha), \alpha)|| \right) |h|^p. \end{aligned}$$

To conclude, take $\rho := \rho_5$, $\delta := \delta_4$, and

$$C := \frac{2}{\sigma} \left(\sup_{(h,\alpha) \in (-\rho_5, \rho_5) \times (-\delta_4, \delta_4)} ||\Psi(h, d_H(\alpha), \alpha)|| \right). \quad \square$$

Before finishing this section, it is worth deriving a particular result from the above discussion. Under assumptions and notation of the previous theorem, suppose additionally that the one step method (1.25) preserves the BT_2 point at the origin. This would not be surprising, for this is the case when dealing with general Runge-Kutta methods (see Theorem 1.6). This means, that for all sufficiently small step-size, the map (1.25) undergoes an $\mathrm{R1}_2$ singularity at the origin, and this consequently implies

$$G(h, 0, 0) = 0,$$

for all h in some interval, say $(-\rho, \rho)$. Consider the following expansion (see (1.34))

$$G(h, d_H(\alpha), \alpha) = F(h, d_H(\alpha), \alpha) + \Psi(h, d_H(\alpha), \alpha) h^p = \Psi(h, d_H(\alpha), \alpha) h^p,$$

therefore we must have

$$G(h, d_H(0), 0) = G(h, 0, 0) = \Psi(h, d_H(0), 0)h^p = 0,$$

for all $h \in (-\rho, \rho)$, and hence $\Psi(h, d_H(0), 0) = 0$ in this interval. This means, that if we expand $\Psi(h, d_H(\cdot), \cdot)$ with respect to α, we obtain

$$\Psi(h, d_H(\alpha), \alpha) = \Gamma(h, \alpha)\alpha,$$

where Γ is some smooth function. By taking this into account in (1.35), we obtain the improved estimate

$$||d_{NS}(h, \alpha) - d_H(\alpha)|| \leq C|\alpha||h|^p, \tag{1.36}$$

for all $(h, \alpha) \in (-\rho, \rho) \times (-\delta, \delta)$, and

$$C := \frac{2}{\sigma} \left(\sup_{(h,\alpha)\in(-\rho,\rho)\times(-\delta,\delta)} ||\Gamma(h, \alpha)|| \right).$$

Note that such an improved estimate can only be obtained when dealing with BT_2 singularities. As we already mentioned (cf. Section 1.4), FH points are always shifted by one-step methods, hence the estimate in Theorem 1.14 is, for FH singularities, already optimal.

1.5.2 Analysis of discretized eigenvalues

As we saw in the previous section, the emanating path of Hopf points is $O(h^p)$-shifted and turned into a path of Neimark-Sacker points by general one-step methods. However, what we are actually computing via (1.5), (1.11) are paths of equilibria with a single pair of eigenvalues with sum equal to 0, product equal to 1, respectively (cf. [6, Theorem 3.3]), which evidently also correspond to the path of Hopf and Neimark-Sacker points we are analyzing.

It is well-known that paths of Hopf points and neutral saddles emanate from a BT_2 point (cf. Section 1.1.1), which can be computed, however, as a unique curve of equilibria with a single pair of eigenvalues with sum equal to 0. Furthermore, these eigenvalues are known to exhibit a singular behavior at the codimension two point, namely, they move along the imaginary axis for say $\alpha < 0$, then at $\alpha = 0$ they collide giving rise to a double, defective eigenvalue equal to 0, and finally for $\alpha > 0$ they move away from each other along the real axis as a neutral saddle. Therefore, this leads us to the question whether the discretized eigenvalues, i.e. the eigenvalues of the one-step map, follow "correctly" this behavior. This is the problem we are to

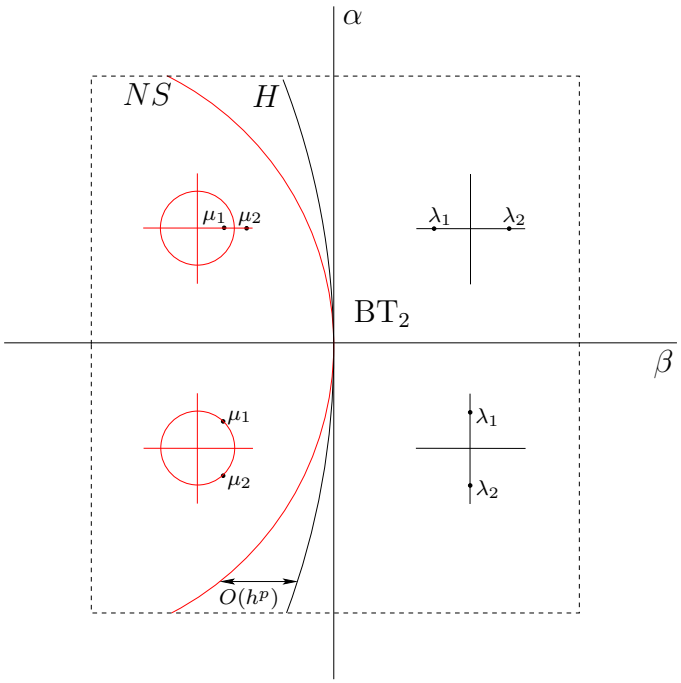

Fig. 1.4: Discretized path of Hopf points and eigenvalues near a BT_2 bifurcation.

take up throughout this section. Note that this is not the case when dealing with the path of Hopf points that emanates from an FH singularity, since they do not present such a singular behavior, and furthermore the discretized eigenvalues are nothing but smooth perturbations of the original ones, for the eigenvalues of the continuous-time system at the FH bifurcation are simple, and they remain simple under small perturbations. This is of course not the case when dealing with BT_2 points. Figure 1.4 illustrates the result we are after. In this figure, the curves labeled by H, NS represent paths of equilibria with a single pair of eigenvalues with sum equal to 0 (i.e. $\lambda_{1,2}$), and product equal to 1 (i.e. $\mu_{1,2}$), respectively.

Before we formally tackle the above outlined problem, some notation and preliminary results will be introduced. Under assumptions and notation of Theorem 1.14, suppose additionally that for all sufficiently small step-size the map (1.25) undergoes an $\mathrm{R1}_2$ singularity at the origin, provided the continuous-time system (1.1) undergoes a generic BT_2 bifurcation at the

origin. Let the following functions be defined by:

$$\begin{aligned} f_x^H(\alpha) &:= f_x(d_H(\alpha),\alpha), \\ \Phi_x^{NS}(h,\alpha) &:= \Phi_x(h,d_{NS}(h,\alpha),\alpha), \\ \psi_x^{NS}(h,\alpha) &:= \psi_x^h(d_{NS}(h,\alpha),\alpha) = I_N + h\Phi_x^{NS}(h,\alpha), \end{aligned} \tag{1.37}$$

for all $(h,\alpha) \in (-\rho,\rho)\times(-\delta,\delta)$. Denote by $\lambda_i(\alpha)$, $\eta_i(h,\alpha)$, $\mu_i(h,\alpha)$, $i = 1,\ldots,N$, the eigenvalues of $f_x^H(\alpha)$, $\Phi_x^{NS}(h,\alpha)$, $\psi_x^{NS}(h,\alpha)$, respectively, $(h,\alpha) \in (-\rho,\rho)\times(-\delta,\delta)$. By (1.37), we can assume that the following relation holds

$$\mu_i(h,\alpha) = 1 + h\eta_i(h,\alpha), \quad i = 1,\ldots,N,$$

and for all $(h,\alpha) \in (-\rho,\rho)\times(-\delta,\delta)$. Moreover, note that by (1.36) and taking into account Definition 1.12, it holds

$$\Phi_x^{NS}(0,\alpha) = f_x(d_{NS}(0,\alpha),\alpha) = f_x^H(\alpha),$$

for all $\alpha \in (-\delta,\delta)$, hence if we expand $\Phi_x^{NS}(\cdot,\alpha)$ with respect to h, we obtain

$$\Phi_x^{NS}(h,\alpha) = f_x^H(\alpha) + \nu_1(h,\alpha)h, \tag{1.38}$$

where ν_1 is some smooth function. On the other hand, the expansion of f_x^H reads

$$f_x^H(\alpha) = f_x^0 + \nu_2(\alpha)\alpha,$$

ν_2 some smooth function. This allows us to conclude

$$\Phi_x^{NS}(0,0) = f_x^H(0) = f_x^0, \tag{1.39}$$

which means that $\Phi_x^{NS}(h,\alpha)$, and $f_x^H(\alpha)$ are smooth perturbations of the same matrix, i.e. f_x^0. This fact will be of a great help for our purposes.

The next goal in this preliminary discussion is to develop a method to, at least theoretically, identify the nature of the eigenvalues along the curves C_H, C_{NS}, namely, a function that distinguishes between Hopf (resp. Neimark-Sacker) and neutral saddle eigenvalues. To accomplish this, assume that $\lambda_{1,2}$, $\mu_{1,2}$ are the pair of eigenvalues with sum equal to 0, product equal to 1 along C_H, C_{NS}, respectively. Figure 1.5 gives us an idea of how to define the functions we need. According to this figure, we can try to construct functions $\kappa_H : (-\delta,\delta) \to \mathbb{R}$, $\kappa_{NS} : (-\rho,\rho)\times(-\delta,\delta) \to \mathbb{R}$, such that:

$$\operatorname{sgn}(\kappa_H(\alpha)) = \begin{cases} -1, & \text{if neutral saddle point,} \\ 0, & \text{if } \mathrm{BT}_2 \text{ point,} \\ 1, & \text{if Hopf point,} \end{cases}$$

$$\operatorname{sgn}(\kappa_{NS}(h,\alpha)) = \begin{cases} -1, & \text{if neutral saddle point,} \\ 0, & \text{if } \mathrm{R1}_2 \text{ point,} \\ 1, & \text{if Neimark-Sacker point.} \end{cases}$$

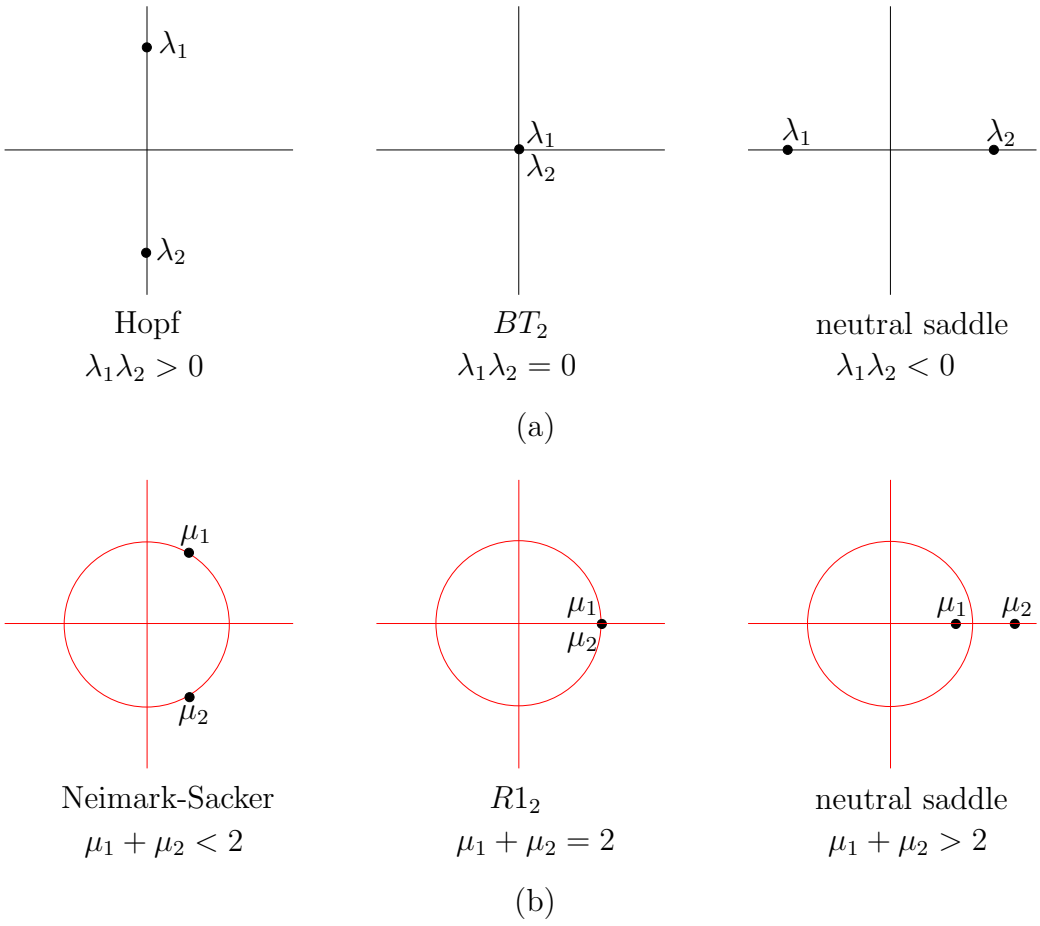

Fig. 1.5: Behavior of the eigenvalues along the curves: (a) C_H; (b) C_{NS}.

Thus, we choose

$$\kappa_H(\alpha) := \lambda_1(\alpha)\lambda_2(\alpha),$$

$\alpha \in (-\delta, \delta)$. As for κ_{NS}, note that the function

$$\tilde{\kappa}_{NS}(h, \alpha) := 2 - (\mu_1(h, \alpha) + \mu_2(h, \alpha)),$$

$(h, \alpha) \in (-\rho, \rho) \times (-\delta, \delta)$ shows the behavior we need. Further methods for detecting and identifying Hopf, and Neimark-Sacker eigenvalues are developed in [54], and suitable formulae for numerical implementations can be found in [29, 44].

Note that as h tends to zero, $\tilde{\kappa}_{NS}(h, \alpha)$ tends 0, regardless α, which is not convenient for our purposes. Nevertheless, this problem can be solved as follows. Note that for all $(h, \alpha) \in (-\rho, \rho) \times (-\delta, \delta)$, it holds:

$$\begin{aligned}
\mu_1(h, \alpha)\mu_2(h, \alpha) &= 1, \\
(1 + h\eta_1(h, \alpha))(1 + h\eta_2(h, \alpha)) &= 1, \\
1 + h(\eta_1(h, \alpha) + \eta_2(h, \alpha)) + h^2\eta_1(h, \alpha)\eta_2(h, \alpha) &= 1, \\
\Rightarrow -h(\eta_1(h, \alpha) + \eta_2(h, \alpha)) &= h^2\eta_1(h, \alpha)\eta_2(h, \alpha),
\end{aligned}$$

and thereby $\tilde{\kappa}_{NS}$ can be rewritten as:

$$\begin{aligned}
\tilde{\kappa}_{NS}(h, \alpha) &= 2 - (\mu_1(h, \alpha) + \mu_2(h, \alpha)), \\
&= 2 - (2 + h(\eta_1(h, \alpha) + \eta_2(h, \alpha))), \\
&= -h(\eta_1(h, \alpha) + \eta_2(h, \alpha)), \\
&= h^2\eta_1(h, \alpha)\eta_2(h, \alpha).
\end{aligned}$$

This allows us then to define

$$\kappa_{NS}(h, \alpha) := \eta_1(h, \alpha)\eta_2(h, \alpha),$$

$(h, \alpha) \in (-\rho, \rho) \times (-\delta, \delta)$. With this machinery, we are able to tackle the problem outlined at the beginning of the section. For this purpose, we will formulate several lemmata, which will help us to achieve the desired result. Throughout this analysis, we will make use of the fact that the eigenvalues of a matrix depend continuously on the coefficients of its characteristic polynomial, and for these coefficients depend continuously on the entries of the matrix, so do the eigenvalues (cf. [11, Section VI.1, VIII.2], [47, Section 10.6]). Thus, the eigenvalues λ_i, η_i, $i = 1, \ldots, N$ depend (at least) continuously on α, (h, α), respectively. Moreover, we will denote by τ_i, $i = 1, \ldots, N$, the eigenvalues of f_x^0, and without loss of generality, we assume $\tau_{1,2} = 0$, provided (1.1) possesses a BT_2 point at the origin. This clearly implies

$$\prod_{i=3}^{N} \tau_i \neq 0. \tag{1.40}$$

The first step of our analysis is to find smooth functions K_H, K_{NS} that could play the same role of κ_H, κ_{NS}, respectively. The reason for doing so is because it is not obvious the differentiability of κ_H, κ_{NS}, at least not in a general context, and our approach will require local Taylor expansions of these functions. This problem is solved by the following two lemmata:

Lemma 1.15. *Let system* (1.1) *undergo a generic* BT_2 *singularity at the origin. Then, there exists a positive constant* $\delta_1 \leq \delta$*, such that*

$$\operatorname{sgn}(K_H(\alpha)) = \operatorname{sgn}(\kappa_H(\alpha)),$$

for all $\alpha \in (-\delta_1, \delta_1)$*, where* $K_H(\alpha) := \varepsilon \det(f_x^H(\alpha))$*,* $\alpha \in (-\delta, \delta)$*,* $\varepsilon := \operatorname{sgn}\left(\prod_{i=3}^N \tau_i\right) \in \{-1, 1\}$.

Proof. Consider $\alpha \in (-\delta, \delta)$. Let us write $\det(f_x^H(\alpha))$ as

$$\det(f_x^H(\alpha)) = W(\alpha)\kappa_H(\alpha),$$

where $W : (-\delta, \delta) \to \mathbb{R}$ is given by

$$W(\alpha) := \prod_{i=3}^{N} \lambda_i(\alpha).$$

By the continuity of λ_i, $i = 1, \ldots, N$, (1.39), and (1.40), it follows

$$\lambda_{1,2}(0) = \tau_{1,2} = 0,$$

and

$$W(0) = \prod_{i=3}^{N} \lambda_i(0) = \prod_{i=3}^{N} \tau_i \neq 0.$$

This allows us to choose a positive constant $\delta_1' \leq \delta$, such that

$$W(\alpha) \neq 0,$$

for all $\alpha \in (-\delta_1', \delta_1')$, and it then follows

$$\operatorname{sgn}(W(\alpha)) = \operatorname{sgn}\left(\prod_{i=3}^{N} \tau_i\right) = \varepsilon,$$

for all $\alpha \in (-\delta_1', \delta_1')$. Thus, we can conclude that:

$$\begin{aligned} \operatorname{sgn}(K_H(\alpha)) &= \varepsilon \operatorname{sgn}(W(\alpha)) \operatorname{sgn}(\kappa_H(\alpha)), \\ &= \varepsilon^2 \operatorname{sgn}(\kappa_H(\alpha)), \\ &= \operatorname{sgn}(\kappa_H(\alpha)), \end{aligned}$$

for all $\alpha \in (-\delta_1', \delta_1')$. Finally, take $\delta_1 := \delta_1'$. □

Lemma 1.16. *Let a general one-step discretization method of order $p \geq 1$ applied to* (1.1) *be given by* (1.25). *Assume:*

(i) system (1.1) *has a generic BT_2 point at the origin,*

(ii) (1.25) *is standard,*

(iii) (1.25) *undergoes an $R1_2$ bifurcation at the origin, for all $0 < |h| < \rho_1$, $\rho_1 \leq \rho$,*

then, there exist positive constants $\delta_2 \leq \delta$, $\rho_2 \leq \rho_1$, such that

$$\operatorname{sgn}(K_{NS}(h,\alpha)) = \operatorname{sgn}(\kappa_{NS}(h,\alpha)),$$

for all $(h,\alpha) \in (-\rho_2,\rho_2)\times(-\delta_2,\delta_2)$, where $K_{NS}(h,\alpha) := \varepsilon \det(\Phi_x^{NS}(h,\alpha))$, $(h,\alpha) \in (-\rho,\rho)\times(-\delta,\delta)$, $\varepsilon := \operatorname{sgn}\left(\prod_{i=3}^{N}\tau_i\right) \in \{-1,1\}$.

Proof. Consider $(h,\alpha) \in (-\rho,\rho)\times(-\delta,\delta)$. Let us write $\det(\Phi_x^{NS}(h,\alpha))$ as

$$\det(\Phi_x^{NS}(h,\alpha)) = Q(h,\alpha)\kappa_{NS}(h,\alpha),$$

where $Q : (-\rho,\rho)\times(-\delta,\delta)\times\mathbb{R} \to \mathbb{R}$ is given by

$$Q(h,\alpha) := \prod_{i=3}^{N}\eta_i(h,\alpha).$$

By the continuity of η_i, $i = 1,\ldots,N$, (1.39), and (1.40), it follows

$$\eta_{1,2}(0,0) = \tau_{1,2} = 0,$$

and

$$Q(0,0) = \prod_{i=3}^{N}\eta_i(0,0) = \prod_{i=3}^{N}\tau_i \neq 0.$$

This allows us to choose positive constants $\delta_2' \leq \delta$, $\rho_2' \leq \rho_1$, such that

$$Q(h,\alpha) \neq 0,$$

for all $(h,\alpha) \in (-\rho_2',\rho_2')\times(-\delta_2',\delta_2')$, and it then follows

$$\operatorname{sgn}(Q(h,\alpha)) = \operatorname{sgn}\left(\prod_{i=3}^{N}\tau_i\right) = \varepsilon,$$

for all $(h,\alpha) \in (-\rho_2',\rho_2')\times(-\delta_2',\delta_2')$. Thus, we can conclude that:

$$\begin{aligned}\operatorname{sgn}(K_{NS}(h,\alpha)) &= \varepsilon\operatorname{sgn}(Q(h,\alpha))\operatorname{sgn}(\kappa_{NS}(h,\alpha)),\\ &= \varepsilon^2\operatorname{sgn}(\kappa_{NS}(h,\alpha)),\\ &= \operatorname{sgn}(\kappa_{NS}(h,\alpha)),\end{aligned}$$

for all $(h,\alpha) \in (-\rho_2',\rho_2')\times(-\delta_2',\delta_2')$. Finally, take $\delta_2 := \delta_2'$, and $\rho_2 := \rho_2'$. □

These two lemmata allow us to use the functions K_H, K_{NS}, instead of κ_H, κ_{NS}. Consequently, we are now able to use Taylor expansions in our approach. In this sense, the following lemma will characterize the first-order expansion of K_H, which will be of a great help in the proof of the main result.

Lemma 1.17. *Let system* (1.1) *undergo a generic* BT_2 *singularity at the origin. Then,*

$$K_H(\alpha) = K_H'(0)\alpha + \theta(\alpha)\alpha^2, \tag{1.41}$$

for all $\alpha \in (-\delta_1, \delta_1)$*, where* θ *is some smooth function, and* $K_H'(0) \neq 0$*.*

Proof. The assertion clearly amounts to showing that $K_H'(0) \neq 0$. Note that $K_H'(0)$ can be expressed as

$$K_H'(0) = \varepsilon \begin{pmatrix} (\det(f_x(x,\beta,\alpha)))_x^T \\ (\det(f_x(x,\beta,\alpha)))_\beta \\ (\det(f_x(x,\beta,\alpha)))_\alpha \end{pmatrix}^T_{(x,\beta,\alpha)=(0,0,0)} \begin{pmatrix} x_H'(0) \\ \beta_H'(0) \\ 1 \end{pmatrix}. \tag{1.42}$$

On the other hand, for the BT_2 point is a regular zero of (1.6), it holds

$$\begin{pmatrix} f_x(x,\beta,\alpha) & f_\beta(x,\beta,\alpha) & f_\alpha(x,\beta,\alpha) \\ g_x(x,\beta,\alpha) & g_\beta(x,\beta,\alpha) & g_\alpha(x,\beta,\alpha) \\ h_x(x,\beta,\alpha) & h_\beta(x,\beta,\alpha) & h_\alpha(x,\beta,\alpha) \end{pmatrix}_{(x,\beta,\alpha)=(0,0,0)} \begin{pmatrix} x_H'(0) \\ \beta_H'(0) \\ 1 \end{pmatrix} \neq 0,$$

where $g := \det(2f_x \odot I_N)$, $h := \det(f_x)$. However, since $(x_H(\alpha), \beta_H(\alpha), \alpha)$ solves (1.5), for all $\alpha \in (-\delta_1, \delta_1)$, it follows that the first $N+1$ elements of the above matrix product vanish. Consequently, $K_H'(0) \neq 0$. □

It is worth pointing out that Lemma 1.17 implies that K_H changes sign at $\alpha = 0$, and hence branches of Hopf points and neutral saddles emanate from the BT_2 singularity along C_H, as expected generically. With this preliminary discussion, we are ready to present the main result of this section, which is formulated in the following:

Theorem 1.18. *Let the assumptions of Lemma 1.16 be fulfilled. Then, there exist positive constants* $\bar{\rho}$*,* $\bar{\delta}$*, such that for all* $(h, \alpha) \in (-\bar{\rho}, \bar{\rho}) \times (-\bar{\delta}, \bar{\delta})$*, it holds*

$$\operatorname{sgn}(K_H(\alpha)) = \operatorname{sgn}(K_{NS}(h, \alpha)).$$

Proof. Choose $\bar{\rho}' := \rho_2$, $\bar{\delta}' := \min(\delta_1, \delta_2)$, and consider $(h, \alpha) \in (-\bar{\rho}', \bar{\rho}') \times (-\bar{\delta}', \bar{\delta}')$. By (1.38), K_{NS} can be expanded as follows

$$K_{NS}(h, \alpha) = K_H(\alpha) + \varrho(h, \alpha)h,$$

ϱ some smooth function. On the other hand, since the origin is an $\mathrm{R1}_2$ point of (1.25) for all $0 < |h| < \bar{\rho}'$, it follows

$$K_{NS}(h, 0) = \varrho(h, 0)h = 0,$$

for $0 < |h| < \bar{\rho}'$, thereby the expansion of K_{NS} can be written as

$$K_{NS}(h, \alpha) = K_H(\alpha) + \varrho_1(h, \alpha)h\alpha,$$

ϱ_1 some smooth function. Combining the above equation with (1.41), we arrive at

$$K_{NS}(h, \alpha) = \alpha(K'_H(0) + \theta(\alpha)\alpha + \varrho_1(h, \alpha)h).$$

Define

$$M_1 := \sup_{\alpha \in (-\bar{\delta}', \bar{\delta}')} |\theta(\alpha)|,$$

and

$$M_2 := \sup_{(h,\alpha) \in (-\bar{\rho}', \bar{\rho}') \times (-\bar{\delta}', \bar{\delta}')} |\varrho_1(h, \alpha)|.$$

Consider $(h, \alpha) \in (-\bar{\rho}'', \bar{\rho}'') \times (-\bar{\delta}'', \bar{\delta}'')$, with $\bar{\rho}'' := \min\left(\bar{\rho}', \frac{|K'_H(0)|}{3M_2}\right)$, $\bar{\delta}'' := \min\left(\bar{\delta}', \frac{|K'_H(0)|}{3M_1}\right)$, hence it follows:

$$\begin{aligned} |\theta(\alpha)\alpha + \varrho_1(h, \alpha)h| &\leq |\theta(\alpha)||\alpha| + |\varrho_1(h, \alpha)||h|, \\ &< \frac{|K'_H(0)|}{3} + \frac{|K'_H(0)|}{3}, \\ &= \frac{2|K'_H(0)|}{3}. \end{aligned}$$

Therefore, we can conclude that:

$$\begin{aligned} \operatorname{sgn}(K_H(\alpha)) &= \operatorname{sgn}(\alpha(K'_H(0) + \theta(\alpha)\alpha)), \\ &= \operatorname{sgn}(\alpha K'_H(0)), \\ &= \operatorname{sgn}(\alpha(K'_H(0) + \theta(\alpha)\alpha + \varrho_1(h, \alpha)h)), \\ &= \operatorname{sgn}(K_{NS}(h, \alpha)), \end{aligned} \tag{1.43}$$

for all $(h, \alpha) \in (-\bar{\rho}'', \bar{\rho}'') \times (-\bar{\delta}'', \bar{\delta}'')$. Finally, take $\bar{\rho} := \bar{\rho}''$ and $\bar{\delta} := \bar{\delta}''$. □

This theorem shows that the eigenvalues of the one-step method follow "correctly" the eigenvalues of the continuous-time system, for sufficiently small step-size, and in an small neighborhood of the BT_2 bifurcation, as illustrated in Figure 1.4. Moreover, by (1.43), it is seen that another function

that allows us to identify the nature of the pair of eigenvalues with zero sum along C_H may be defined as

$$\tilde{K}_H(\alpha) := \xi_0 \alpha,$$

for α sufficiently small, and $\xi_0 := K_H'(0)$ given by (1.42). This means that the sign of the coefficient $K_H'(0)$ completely determines how the branches of C_H (and consequently of C_{NS}) unfold at the BT_2 point.

1.6 Intersection of the discretized fold and Hopf curves

We conclude the theoretical part of this chapter with the analysis of the intersection of the discretized paths of fold and Hopf points. It is assumed that the continuous-time system (1.1) undergoes a generic BT_2 or FH point at the origin, and the system is discretized via general one-step methods. Throughout this section, we assume $\alpha \in \mathbb{R}^2$ to be the parameter of system (1.1).

Curves of fold and Hopf points are known to emanate from the mentioned codimension two singularities (see Sections 1.1.1, 1.1.2). Denote then these curves by $C_F, C_H : (-\epsilon, \epsilon) \to \mathbb{R}^{N+2}$. Generically, it is expected that the projections of C_F and C_H onto the parameter space intersect tangentially at the codimension two singularity (see Figures 1.1, 1.2). Likewise, C_F and C_H are known to intersect transversally (in full space $\mathbb{R}^{N+2}$) at the bifurcation. Thus, the question we are to take up is whether this generic behavior persists under general one-step methods, i.e., whether the discretized fold and Hopf curves intersect tangentially (resp. transversally) in parameter space (resp. in full space). In this sense, the genericity of the BT_2 and FH point (as explicitly defined in Sections 1.1.1, 1.1.2) will be shown to induce a generic intersection of the discretized curves. For the sake of completeness of our discussion, we will firstly prove that the defined genericity conditions indeed imply the expected generic intersection of C_F and C_H at the codimension two point. We accomplish this task in the following:

Theorem 1.19. *Let system* (1.1) *undergo a generic BT_2 or FH singularity at the origin. Then, there exist paths of fold and Hopf points of* (1.1) *which intersect transversally (resp. tangentially) at the codimension two point in full space (resp. parameter space).*

Proof. In the proof of Theorem 1.14, it was shown that the genericity of the

codimension two points, i.e., the invertibility of the following matrix

$$A^0 := \begin{pmatrix} f_x^0 & f_\alpha^0 \\ g_x^0 & g_\alpha^0 \\ h_x^0 & h_\alpha^0 \end{pmatrix},$$

where $g := \det(2f_x \odot I_N)$, $h := \det(f_x)$, implies the regularity of system (1.5) at the origin. Hence, we proved the existence of an emanating path of Hopf points. Similarly, for system (1.4) is also regular at the origin, the existence of a fold curve is guaranteed.

Thus, consider regular, smooth parametrizations of the fold and Hopf curves denoted by $C_F := (x_F, \alpha_F) : (-\epsilon, \epsilon) \to \mathbb{R}^N \times \mathbb{R}^2$, $C_H := (x_H, \alpha_H) : (-\epsilon, \epsilon) \to \mathbb{R}^N \times \mathbb{R}^2$, $\epsilon > 0$, respectively. The intersection of these curves can be found as the solution of the system

$$\begin{cases} f(x,\alpha) &= 0, \\ \det(2f_x(x,\alpha) \odot I_N) &= 0, \\ \det(f_x(x,\alpha)) &= 0, \end{cases}$$

which is, by assumption, regular at the origin, i.e., it possesses the isolated solution $(x, \alpha) = (0, 0)$. Thus, C_F and C_H intersect at the origin, and without loss of generality we assume $C_F(0) = C_H(0) = 0$. The next step is to show that these curves intersect tangentially in parameter space. Firstly, note that A^0 has full rank, i.e. $\operatorname{rank}(A^0) = N + 2$, thereby we must have $\operatorname{rank}\begin{pmatrix} f_x^0 & f_\alpha^0 \end{pmatrix} = N$. Recall that due to the codimension two point, f_x^0 has rank defect equal to 1, thus it holds

$$(a, b) := p_0^T f_\alpha^0 \neq 0,$$

where p_0 is a left eigenvector of f_x^0 corresponding to the eigenvalue equal to 0. Since C_F and C_H represent equilibria of (1.1), we can follow:

$$\begin{aligned} f(x_F(s), \alpha_F(s)) &= 0, \\ \Rightarrow f_x(x_F(s), \alpha_F(s))x'_F(s) + f_\alpha(x_F(s), \alpha_F(s))\alpha'_F(s) &= 0, \end{aligned}$$

for $s \in (-\epsilon, \epsilon)$, and by evaluating the above expression at $s = 0$, we arrive at

$$f_x^0 x'_F(0) + f_\alpha^0 \alpha'_F(0) = 0.$$

Likewise, we can show

$$f_x^0 x'_H(0) + f_\alpha^0 \alpha'_H(0) = 0.$$

By multiplying both sides of the above equations by the left by p_0^T, we obtain

$$(a,b)\alpha_F'(0) = (a,b)\alpha_H'(0) = 0,$$

which implies that α_F, α_H are tangential at the origin, and furthermore the common tangent vector may be given by $(-b,a)^T = (-p_0^T f_{\alpha_2}^0, p_0^T f_{\alpha_1}^0)^T$. It is left to show that C_F and C_H intersect transversally in full space. By the contrary, suppose that this is not true, namely, there exists a nonzero constant K, such that

$$C_F'(0) = KC_H'(0).$$

Since C_F, C_H are solutions of (1.4), (1.5), respectively, it follows

$$\begin{pmatrix} f_x^0 & f_\alpha^0 \\ g_x^0 & g_\alpha^0 \end{pmatrix} C_H'(0) = 0,$$

and

$$\begin{pmatrix} f_x^0 & f_\alpha^0 \\ h_x^0 & h_\alpha^0 \end{pmatrix} C_F'(0) = 0,$$

but since $C_F'(0) = KC_H'(0)$ holds, we conclude that

$$\begin{pmatrix} f_x^0 & f_\alpha^0 \\ g_x^0 & g_\alpha^0 \\ h_x^0 & h_\alpha^0 \end{pmatrix} C_F'(0) = 0,$$

which contradicts the invertibility of A^0. Thus, C_F and C_H intersect transversally at the origin. □

It is worth having presented the above discussion, for a similar approach will be applied for proving the main result of this section, namely, the generic intersection of the discretized fold and Hopf curves. Roughly speaking, we will see that genericity "persists" under general one-step methods, although we have not formally defined genericity of codimension two points in discrete-time systems, and that topic will not be discussed in detail in the present work. So, the main result of this section is presented in the following:

Theorem 1.20. *Let a general one-step discretization method of order $p \geq 1$ applied to* (1.1) *be given by* (1.25). *Assume:*

(i) (1.25) *is standard,*

(ii) system (1.1) *has a generic BT_2 or FH point at the origin.*

Further, let

$$\begin{aligned} C_F := (x_F, \alpha_F) &: (-\rho, \rho) \times (-\epsilon, \epsilon) \to \mathbb{R}^N \times \mathbb{R}^2, \\ C_{NS} := (x_{NS}, \alpha_{NS}) &: (-\rho, \rho) \times (-\epsilon, \epsilon) \to \mathbb{R}^N \times \mathbb{R}^2, \end{aligned}$$

with $\epsilon > 0$, $0 < \rho \leq h_0$ (so that the conclusions of Theorems 1.13 and 1.14 hold), and $C_F(0,0) = C_{NS}(0,0) = 0$, be smooth, regular parametrizations of the curves of fold and Neimark-Sacker points of (1.25)*, respectively. Then, C_F and C_{NS} intersect transversally (resp. tangentially) at the discretized codimension two point in full space (resp. parameter space) for all $h \in (-\rho, \rho)$.*

Some remarks before presenting the proof of this theorem are in order. We have seen that a BT_2 point persists at the same position under general Runge-Kutta methods, and they are turned into a $\mathrm{R1}_2$ point by the method, provided the step-size is sufficiently small. However, under general p-th order one-step methods, it can be shown that a BT_2 point is smoothly $O(h^p)$-shifted. In fact, the very same arguments as those used in Theorem 1.13 can be employed in order to show this assertion. Therefore, in the proof of Theorem 1.20, we will not assume that the one-step method preserves a BT_2 point at the same position. Moreover, the existence of a curve of discretized fold points can be deduced as in the Hopf case (cf. Theorem 1.14), and similarly, we will not assume that this curve remains at the same position, as it happens under general Runge-Kutta methods (see the introduction of the chapter). The reason for doing so is that in this way, we can cover simultaneously the two cases, i.e. BT_2 and FH bifurcations. Particular results (e.g. when dealing with Runge-Kutta methods) will be of course consistent with and covered by the general approach we are to employ. With these few remarks, we are ready to present:

Proof of Theorem 1.20. We will firstly show that the curves C_F and C_{NS} actually intersect at the discretized codimension two point. This point, at which the curves intersect, can be found as a solution of

$$\left\{ \begin{array}{rcl} E(h, x, \alpha) &=& 0, \\ H(h, x, \alpha) &=& 0, \\ F(h, x, \alpha) &=& 0, \end{array} \right. \tag{1.44}$$

where $E : (-\rho, \rho) \times \bar{\Omega} \times \bar{\Lambda} \to \mathbb{R}^N$, $H, F : (-\rho, \rho) \times \bar{\Omega} \times \bar{\Lambda} \to \mathbb{R}$ are defined

by

$$\begin{aligned} E(h,x,\alpha) &:= \frac{1}{h}(\psi^h(x,\alpha)-x), \\ H(h,x,\alpha) &:= \det\left(\frac{1}{h}(\psi^h_x(x,\alpha)\odot\psi^h_x(x,\alpha)-I_m)\right), \\ F(h,x,\alpha) &:= \det\left(\frac{1}{h}(\psi^h_x(x,\alpha)-I_N)\right), \end{aligned}$$

(cf. (1.28)). In the proof of Theorem 1.13, we saw that system (1.44) has for every $h \in (-\rho,\rho)$ a unique solution $(x_0(h),\alpha_0(h))$ (which in this case represent an FN or an $R1_2$ point of (1.25)). Thus, it follows that C_F and C_{NS} intersect at this point, and without loss of generality, we suppose that for every $h \in (-\rho,\rho)$ there exists $\tilde{s}_h, \bar{s}_h \in (-\epsilon,\epsilon)$, such that $C_F(h,\tilde{s}_h) = C_{NS}(h,\bar{s}_h) = (x_0(h),\alpha_0(h))$. Next, we will see that C_F and C_{NS} intersect tangentially in parameter space.

In what follows, we carry out the analysis for $h \neq 0$, since at $h = 0$ the conclusions of the theorem clearly hold. This is readily seen by noticing that the curves C_F, C_{NS} converge uniformly to their continuous counterpart (see estimate (1.31)), thereby for $h = 0$ the conclusions of the present theorem already follow from Theorem 1.19.

Recall that the curves C_F, C_{NS} represent equilibria of (1.25), thus it holds

$$E(h,x_F(h,s),\alpha_F(h,s)) = 0,$$

and hence[4]

$$E_x(h,x_F(h,s),\alpha_F(h,s))x'_F(h,s) + E_\alpha(h,x_F(h,s),\alpha_F(h,s))\alpha'_F(h,s) = 0,$$

for all $(h,s) \in (-\rho,\rho)\times(-\epsilon,\epsilon)$, and by evaluating the above expression at $s = \tilde{s}_h$, we arrive at

$$E_x(h,x_0(h),\alpha_0(h))x'_F(h,\tilde{s}_h) + E_\alpha(h,x_0(h),\alpha_0(h))\alpha'_F(h,\tilde{s}_h) = 0. \quad (1.45)$$

Likewise, we can show

$$E_x(h,x_0(h),\alpha_0(h))x'_{NS}(h,\bar{s}_h) + E_\alpha(h,x_0(h),\alpha_0(h))\alpha'_{NS}(h,\bar{s}_h) = 0. \quad (1.46)$$

Note that for every $0 < |h| < \rho$ there exists a nonzero vector $p_{0h} \in \mathbb{R}^N$, such that

$$p_{0h}^T E_x(h,x_0(h),\alpha_0(h)) = 0,$$

[4]Throughout this discussion, the symbol $'$ means derivative with respect to s.

since $E_x(h, x_0(h), \alpha_0(h))$ has rank defect equal to 1 (see the third equation in (1.44)). Furthermore, due to the invertibility of (for $(x_0(h), \alpha_0(h))$ is a regular zero of (1.44))

$$A^0(h) := \begin{pmatrix} E_x(h, x_0(h), \alpha_0(h)) & E_\alpha(h, x_0(h), \alpha_0(h)) \\ H_x(h, x_0(h), \alpha_0(h)) & H_\alpha(h, x_0(h), \alpha_0(h)) \\ F_x(h, x_0(h), \alpha_0(h)) & F_\alpha(h, x_0(h), \alpha_0(h)) \end{pmatrix},$$

it follows that $\operatorname{rank}\left(\begin{pmatrix} E_x(h, x_0(h), \alpha_0(h)) & E_\alpha(h, x_0(h), \alpha_0(h)) \end{pmatrix}\right) = N$, for all $h \in (-\rho, \rho)$. Consequently, it holds

$$(a_h, b_h) := p_{0h}^T E_\alpha(h, x_0(h), \alpha_0(h)) \neq 0,$$

for all $0 < |h| < \rho$. By multiplying both sides of (1.45) and (1.46) by the left by p_{0h}^T, we obtain

$$(a_h, b_h)\alpha'_F(h, \tilde{s}_h) = (a_h, b_h)\alpha'_{NS}(h, \bar{s}_h) = 0,$$

which implies that α_F and α_{NS} meet tangentially at $\alpha = \alpha_0(h)$, for all $0 < |h| < \rho$. It remains to show the transversal intersection of the curves in full space. By the contrary, suppose that this is not true, namely, there exists a $0 \neq h_c \in (-\rho, \rho)$, and a nonzero constant K, such that

$$C'_F(h_c, \tilde{s}_{h_c}) = KC'_{NS}(h_c, \bar{s}_{h_c}).$$

Since C_F, C_H are solutions of

$$\begin{cases} E(h, x, \alpha) &= 0, \\ F(h, x, \alpha) &= 0, \end{cases}$$

and

$$\begin{cases} E(h, x, \alpha) &= 0, \\ H(h, x, \alpha) &= 0, \end{cases}$$

respectively, it follows

$$\begin{pmatrix} E_x(h_c, x_0(h_c), \alpha_0(h_c)) & E_\alpha(h_c, x_0(h_c), \alpha_0(h_c)) \\ F_x(h_c, x_0(h_c), \alpha_0(h_c)) & F_\alpha(h_c, x_0(h_c), \alpha_0(h_c)) \end{pmatrix} C'_F(h_c, \tilde{s}_{h_c}) = 0,$$

and

$$\begin{pmatrix} E_x(h_c, x_0(h_c), \alpha_0(h_c)) & E_\alpha(h_c, x_0(h_c), \alpha_0(h_c)) \\ H_x(h_c, x_0(h_c), \alpha_0(h_c)) & H_\alpha(h_c, x_0(h_c), \alpha_0(h_c)) \end{pmatrix} C'_{NS}(h_c, \bar{s}_{h_c}) = 0,$$

but since $C'_F(h_c, \tilde{s}_{h_c}) = KC'_{NS}(h_c, \bar{s}_{h_c})$ holds, we conclude that

$$\begin{pmatrix} E_x(h_c, x_0(h_c), \alpha_0(h_c)) & E_\alpha(h_c, x_0(h_c), \alpha_0(h_c)) \\ H_x(h_c, x_0(h_c), \alpha_0(h_c)) & H_\alpha(h_c, x_0(h_c), \alpha_0(h_c)) \\ F_x(h_c, x_0(h_c), \alpha_0(h_c)) & F_\alpha(h_c, x_0(h_c), \alpha_0(h_c)) \end{pmatrix} C'_F(h_c, \tilde{s}_{h_c}) = 0,$$

which contradicts the invertibility of $A^0(h_c)$. Thus, C_F and C_{NS} intersect transversally at $(x_0(h), \alpha_0(h))$ for all $0 < |h| < \rho$. □

1.7 Numerical examples

In this section, our aim is to numerically illustrate the main results obtained in this chapter. For this purpose, we consider the following continuous-time, dimensionless system:

$$\begin{aligned} \dot{x} &= -\left(\frac{\beta+\alpha}{R}\right)x + \frac{\alpha}{R}y - \frac{C}{R}x^3 + \frac{D}{R}(y-x)^3 - \frac{E}{R}x^5 + \frac{F}{R}(y-x)^5, \\ \dot{y} &= \alpha x - (\alpha+G)y - z - D(y-x)^3 - Hy^3 - F(y-x)^5 - Iy^5, \quad (1.47) \\ \dot{z} &= y, \end{aligned}$$

with state variables $(x, y, z) \in \mathbb{R}^3$, and parameters $\beta, \alpha, C, D, E, F, G, H, I$, $R \in \mathbb{R}$, $R > 0$. This system describes the dynamics of a modified van der Pol-Duffing oscillator. A thorough analysis of this oscillator concerning both local, as well as global phenomena can be found in [1], [25]. In these articles, the authors provide a physical analysis of the oscillator's circuit, which is modeled by system (1.47), and furthermore, a stratification of the parameter space via eigenvalue analysis is given. A more general discussion concerning the dynamics of this type of circuits can be found in [43, Chapter 7].

Throughout this section, we assume β, α to be our bifurcation parameters, and we let $C = 1$, $D = -5$, $E = 1$, $F = 1$, $G = -1.5$, $H = 1$, $I = 1$, $R = 3$ fixed. Moreover, the numerical computations will be performed with the continuation software CONTENT ([45]). In some cases, the numerical data will be exported to MATLAB for further numerical manipulations.

1.7.1 Persistence of BT_2 points

We begin our numerical experiments by showing that BT_2 points persist at the same position, and that they are turned into $R1_2$ points under Runge-Kutta methods (cf. Theorem 1.6). For this purpose, we will firstly find a BT_2 point for system (1.47). We choose $(x_{ini}, y_{ini}, z_{ini}) = (0, 0.5, 0)$, $(\beta_{ini}, \alpha_{ini}) = (-8, 9.5)$ as initial data for the continuation of equilibria, and we then let β freely vary. The thus obtained curve is plotted in Figure 1.6. With this procedure, we found: three neutral saddles, two Hopf points, one fold, and one branching point, labeled by NTS, H, LP, and BP, respectively. The next step is to switch to a codimension one singularity that could lead us to the BT_2 we are looking for, that is, to switch to an NTS, H, or LP point. For this purpose, we note that according to Figure 1.6, an NTS and an LP point lie very close to each other, which gives rise to the possibility that a fold and a Hopf curve could be emanating from the same codimension two singularity (either a BT_2 or an FH point). Thus, we switch to the NTS point that lies

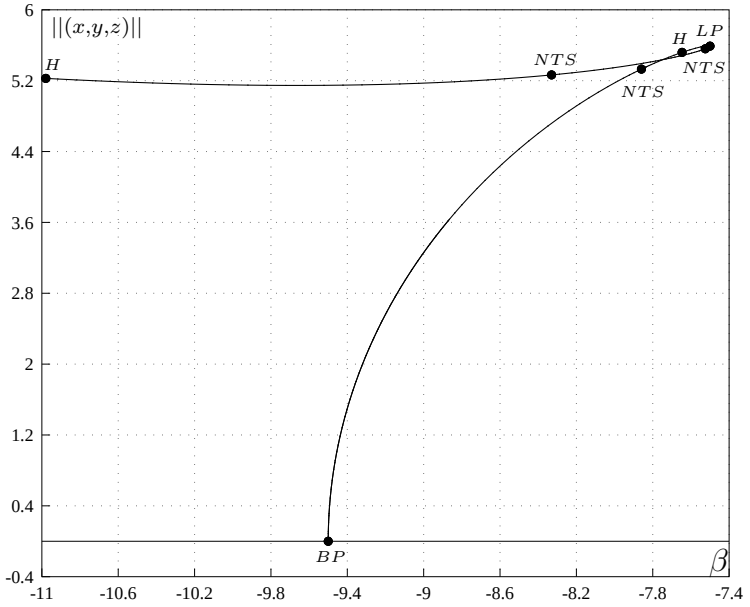

Fig. 1.6: Continuation of equilibria of (1.47) for $\alpha = 9.5$ fixed.

close to LP, which is located at $(x_{NTS}, y_{NTS}, z_{NTS}) \approx (-1.0541, 0, -5.459)$, $(\beta_{NTS}, \alpha_{NTS}) \approx (-7.5247, 9.5)$. The continuation of the neutral saddle curve is shown in Figure 1.7. Along this curve, we found a BT_2 and a generalized Hopf point, labeled by BT_2, GH, respectively. The BT_2 point is then located at $(x_{BT}, y_{BT}, z_{BT}) = (-1, 0, -4.26794919243109)$, $(\beta_{BT}, \alpha_{BT}) = (-6.26794919243109, 8.26794919243109)$, and with normal form coefficients $a = 0.412535$, $b = -4.19772$. This is the information of the continuous-time system we were after.

The next part of the experiment is to discretize system (1.47) by a Runge-Kutta method in order to see whether the BT_2 point found is actually preserved by the method. For this purpose, we choose the 3-th order method of Runge (cf. [36]) with an initial step-size $h_0 = 0.13$. By using the same procedure and initial data as that used for the continuous-time system, we obtain a curve of equilibria of the one-step method, which is shown in Figure 1.8. Similarly, we found: three neutral saddles, two Neimark-Sacker points, one fold, and one branching point, labeled by NTS, NS, LP, and BP, respectively. Then, we switch to the NTS point closest to LP, which is located at $(\tilde{x}_{NTS}, \tilde{y}_{NTS}, \tilde{z}_{NTS}) \approx (-1.0541, 0, -5.459)$, $(\tilde{\beta}_{NTS}, \tilde{\alpha}_{NTS}) \approx (-7.5247, 9.5)$, and then we continue this point with respect to β and α. The obtained curve is plotted in Figure 1.9. Along this curve, we found an $\mathrm{R1}_2$ and a degenerate Neimark-Sacker point, labeled by $R1_2$, DN, respectively. The

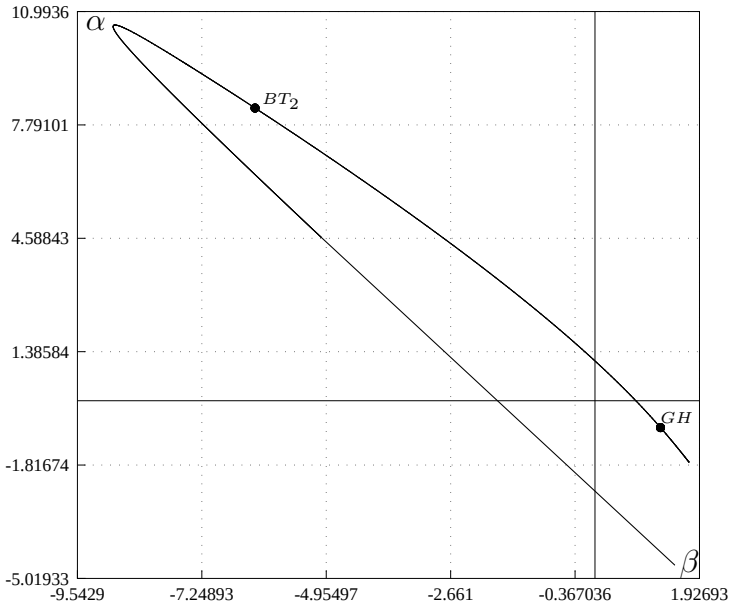

Fig. 1.7: Continuation of the neutral saddle curve of (1.47).

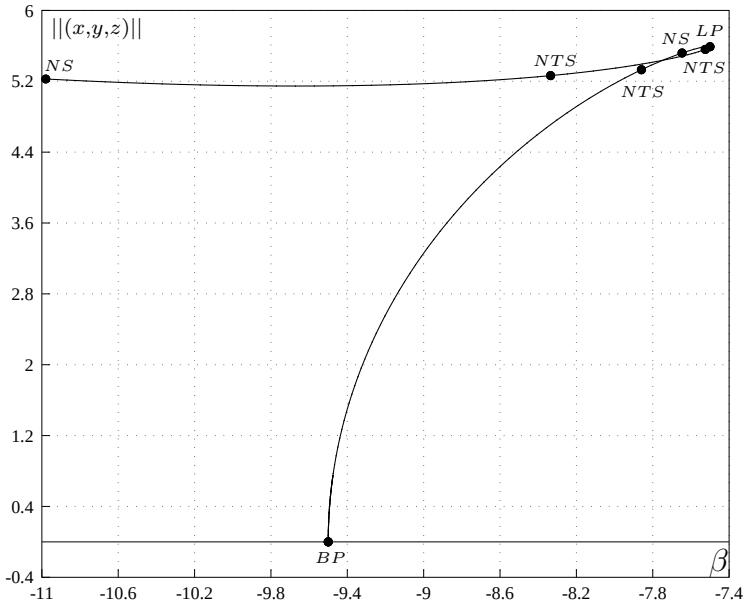

Fig. 1.8: Continuation of equilibria of the one-step method for $\alpha = 9.5$ fixed.

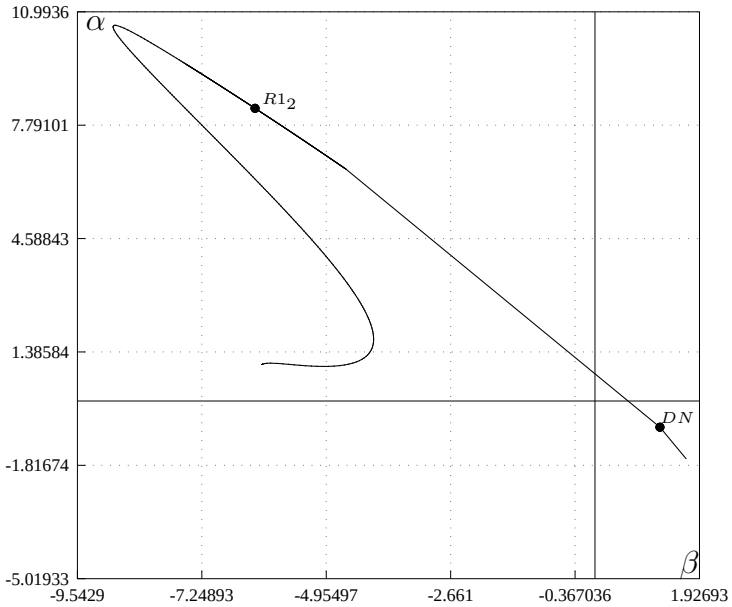

Fig. 1.9: Continuation of the neutral saddle curve of the one-step method.

$\mathrm{R1}_2$ point is then located at $(x_{R1}, y_{R1}, z_{R1}) = (-1, 0, -4.26794919243116)$, $(\beta_{R1}, \alpha_{R1}) = (-6.26794919243116, 8.26794919243116)$, and with normal form coefficients $\tilde{a} = 0.00697184$, $\tilde{b} = -0.546982$. Note that this point lies very close to the BT_2 point obtained for the continuous-time system. The next step is to investigate how the $\mathrm{R1}_2$ point of the one-step method is affected as we vary the step-size. For this purpose, we define the distance function

$$\begin{aligned} Dist_{BT}(h) \;:=\; & ||(x_{R1}(h), y_{R1}(h), z_{R1}(h), \beta_{R1}(h), \alpha_{R1}(h)) \\ & -(x_{BT}, y_{BT}, z_{BT}, \beta_{BT}, \alpha_{BT})||, \end{aligned}$$

for $h > 0$ small, and $||\cdot||$ represents the Euclidean norm. The result is shown in Figure 1.10. In this picture, we let the step-size vary from $h = 0.05$ to $h = 0.3$, but we plotted the logarithm of the variables in order to detect any evidence of an $O(h^p)$-shift of the BT_2 point. However, no such evidence appeared but the distance remained always below the tolerance used for the computations, which allows us to confirm the prediction of Theorem 1.6, i.e., that the BT_2 point persists at the same position under Runge-Kutta methods.

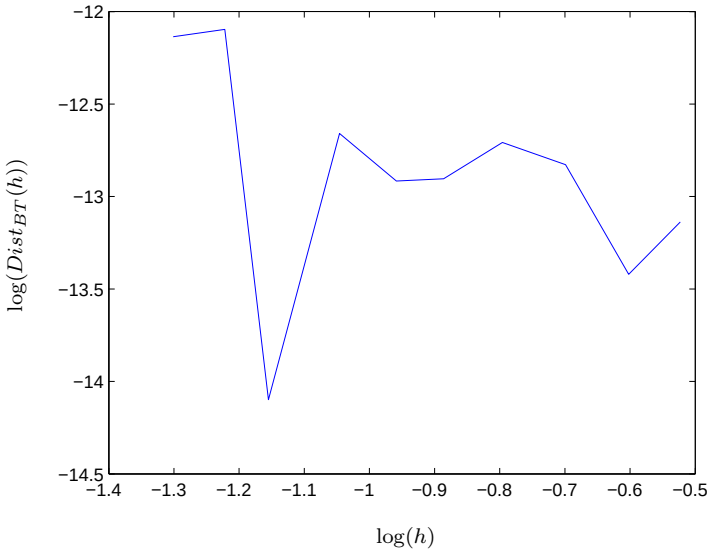

Fig. 1.10: Distance between BT_2 and $R1_2$ points for different values of step-size.

1.7.2 $O(h^p)$-shift of FH points

In this experiment, our purpose is to illustrate the theoretical result obtained in Section 1.4, namely, we want to observe whether FH points are $O(h^p)$-shifted and turned into FN points by p-th order methods (cf. Theorem 1.13). To achieve this, we need firstly to find an FH point of system (1.47). As we saw in the previous example, curves of fold and Hopf points are close to each other, and thus, a BT_2 point was encountered. However, in Figure 1.7, we observed that along the curve of neutral saddles no FH point is detected. Therefore, we will rather switch from the BT_2 singularity to the path of fold points, and then we will try to find an FH singularity along this curve. The continuation of the fold curve is shown in Figure 1.11. Thus, we find an FH point at $(x_{FH}, y_{FH}, z_{FH}) = (-1, 0, -7.5)$, $(\beta_{FH}, \alpha_{FH}) = (-9.5, 11.5)$. Furthermore, we also encountered two BT_2 points; one of them corresponds to that found in the previous example. Next, we discretize again system (1.47) by Runge's method, and then we try to find an FN point of the one-step map. In Figure 1.12, we show the continuation of the fold curve emanating from the $R1_2$ point found in the previous example. Along this curve, we detected an FN point at $(x_{FN}, y_{FN}, z_{FN}) = (-1, 0, -7.50001140949743)$, $(\beta_{FN}, \alpha_{FN}) = (-9.50001140949743, 11.5000114094974)$, which lies close to the FH point encountered before. Additionally, we found two $R1_2$ points;

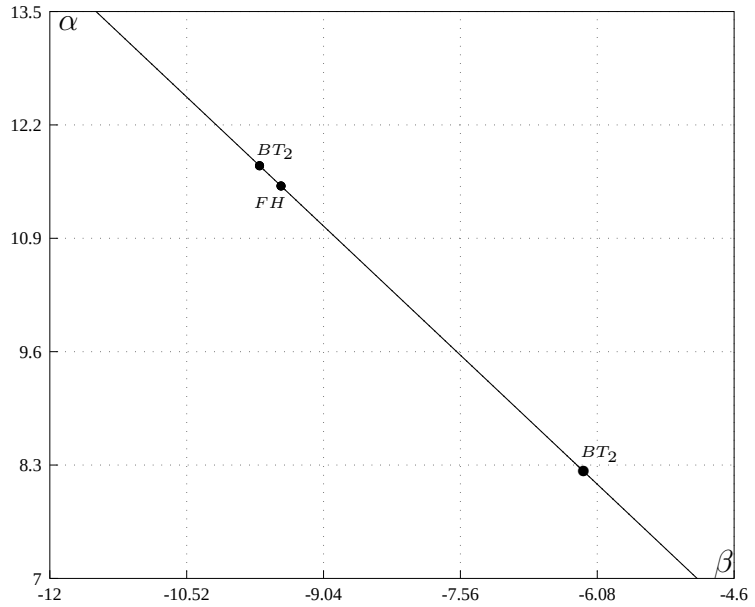

Fig. 1.11: Continuation of the fold curve of (1.47).

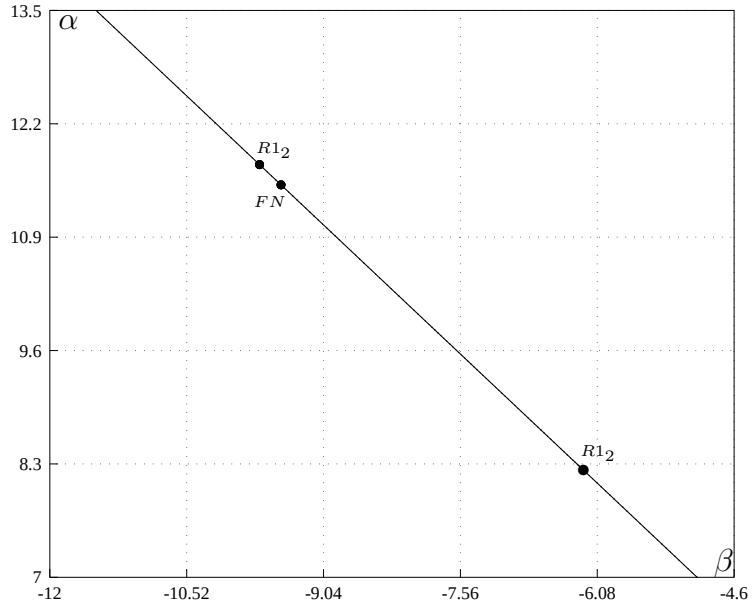

Fig. 1.12: Continuation of the fold curve of the one-step method.

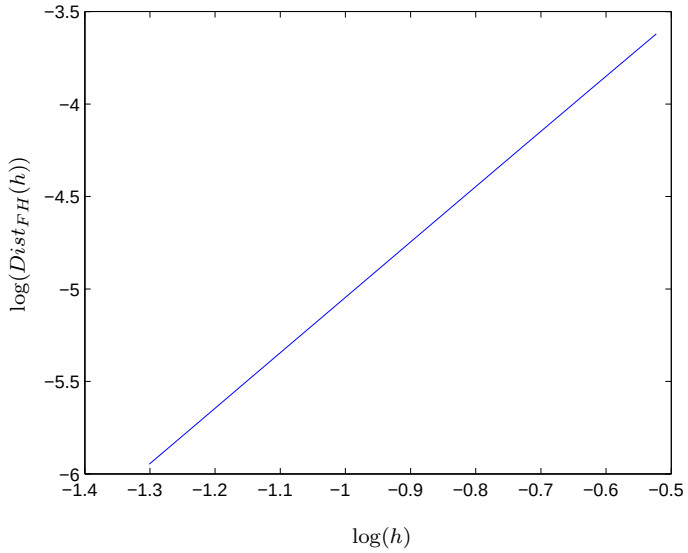

Fig. 1.13: Distance between FH and FN points for different values of step-size.

one of them corresponds to that detected in the previous example. The next step is to investigate how this FN point is affected under variation of the step-size. To accomplish this, we define the distance function

$$\begin{aligned} Dist_{FH}(h) \;:=\; & ||(x_{FN}(h), y_{FN}(h), z_{FN}(h), \beta_{FN}(h), \alpha_{FN}(h)) \\ & -(x_{FH}, y_{FH}, z_{FH}, \beta_{FH}, \alpha_{FH})||, \end{aligned}$$

for $h > 0$ small, and $||\cdot||$ represents again the Euclidean norm. Figure 1.13 shows the behavior of $Dist_{FH}$ with respect to the step-size. In contrast to the previous example, we do find in this case an $O(h^p)$-shift of the FH point, whose order can be estimated by the slope of the quasi-straight line obtained. This slope is $m \approx 2.9931 \approx 3$, which is consistent with Theorem 1.13.

It is worth noting that the fold curve of the one-step method is the same as the one for system (1.47) (see the introduction of the Chapter), however, we observed that the FN point is always $O(h^p)$-far from the FH point, which means that the FN singularity moves along the (discretized) fold curve, as the step-size varies.

1.7.3 Discretized Hopf curve

The purpose of this experiment is to numerically illustrate the result obtained in Section 1.5.1. That is, we want to observe whether the emanating path of

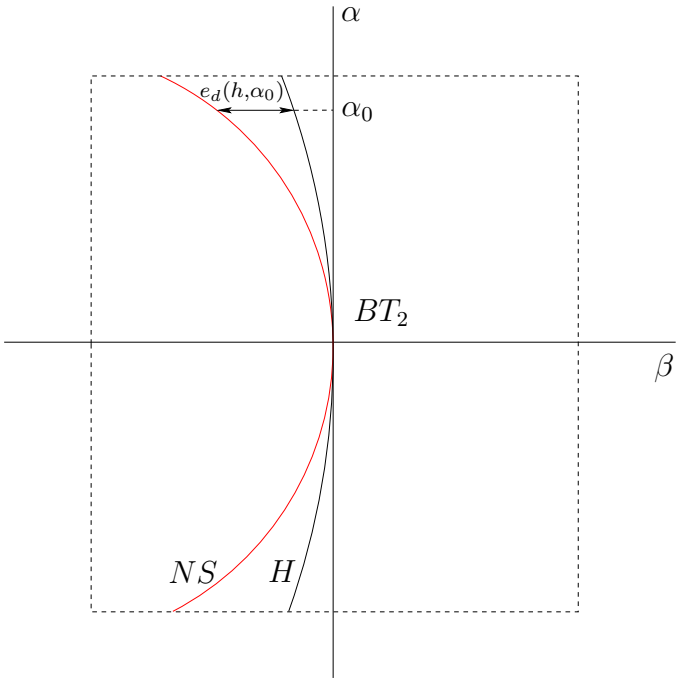

Fig. 1.14: Interpretation of the distance function on parameter space.

Hopf points is $O(h^p)$-shifted by one-step methods. In particular, we will deal with the Hopf curve that emanates from the BT_2 point found in Section 1.7.1. As in the previous examples, we will discretize system (1.47) via Runge's method. Under notation of Theorem 1.14, we define the following distance function

$$Dist_H(h,\alpha) := ||d_{NS}(h,\alpha) - d_H(\alpha)||,$$

for $h > 0$, $|\alpha - \alpha_{BT}|$ small, and $||\cdot||$ represents, as before, the Euclidean norm. Thus, our aim is to investigate the behavior of $Dist_H$, as (h,α) vary. In Figure 1.14, we illustrate the meaning of the above distance function. In this picture, e_d represents the β-component of $Dist_H$. By repeatedly fixing α from $\alpha = 7.41663851586445$ to $\alpha = 9.09659824492632$, and letting h vary from $h \approx 0.05$ to $h = 0.3$, for each α fixed, we obtained a surface plot of $Dist_H$ which is shown in Figure 1.15. In this picture, two facts draw special attention. Firstly, recall that the singularity, i.e. the BT_2 point, is located along the line $\alpha = \alpha_{BT} \approx 8.26$. Thus, it is observed that $Dist_H(h,\alpha)$ tends to zero, as α tends to the singularity, regardless h. This fact is analytically seen in (1.36), and schematically seen in Figure 1.14. Secondly, it is also noted that $Dist_H(h,\alpha)$ tends to zero, as h tends to zero, regardless α, which means that $Dist_H$ is uniformly bounded, however, we do not know to which order

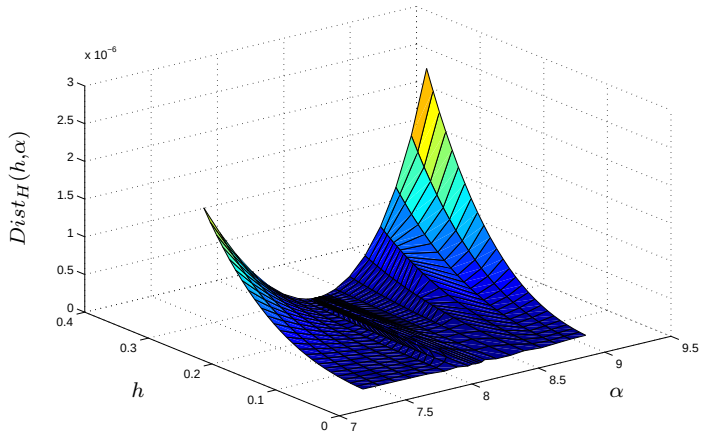

Fig. 1.15: Behavior of $Dist_H$ with respect to (h, α).

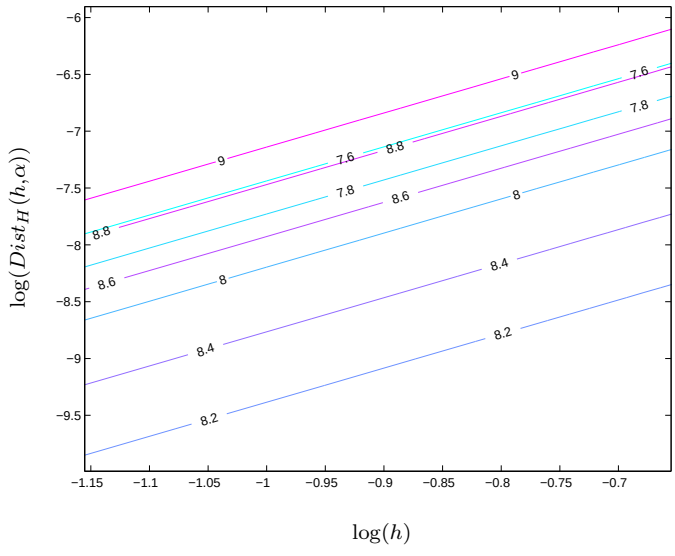

Fig. 1.16: Behavior of $Dist_H$ with respect to h, for several, fixed α's.

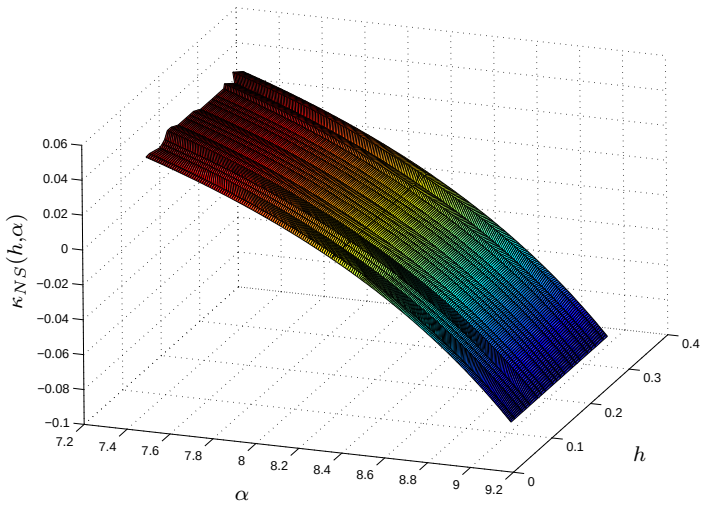

Fig. 1.17: Behavior of κ_{NS} with respect to (h, α).

can this function be bounded. For determining the order, we will analyze the behavior of $Dist_H$ with respect to h, for several, fixed α's. In Figure 1.16, this behavior is shown. In this picture, we plotted the logarithm of the variables, so that we can determine the order as the slope of the quasi-straight lines obtained. The labels on the lines represent, approximately, the fixed value of α used. Thus, it is seen that the slope of the lines are approximately the same, that is, $m \approx 3.0029 \approx 3$, which is consistent with Theorem 1.14.

Moreover, it is worth taking this experiment to also illustrate the main result of Section 1.5.2, i.e., we will try to verify whether the branches of the Neimark-Sacker curve of the one-step method discretize "correctly" the branches of the Hopf curve of system (1.47). More precisely, under notation of Section 1.5.2, we will numerically see whether the following relation is satisfied

$$\operatorname{sgn}(\kappa_H(\alpha)) = \operatorname{sgn}(\kappa_{NS}(h, \alpha)),$$

for $h > 0$, $|\alpha - \alpha_{BT}|$ small (cf. Theorem 1.18). Thus, we fix repeatedly h from $h = 0.05$ to $h = 0.3$, and let α vary from $\alpha \approx 7.4$ to $\alpha = 9.1$, for each h fixed. As we do so, we evaluate κ_{NS} at each pair (h, α), and thereby we obtain Figure 1.17. In this picture, it can be seen that κ_{NS} changes sign at $\alpha = \alpha_{BT} \approx 8.26$, regardless h, which means that the $\alpha < \alpha_{BT}$- (resp. $\alpha > \alpha_{BT}$-) branch of C_{NS} corresponds to Neimark-Sacker points (resp. neutral saddles). Next, let us check whether the Hopf curve also presents this

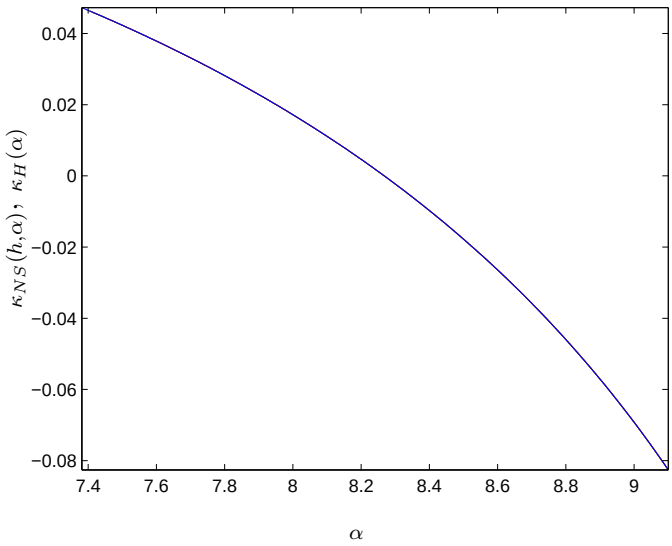

Fig. 1.18: Behavior of κ_H, κ_{NS} with respect to α, for several, fixed h's.

behavior. For this purpose, we will plot κ_H and κ_{NS}, for several, fixed h's. The result is shown in Figure 1.18. In this picture, it can be noted that the $\kappa_{NS}(h,\cdot)$'s lie very close to κ_H. In order to see that κ_H and the $\kappa_{NS}(h,\cdot)$'s actually change sign at the same point $\alpha = \alpha_{BT}$, let us plot an enlargement of Figure 1.18 near the singularity. The result is presented in Figure 1.19. In this picture, we can distinguish two lines; the one labeled by A correspond to κ_H, and the $\kappa_{NS}(h,\cdot)$'s are grouped in the line labeled by B. Thereby, we observe that the conclusion of Theorem 1.18 is verified in this example.

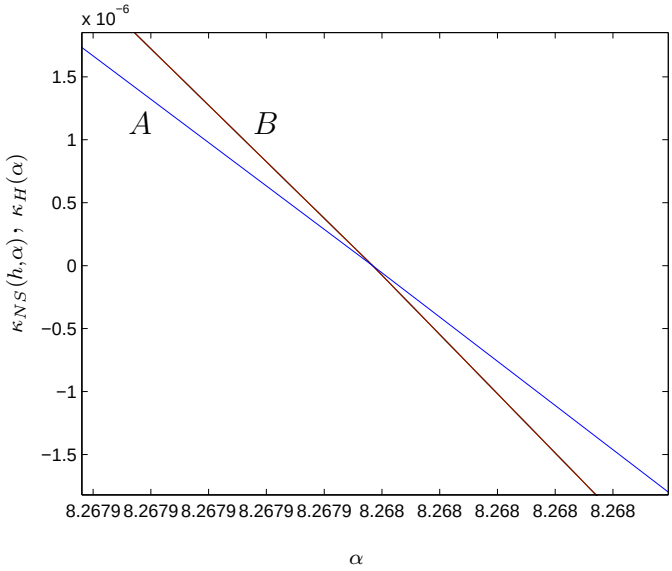

Fig. 1.19: Behavior of κ_H, κ_{NS} with respect to α, for several, fixed h's (enlargement of a region around the singularity).

Chapter 2

Numerical analysis of homoclinic tangencies near $\mathrm{R1}_2$ points

> "Everything should be made as simple as possible, but not simpler"
> Albert Einstein

In the previous chapter, our attention was devoted to the local analysis of continuous-time systems under discretizations. In particular, we proved that BT_2 points are turned into $\mathrm{R1}_2$ points by Runge-Kutta methods. The local bifurcation diagram was shown to be preserved up to an $O(h^p)$-shift of the Hopf curve by one-step methods of order $p \geq 1$. Moreover, it is well-known that a curve of homoclinic orbits emanates from a BT_2 point, however, the effect of one-step methods on the whole homoclinic curve is not completely understood yet. Nevertheless, if we consider just one point on the homoclinic curve, with one parameter fixed, then the effect of discretization methods is largely analyzed in [9, 24]. On the other hand, the presence of discrete homoclinic orbits near $\mathrm{R1}_2$ points is well-known. This fact can be proven via flow interpolation (cf. Section 1.2.1 and Lemma 1.4).

In this chapter, we want to perform a numerical analysis of the discrete homoclinic orbits emanating from $\mathrm{R1}_2$ points. The main result will be a theory-based procedure for starting the continuation of tangential homoclinic orbits from an $\mathrm{R1}_2$ point. With this procedure we will be able to quantitatively explore the homoclinic structure in various examples. In particular, we

devote special attention to the normal form of the $1:1$ resonance, since this is qualitatively the core of any discrete system undergoing such singularity.

This chapter is organized in the following way. In the first section, we formally define the objects we will deal with, and also mention the already known, related numerical methods, which will be largely used throughout the numerical examples. The subsequent sections are devoted to developing the theory-based starting procedure. As the homological equation will be one of the main tools for the derivation of the starting procedure, we will dedicate a complete section to discussing several aspects of it. Then, we apply the procedure to several examples, in particular to the normal form of the $1:1$ resonance.

2.1 Theoretical and numerical background

Let $f(\cdot,\alpha)$, $f \in C^k(\mathbb{R}^N \times \mathbb{R}^p, \mathbb{R}^N)$, $k \geq 1$, be a diffeomorphism for all $\alpha \in \mathbb{R}^p$. Throughout this section, we consider the discrete-time system

$$x \mapsto f(x,\alpha). \tag{2.1}$$

Definition 2.1. *Suppose that $\xi \in \mathbb{R}^N$ is a hyperbolic equilibrium of (2.1) at $\alpha = \alpha_0$. An orbit $x_{\mathbb{Z}} \in \left(\mathbb{R}^N\right)^{\mathbb{Z}}$ of (2.1) is referred to as homoclinic with respect to ξ (in short homoclinic) if*

$$\lim_{n\to\pm\infty} x_n = \xi.$$

The main objects of study in this chapter are tangential homoclinic orbits, which are formally defined as follows:

Definition 2.2. *A homoclinic orbit $x_{\mathbb{Z}} \in \left(\mathbb{R}^N\right)^{\mathbb{Z}}$ of (2.1) is referred to as r-tangential, r some nonnegative integer, if the homogeneous difference equation*

$$u_{n+1} = f_x(x_n,\alpha_0)u_n, \quad n \in \mathbb{Z}$$

has r linearly independent bounded solutions. Furthermore, an r-tangential homoclinic orbit $x_{\mathbb{Z}} \in \left(\mathbb{R}^N\right)^{\mathbb{Z}}$ is called nondegenerate with respect to the parameter $\alpha \in \mathbb{R}^p$, if $p = r$, and every bounded solution $(u_{\mathbb{Z}},\mu) \in \left(\mathbb{R}^N\right)^{\mathbb{Z}} \times \mathbb{R}^p$, of the difference equation

$$u_{n+1} = f_x(x_n,\alpha_0)u_n + f_\alpha(x_n,\alpha_0)\mu, \quad n \in \mathbb{Z}$$

satisfies $\mu = 0$.

Along this chapter, we will deal with 1-tangential (in short tangential) and transversal homoclinic orbits (i.e. 0-tangential homoclinic orbits).

Before presenting the numerical methods for the computation of homoclinic orbits, it is worth introducing two theorems that characterize these objects as solutions of a suitably defined operator. In fact, the numerical methods we will work with can be seen as truncated versions of the underlying operator. To do so, we firstly need to define some Banach spaces over which the (truncated) operator will act. Let $N_+, N_- \in \mathbb{Z} \cup \{\pm\infty\}$, $N_- < 0 < N_+$. Define the discrete intervals

$$J := [N_-, N_+] \cap \mathbb{Z},$$

and

$$\hat{J} := [N_-, N_+ - 1] \cap \mathbb{Z},$$

if $N_+ < \infty$. Define the space of bounded sequences

$$S_J^N := \left\{ x_J \in \left(\mathbb{R}^N\right)^J : \sup_{n \in J} ||x_n|| < \infty \right\},$$

where $||\cdot||$ is any norm in $\mathbb{R}^N$. It is well-known that S_J^N equipped with the norm

$$||x_J||_\infty := \sup_{n \in J} ||x_n||,$$

$x_J \in S_J^N$, is a Banach space. Furthermore, we allow $J = \mathbb{Z}$, and thus we obtain the Banach space $S_{\mathbb{Z}}^N$. With this basic setup we can now define the operator

$$\Gamma : \begin{array}{ccc} S_{\mathbb{Z}}^N \times \mathbb{R}^p & \to & S_{\mathbb{Z}}^N \\ (x_{\mathbb{Z}}, \alpha) & \mapsto & (x_{n+1} - f(x_n, \alpha))_{n \in \mathbb{Z}} \end{array}.$$

By means of this operator, a homoclinic orbit (in the sense of Definition 2.1) can be regarded as the solution of the infinite boundary value problem

$$\left\{ \begin{array}{rcl} \Gamma(x_{\mathbb{Z}}, \alpha_0) & = & 0, \\ \lim_{n \to \pm\infty} x_n & = & \xi. \end{array} \right. \tag{2.2}$$

The following theorem characterizes tangential and transversal homoclinic orbits in terms of the operator Γ:

Theorem 2.3. *Let $p = 1$, and $x_{\mathbb{Z}} \in S_{\mathbb{Z}}^N$ be a homoclinic orbit of (2.1) at $\alpha = \alpha_0$. Then, the following assertions hold:*

(i) $x_{\mathbb{Z}}$ is transversal, if and only if $x_{\mathbb{Z}}$ is a regular zero of $\Gamma(\cdot, \alpha_0)$,

(ii) $x_{\mathbb{Z}}$ *is tangential and nondegenerate with respect to* α*, if and only if* $(x_{\mathbb{Z}}, \alpha_0)$ *is a turning point of* Γ *in* α*.*

Proof. See [40, Theorem 3.4], and [41, Proposition 2.1.3]. □

Now that we have formally introduced the objects we want to work with, we can start with the numerical part of this section, i.e., with the numerical computation of transversal and tangential homoclinic orbits. Let us then begin with the approximation of transversal homoclinic orbits. The main idea is to replace the infinite boundary value problem (2.2) by a finite, truncated one. To do so, define the operator

$$\hat{\Gamma}: \begin{array}{rcl} S_J^N \times \mathbb{R}^p & \to & S_J^N \\ (x_J, \alpha) & \mapsto & ((x_{n+1} - f(x_n, \alpha))_{n \in \hat{J}}, b(x_{N_-}, x_{N_+}, \alpha)) \end{array},$$

where $b : \mathbb{R}^{2N} \times \mathbb{R}^p \to \mathbb{R}^N$ represents a boundary condition. In particular, we will consider periodic and projection boundary conditions. Let $\bar{x}_{\mathbb{Z}} \in S_{\mathbb{Z}}^N$ be a transversal homoclinic orbit of (2.1) at $\alpha = \alpha_0$ with respect to the equilibrium $\xi \in \mathbb{R}^N$. Let $-N_-, N_+$ be sufficiently large. Then, under certain assumptions, the operator $\hat{\Gamma}(\cdot, \alpha_0)$ has a unique zero $x_J \in S_J^N$ close to $\bar{x}|_J$, and the following estimate holds (cf. [41, Theorem 3.1.2])

$$||\bar{x}|_J - x_J||_\infty \leq C(||\bar{x}_{N_-} - \xi||^s + ||\bar{x}_{N_+} - \xi||^s), \tag{2.3}$$

where C is a positive constant, and $s = 1, 2$, provided b is a periodic, projection boundary condition, respectively.

As for the numerical computation of tangential homoclinic orbits, Theorem 2.3 allows us to intuitively deduce that tangential homoclinic orbits can be approximated by turning points of the operator $\hat{\Gamma}$, with $p = 1$ (see [41, Chapter 7] for a rigorous discussion). Thus, we will approximate tangential homoclinic orbits by zeroes of the following operator

$$\hat{\Upsilon}: \begin{array}{rcl} S_J^N \times S_J^N \times \mathbb{R}^p & \to & S_J^N \times S_J^N \times \mathbb{R} \\ (x_J, u_J, \alpha) & \mapsto & \begin{pmatrix} \hat{\Gamma}(x_J, \alpha) \\ \hat{\Gamma}_{x_J}(x_J, \alpha) u_J \\ \sum_{i=N_-}^{N_+} ||u_i||^2 - 1 \end{pmatrix} \end{array},$$

where $||\cdot||$ represents the Euclidean norm in $\mathbb{R}^N$. In what follows, we write $\hat{\Gamma}^T, \hat{\Upsilon}^T$ (resp. $\hat{\Gamma}^P, \hat{\Upsilon}^P$) to denote the use of periodic (resp. projection) boundary conditions. For a detailed discussion about the numerical approximation of transversal, tangential, and other degenerate types of discrete homoclinic orbits we refer to [7, 10, 39, 40, 41].

We want to finish this section by pointing out some interesting facts about the homoclinic structure of the normal form of the 1 : 1 resonance. Consider the following system

$$\begin{pmatrix} x_1 \\ x_2 \end{pmatrix} \mapsto \begin{pmatrix} x_1 + x_2 \\ x_2 + \beta + \alpha x_2 + x_1^2 + x_1 x_2 \end{pmatrix}, \tag{2.4}$$

where $(x_1, x_2) \in \mathbb{R}^2$, $(\beta, \alpha) \in \mathbb{R}^2$, which is a particular, truncated version of the normal form (1.9). The local bifurcation diagram is shown in Figure 2.1. In this picture, the curves labeled by F, NS correspond to paths of fold, Neimark-Sacker points, respectively. Of course, only one branch of NS represents Neimark-Sacker points, the other one consists of neutral saddles. On the other hand, the curves labeled by T_1, T_2 represent homoclinic tangencies, which meet, together with NS, tangentially at the origin. Between T_1 and T_2, system (2.4) exhibits a transversal homoclinic structure, which is limited by the homoclinic tangencies. This structure is schematically represented in Figure 2.2, for $\alpha = \alpha_0$ fixed (see Figure 2.1). In this picture, ξ, W^s_ξ, and W^u_ξ stand for an equilibrium of (2.4), the stable, and the unstable manifolds with respect to ξ, respectively.

In Figure 2.1, the distance between T_1 and T_2 is somewhat exaggerated. Actually, this distance is exponentially bounded with respect to one parameter, that is

$$|T_1(\alpha) - T_2(\alpha)| < c_1 e^{-\frac{c_2}{\alpha}},$$

for all $0 < \alpha < c_3$, where $c_{1,2,3} > 0$ are some real constants (cf. [13, 44]). This means that the complete homoclinic structure of system (2.4) survives in an exponentially small sector of the parameter space. This sector is precisely what we want to study numerically.

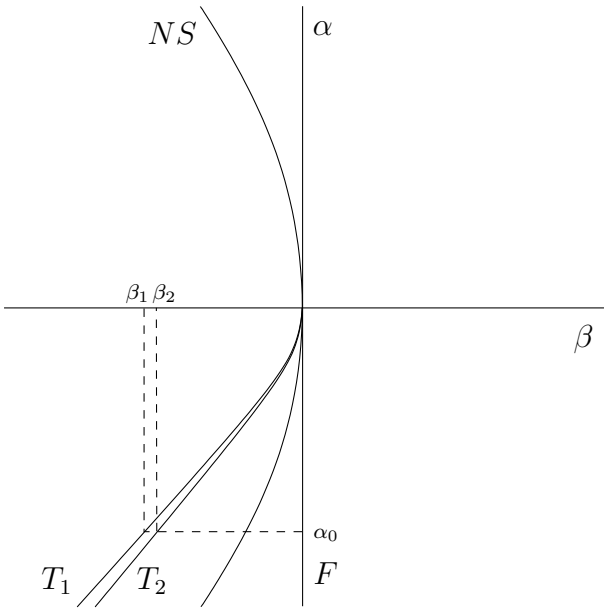

Fig. 2.1: Local bifurcation diagram of system (2.4).

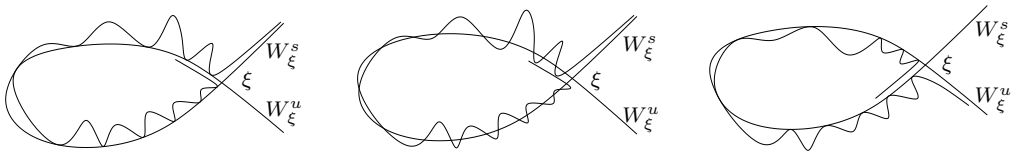

$\beta=\beta_1$ $\beta_1<\beta<\beta_2$ $\beta=\beta_2$

Fig. 2.2: Behavior of stable and unstable manifolds of system (2.4) for $\alpha = \alpha_0$ fixed.

2.2 Computing a first homoclinic tangency near an R1$_2$ point

A typical problem in the numerical analysis of homoclinic orbits is the choice of an appropriate initial guess that could lead us, via e.g. Newton iterations, to the homoclinic connection we want to analyze. In our case, we have a well-posed problem given in terms of the operator $\hat{\Upsilon}$ (see Section 2.1), and what we want to construct is a theory-based starting procedure, by means of which we can obtain an "educated" initial guess for the solution of the underlying well-posed problem, whose solutions correspond to the numerical approximation of the homoclinic tangencies we are interested in.

What is commonly done is to set a first approximating orbit to

$$(\ldots, \xi, \ldots, \xi, x_1, \ldots, x_r, \xi, \ldots, \xi, \ldots),$$

where ξ represents an equilibrium point and x_i, $i = 1, \ldots, r$, $r \in \mathbb{N}$ are, basically, randomly chosen vectors on the state space. This method is successfully applied, e.g., in [40, 41]. This is of course a purely trial and error-based method, where the user relies entirely on "luck" or brute force. Therefore, the user has essentially no control over the outcome of the Newton iterations, and it can easily happens that a spurious solution is obtained, which is a significant disadvantage.

Another approach consists of finding the intersections of the stable and unstable manifolds and using these intersections as an initial guess (see Figure 2.2). By doing so, a transversal homoclinic orbit is generically obtained via Newton iterations. Once this is done, the transversal orbit is continued with respect to one parameter until a turning point of the defining system is found. Finally, this turning point is used as initial guess of the homoclinic tangency (cf. [31]). However, the disadvantage of this method is that for finding an approximation of the transversal orbits, the stable and unstable manifolds of the system need to be numerically approximated, which is itself a problem. Furthermore, this technique is only reasonably applicable when working with planar systems. Moreover, since the systems we deal with depend on parameters, we have to at least approximately know at which parameter-values the homoclinic connection occurs, so that the manifolds intersect at all.

Thus, our main concern throughout this section will be the construction of a theory-based method that allows us to start the continuation of tangential homoclinic orbits from an R1$_2$ point, with no restriction of the dimension of the system. The basic idea is the following. We assume we are given a parameter-dependent, discrete-time dynamical system which undergoes an

R1$_2$ singularity at the origin. By means of the homological equation (cf. Section 2.2.1), we perform a quantitative center manifold reduction, so that, up to a certain order, we can transform orbits of the normal form to orbits of the original system. Then, we make use of Lemma 1.4, which allows us to approximate the normal form by the 1-flow of a vector field which undergoes a generic BT$_2$ singularity at the origin (cf. Section 1.2.1). By doing this, we merely transform the original discrete problem into a continuous one. Consequently, we just need to apply any of the known techniques for starting the continuation of homoclinic orbits from a BT$_2$ point. In our case, we will apply the method described in Appendix B.1 (cf. [5]). After this, we need to transform the thus obtained approximating orbit back to the normal form, via Lemma 1.4, and finally to the original system, by means of the quantitative center manifold reduction. Once this is achieved, the so obtained initial guess can be used for starting the Newton iterations in order to obtain the approximation of a homoclinic tangency.

2.2.1 The homological equation for maps

An important task in the numerical analysis of dynamical systems is the verification of nondegeneracy conditions at bifurcation points, which amounts to computing the coefficients of the normal form of the underlying singularity. In this way, very useful information about the local behavior of a system can be obtained (cf. Section 1.3.3). To accomplish this, several techniques may be employed, however, the homological-equation-approach has proven to be an efficient and direct method, which allows not only the derivation of compact formulae for the computation of normal form coefficients but also the Taylor expansion of the center manifold up to a certain order, in an iterative manner. The order the center manifold can be expanded up to depends directly on the order of expansion of the underlying normal form. In Section 2.2.2, we will use the homological equation for deriving quantitative relations between orbits of the normal form and of the original system.

The homological-equation-approach has been employed, e.g., in [44, Section 9.7], [50, Section 3.1 and 3.3.2], [30], [46]. The basic idea can be explained as follows. Suppose we are given a discrete-time system

$$x \mapsto f(x, \alpha), \tag{2.5}$$

where $f \in C^k(\Omega_f \times \Lambda_f, \mathbb{R}^N)$, $k \geq 1$ sufficiently large, and $0 \in \Omega_f \subset \mathbb{R}^N$, $0 \in \Lambda_f \subset \mathbb{R}^p$ are open sets. Assume that:

A$_1$ f_x^0 has $N_0 \geq 1$ eigenvalues on the unit circle, and

A$_2$ the system obtained by restriction of (2.5) to a center manifold can be smoothly transformed near the origin to some normal form

$$w \mapsto G(w, \beta), \tag{2.6}$$

where $G : \mathbb{R}^{N_0} \times \mathbb{R}^p \to \mathbb{R}^{N_0}$ is a smooth map.

The shape of G (but not its coefficients) is supposed to be known up to a certain order. Finally, the parameter-dependent center manifold is assumed to be locally parametrized by $(w, \beta) \in \mathbb{R}^{N_0} \times \mathbb{R}^p$, by means of a smooth function

$$Q : \mathbb{R}^{N_0} \times \mathbb{R}^p \to \mathbb{R}^N .$$

Thus, the invariance of the center manifold allows us to presume the existence of a smooth, invertible parameter transformation $K : \mathbb{R}^p \to \mathbb{R}^p$, such that the equation

$$f(Q(w, \beta), K(\beta)) = Q(G(w, \beta), \beta) \tag{2.7}$$

holds locally. The above equation is the so-called homological equation. The use and applications related to this equation are largely explained in the references cited above. However, a formal statement which actually guarantees the existence of the maps Q, K, so that (2.7) holds, seems not to be available. Consequently, we will discuss in this section the existence of the underlying maps. For this purpose, we need firstly to formalize the notion of local smooth equivalence and local invariance (cf. [20]).

Definition 2.4. *Consider the discrete system* (2.5) *and*

$$y \mapsto g(y, \gamma), \tag{2.8}$$

where $g \in C^k(\Omega_g \times \Lambda_g, \mathbb{R}^N)$, $k \geq 1$ *sufficiently large,* $0 \in \Omega_g \subset \mathbb{R}^N$, $0 \in \Lambda_g \subset \mathbb{R}^p$ *are open sets, and the origin is an equilibrium of* (2.5). *Systems* (2.5) *and* (2.8) *are said to be locally, smoothly equivalent at the origin, if there exist neighborhoods* $X_i \subset \Omega_f$ *of* $x = 0$, $Y_i \subset \Omega_g$ *of* $y = 0$, $i = 1, 2$, $\Gamma_f \subset \Lambda_f$ *of* $\alpha = 0$, $\Gamma_g \subset \Lambda_g$ *of* $\gamma = 0$, *and maps* $h : X_1 \cup X_2 \times \Gamma_f \to Y_1 \cup Y_2$, $P : \Gamma_f \to \Gamma_g$, *such that:*

(i) $h(\cdot, \alpha)$ *is a diffeomorphism for all* $\alpha \in \Gamma_f$, *and* $h(0, 0) = 0$,

(ii) P *is a diffeomorphism, and* $P(0) = 0$,

(iii) $h(X_1, \alpha) \subset Y_1$, $h(X_2, \alpha) \subset Y_2$, *for all* $\alpha \in \Gamma_f$,

(iv) $f(X_1, \alpha) \subset X_2$, *for all* $\alpha \in \Gamma_f$, *and* $g(Y_1, \gamma) \subset Y_2$, *for all* $\gamma \in \Gamma_g$, *and*

(v) the equation

$$g(h(x,\alpha),P(\alpha)) = h(f(x,\alpha),\alpha)$$

holds for all $(x,\alpha) \in X_1 \times \Gamma_f$.

Definition 2.5. *Let* $0 \in \mathbb{R}^N$ *be an equilibrium of the discrete system*

$$z \mapsto F(z), \tag{2.9}$$

with $F : \Omega_F \to \mathbb{R}^N$ *smooth,* $0 \in \Omega_F \subset \mathbb{R}^N$ *open. A set* $0 \in M \subset \Omega_F$ *is said to be locally invariant under* (2.9) *at* $z = 0$*, if there exists an open set* $0 \in V \subset \Omega_F$*, such that:*

$$\begin{aligned} \forall z \in V \cap M : F(z) \in V &\Rightarrow F(z) \in M, \\ \forall z \in V : F(z) \in V \cap M &\Rightarrow z \in M. \end{aligned}$$

With this basic setup we are ready to formulate the main result of this section in the following:

Theorem 2.6. *Consider system* (2.5) *with* $\boldsymbol{A}_1$, $\boldsymbol{A}_2$*. Suppose that a parameter-dependent center manifold of* (2.5) *is locally given by*

$$W^C_\alpha := \{x \in \mathbb{R}^N : x = H(u,\alpha), (u,\alpha) \in \Omega_{CM} \times \Lambda_{CM}\},$$

where $H : \Omega_{CM} \times \Lambda_{CM} \to \Omega_f$ *is smooth,* $0 \in \Omega_{CM} \subset \mathbb{R}^{N_0}$, $0 \in \Lambda_{CM} \subset \Lambda_f$ *are open sets,* $H(0,0) = 0$*, and* $H_u(u,\alpha)$ *has full rank for all* $(u,\alpha) \in \Omega_{CM} \times \Lambda_{CM}$*. Then, there exist a local reparametrization of* W^C_α *given in terms of some smooth function* $Q : \mathbb{R}^{N_0} \times \mathbb{R}^p \to \mathbb{R}^N$ *and a smooth parameter transformation* $K : \mathbb{R}^p \to \mathbb{R}^p$*, such that the homological equation*

$$f(Q(w,\beta),K(\beta)) = Q(G(w,\beta),\beta) \tag{2.10}$$

holds locally.

Proof. Choose sufficiently small, open sets $0 \in U_1 \subset \Omega_{CM}$, $0 \in \Lambda_1 \subset \Lambda_{CM}$, in such a way that $H(U_1,\Lambda_1) \subset V \cap W^C_\alpha$, V given by Definition 2.5, with $M := W^C_\alpha$, and $F := (f, I_\alpha)$[1], where I_α is the identity function in the parameter space $\mathbb{R}^p$. Take any $x := H(u,\alpha) \in W^C_\alpha$, $(u,\alpha) \in U_1 \times \Lambda_1$, sufficiently close to the origin. Then, by the local invariance of W^C_α, we have that $f(x,\alpha) \in W^C_\alpha$, which implies that there exists a $v \in U_1$, such that

$$f(x,\alpha) = f(H(u,\alpha),\alpha) = H(v,\alpha). \tag{2.11}$$

[1]The function F defines the extended system where the parameter-dependent center manifold of (2.5) is derived from.

By means of Theorem A.3, we can write v explicitly in terms of (u, α), thereby we obtain a discrete system

$$u \mapsto v = \Phi(u, \alpha) := \tau(f(H(u, \alpha), \alpha), \alpha), \tag{2.12}$$

where $\Phi : U_1 \times \Lambda_1 \to \mathbb{R}^{N_0}$ is seen to be smooth. System (2.12) is merely the restriction of (2.5) to the center manifold W^C_α. Therefore, by $\mathbf{A}_2$, (2.12) is locally, topologically equivalent to the normal form (2.6). Hence, according to Definition 2.4, there exist sufficiently small, open sets $0 \in \Theta \subset \mathbb{R}^{N_0}$, $0 \in \Delta \subset \mathbb{R}^p$, and locally defined, smooth maps $h : \mathbb{R}^{N_0} \times \mathbb{R}^p \to \mathbb{R}^{N_0}$, $P : \mathbb{R}^p \to \mathbb{R}^p$, such that

$$\Phi(h(w, \beta), P(\beta)) = h(G(w, \beta), \beta), \tag{2.13}$$

holds for all $(w, \beta) \in \Theta \times \Delta$. Consider any $u := h(w, \beta)$, $\alpha := P(\beta)$, $(w, \beta) \in \Theta \times \Delta$. Then, by combining (2.11), (2.12), and (2.13), it follows:

$$\begin{aligned} f(H(u, \alpha), \alpha) &= H(\Phi(u, \alpha), \alpha), \\ f(H(h(w, \beta), P(\beta)), P(\beta)) &= H(\Phi(h(w, \beta), P(\beta)), P(\beta)), \\ \Rightarrow f(H(h(w, \beta), P(\beta)), P(\beta)) &= H(h(G(w, \beta), \beta), P(\beta)). \end{aligned}$$

Finally, reparametrize W^C_α by means of $Q(w, \beta) := H(h(w, \beta), K(\beta))$, $K := P$, $(w, \beta) \in \Theta \times \Delta$, then the last equation above turns into

$$f(Q(w, \beta), K(\beta)) = Q(G(w, \beta), \beta),$$

which holds for all $(w, \beta) \in \Theta \times \Delta$. □

It is worth noting that Theorem 2.6 not only proves the existence of the maps Q, K, such that the homological equation locally holds but also shows how these maps can be constructed from any parametrization of a center manifold. Also, note that

$$Q_w(w, \beta) = H_u(h(w, \beta), K(\beta))h_w(w, \beta)$$

has full rank for all $(w, \beta) \in \Theta \times \Delta$, for $h(\cdot, \beta)$ is a diffeomorphism, which means that the reparametrization of the center manifold is well-defined. On the other hand, if we consider system (2.5) evaluated at $\alpha = 0$, then the homological equation (omitting parameters) reads

$$f(Q(w)) = Q(G(w)),$$

which is the form most widely used for the computation of critical coefficients of normal forms (see e.g. [44]).

2.2.2 Parameter-dependent center manifold reduction

Consider a discrete-time system

$$x \mapsto f(x, \alpha), \tag{2.14}$$

where $f \in C^k(\Omega_f \times \Lambda_f, \mathbb{R}^N)$, $k \geq 1$ sufficiently large, and $0 \in \Omega_f \subset \mathbb{R}^N$, $0 \in \Lambda_f \subset \mathbb{R}^2$ are open sets. Furthermore, assume that the origin is an R1$_2$ point of (2.14).

In the previous section, we showed the validity of the homological equation in some neighborhood of the origin. Now we will use the homological equation for deriving local, explicit relations between orbits of the normal form of the 1 : 1 resonance and orbits of system (2.14), together with parameter transformations. For this purpose, we write the homological equation in the following way

$$f(H(u, \delta), K(\delta)) = H(G(u, \delta), \delta), \tag{2.15}$$

with:

$$\begin{aligned} G(u,\delta) &:= \begin{pmatrix} u_1 + u_2 \\ u_2 + \delta_1 + \delta_2 u_2 + a u_1^2 + b u_1 u_2 + O_G((u_1^2 + |u_1 u_2|)||\delta||) \end{pmatrix} \\ &\quad + O_G(||u||^3), \\ K(\delta) &:= K_1 \delta + O_K(||\delta||^2), \\ H(u,\delta) &:= \begin{pmatrix} v_0 & v_1 \end{pmatrix} u + D\delta + O_H(||u||^2 + ||u||||\delta|| + ||\delta||^2), \end{aligned}$$

where $u := (u_1, u_2) \in \mathbb{R}^2$, $\delta := (\delta_1, \delta_2) \in \mathbb{R}^2$, the O_i-symbol, $i = G, K, H$, stands for higher order terms, a, b are the normal form coefficients, and v_0, v_1, p_0, p_1 denote the critical right and left generalized eigenvectors of f_x^0, respectively. Furthermore, the critical eigenvectors are supposed to be biorthogonal (cf. Definition 1.3). On the other hand, $K_1 \in \mathbb{R}^{2,2}$, and $D \in \mathbb{R}^{N,2}$ are quantities to be computed by means of the homological equation. Throughout the computations, we consider the Taylor expansion of f

$$f(x, \alpha) = f_x^0 x + f_\alpha^0 \alpha + \frac{1}{2} B(x, x) + O_f(||x||^3 + ||\alpha||^2 + ||x||||\alpha||),$$

where $B(\cdot, \cdot) := f_{xx}^0[\cdot, \cdot]$ (see Definition 1.3).

With this basic setup, we are ready to perform the numerical center manifold reduction. Thus, replace G, K, H, and f, as given explicitly above, in the homological equation. By doing so, we obtain:

$$\begin{aligned} &f_x^0 H(u,\delta) + f_\alpha^0 K(\delta) + \frac{1}{2} B(H(u,\delta), H(u,\delta)) + O_f(||H(u,\delta)||^3 + ||K(\delta)||^2 \\ &+ ||H(u,\delta)||||K(\delta)||) = \begin{pmatrix} v_0 & v_1 \end{pmatrix} G(u,\delta) + D\delta + O_H(||G(u,\delta)||^2 \\ &\qquad + ||G(u,\delta)||||\delta|| + ||\delta||^2), \end{aligned}$$

$$
\begin{aligned}
&u_1v_0 + u_2(v_0+v_1) + f_x^0 D\delta + O_H(||u||^2 + ||u||||\delta|| + ||\delta||^2) + f_\alpha^0 K_1\delta \\
&+ O_K(||\delta||^2) + \frac{1}{2}u_1^2 B(v_0,v_0) + u_1u_2B(v_0,v_1) + \frac{1}{2}u_2^2B(v_1,v_1) + \frac{1}{2}B(D\delta \\
&+ O_H(||u||^2 + ||u||||\delta|| + ||\delta||^2), 2(u_1v_0+u_2v_1) + D\delta + O_H(||u||^2 + ||u||||\delta|| \\
&+ ||\delta||^2)) + O_f(||H(u,\delta)||^3 + ||K(\delta)||^2 + ||H(u,\delta)||||K(\delta)||) \\
&= (u_1+u_2+O_G(||u||^3))v_0 + (u_2+\delta_1+\delta_2u_2+au_1^2+bu_1u_2 \\
&+ O_G((u_1^2+|u_1u_2|)||\delta||) + O_G(||u||^3))v_1 + D\delta + O_H(||G(u,\delta)||^2 \\
&+ ||G(u,\delta)||||\delta|| + ||\delta||^2).
\end{aligned}
$$

By collecting the linear terms in δ of the last equation, we arrive at

$$f_x^0 D\delta + f_\alpha^0 K_1\delta = \begin{pmatrix} v_1 & 0 \end{pmatrix}\delta + D\delta,$$

and hence it follows

$$(f_x^0 - I_N)D = \begin{pmatrix} v_1 & 0 \end{pmatrix} - f_\alpha^0 K_1. \tag{2.16}$$

Next, the biorthogonality of the critical eigenvectors can be used in order to simplify the above relation. Let us then multiply both sides of the last equation by p_0^T. By doing so, we obtain the following equation

$$\begin{pmatrix} 1 & 0 \end{pmatrix} = \begin{pmatrix} \beta_1 & \beta_2 \end{pmatrix} K_1, \tag{2.17}$$

where

$$0 \neq \begin{pmatrix} \beta_1 & \beta_2 \end{pmatrix} := p_0^T f_\alpha^0$$

is a transversality condition that must be satisfied. The equation (2.17) does not determine K_1 uniquely, however, a possible choice is readily given by

$$K_1 = \frac{1}{\beta_1^2+\beta_2^2}\begin{pmatrix} \beta_1 & \sigma\beta_2 \\ \beta_2 & -\sigma\beta_1 \end{pmatrix},$$

where $\sigma \in \{1,-1\}$. Once we have determined K_1, D is immediately obtained from (2.16) by, e.g., bordering techniques (cf. [6]). It is only left to compute the normal form coefficients a, b. These coefficients are well-known and given by (cf. [50]):

$$
\begin{aligned}
a &= \frac{1}{2}p_0^T B(v_0,v_0), \\
b &= p_1^T B(v_0,v_0) + p_0^T B(v_0,v_1),
\end{aligned}
$$

(see also Definition 1.3). At this point, an explicit, linear approximation of the center manifold, as well as of the parameter transformation are ready to be used for the computation of orbits of the original system (2.14) from orbits of the normal form.

We want to conclude this section by showing how the homological equation and the numerical center manifold reduction we just derived above will actually help us to construct the starting procedure for the continuation of homoclinic tangencies from an R1$_2$ point. Namely, we have the following:

Theorem 2.7. *Let system* (2.14) *have an R1$_2$ point at the origin. Let* $0 \in \Omega_H \subset \mathbb{R}^2$, $0 \in \Lambda_H \subset \mathbb{R}^2$ *be open sets, such that the homological equation* (2.15) *holds for all* $(u, \delta) \in \Omega_H \times \Lambda_H$ *(cf. Theorem 2.6). Let* $u_{\mathbb{Z}} \in S^2_{\mathbb{Z}}$ *be a tangential homoclinic orbit of the normal form* $u \mapsto G(u, \delta)$ *at* $\delta = \delta_0 \in \Lambda_H$, *so that* $u_i \in \Omega_H$, *for all* $i \in \mathbb{Z}$. *Furthermore, denote by* $U_{\mathbb{Z}} \in S^2_{\mathbb{Z}}$ *a nontrivial solution of the equation*

$$U_{n+1} = G_u(u_n, \delta_0)U_n, \quad n \in \mathbb{Z}\,. \tag{2.18}$$

Then, system (2.14) *has a tangential homoclinic orbit* $x_{\mathbb{Z}} \in S^N_{\mathbb{Z}}$ *at* $\alpha = \alpha_0 := K(\delta_0)$, *which is explicitly given by*

$$x_i := H(u_i, \delta_0), \quad i \in \mathbb{Z}\,. \tag{2.19}$$

Furthermore, the sequence $X_{\mathbb{Z}} \in S^N_{\mathbb{Z}}$ *defined as*

$$X_i := H_u(u_i, \delta_0)U_i, \quad i \in \mathbb{Z} \tag{2.20}$$

satisfies

$$X_{n+1} = f_x(x_n, \alpha_0)X_n, \quad n \in \mathbb{Z}\,. \tag{2.21}$$

Proof. Let us begin by showing that $x_{\mathbb{Z}}$ is a homoclinic orbit of (2.14). We then must firstly verify that $x_{\mathbb{Z}}$ is an orbit of (2.14). For this purpose, let $n \in \mathbb{Z}$ arbitrary. It follows

$$x_{n+1} = H(u_{n+1}, \delta_0) = H(G(u_n, \delta_0), \delta_0).$$

By taking into account the homological equation, we arrive at

$$x_{n+1} = H(G(u_n, \delta_0), \delta_0) = f(H(u_n, \delta_0), K(\delta_0)) = f(x_n, \alpha_0),$$

hence $x_{\mathbb{Z}}$ is indeed an orbit of (2.14). Now we will see that this orbit is homoclinic. Note that

$$\lim_{n \to \pm\infty} u_n = u_{eq},$$

where $u_{eq} \in \Omega_H$ is an equilibrium of the normal form. Consequently, we have that

$$\lim_{n\to\pm\infty} x_n = \lim_{n\to\pm\infty} H(u_n, \delta_0) = H(u_{eq}, \delta_0) =: x_{eq} \in \Omega_f.$$

Thus, it remains to show that x_{eq} is an equilibrium of (2.14). By the homological equation, it follows

$$f(x_{eq}, \alpha_0) = f(H(u_{eq}, \delta_0), K(\delta_0)) = H(G(u_{eq}, \delta_0), \delta_0) = H(u_{eq}, \delta_0) = x_{eq}.$$

Therefore, $x_{\mathbb{Z}}$ is a homoclinic orbit of (2.14). Now we have to show that $x_{\mathbb{Z}}$ is tangential, which amounts to proving that $X_{\mathbb{Z}}$ satisfies (2.21). To achieve this, we need the following relation

$$f_x(H(u,\delta), K(\delta))H_u(u,\delta) = H_u(G(u,\delta),\delta)G_u(u,\delta), \tag{2.22}$$

$(u, \delta) \in \Omega_H \times \Lambda_H$, which is obtained by differentiation with respect to u of the homological equation. Let $n \in \mathbb{Z}$ arbitrary. We have that

$$X_{n+1} = H_u(u_{n+1}, \delta_0)U_{n+1} = H_u(G(u_n, \delta_0), \delta_0)U_{n+1}.$$

By taking into account (2.18) and (2.22), it follows:

$$\begin{aligned} X_{n+1} &= H_u(G(u_n, \delta_0), \delta_0)U_{n+1}, \\ &= H_u(G(u_n, \delta_0), \delta_0)G_u(u_n, \delta_0)U_n, \\ &= f_x(H(u_n, \delta_0), K(\delta_0))H_u(u_n, \delta_0)U_n, \\ &= f_x(x_n, \alpha_0)X_n. \quad \square \end{aligned}$$

2.2.3 Flow approximation

In the past section, the homological equation played the central role both in the center manifold reduction, as well as in the transformation of homoclinic orbits of the normal form to homoclinic orbits of the original system (2.14). In fact, Theorem 2.7 provides us with formulae (2.19), (2.20), which allow the construction of tangential homoclinic orbits of system (2.14), provided a tangential homoclinic orbit of the normal form is available. In practice, we will of course be only able to approximate the homoclinic orbits of the original system, for the center manifold and the parameter transformation are only known up to a certain order. In other words, the problem of obtaining a first approximation of a tangential homoclinic orbit of an arbitrary N-dimensional system has been translated into approximating such orbits, but of the normal form, namely, the dimension of the problem has been reduced.

In the present section, our efforts will be then dedicated to approximating tangential homoclinic orbits of the normal form of the $1:1$ resonance.

For this purpose, Lemma 1.4 will be of a great help, since it allows us to approximate the normal form by the 1-flow of a vector field (see Section 1.2.1), i.e., we transform the discrete problem into a continuous one. The advantage of doing this is that the dynamics of the approximating vector field is described by the well-known Bogdanov-Takens theory, and, in particular, the starting procedure for the continuation of homoclinic orbits near a BT_2 point is available (cf. Algorithm B.1). It would remain to know how to actually construct an approximating, discrete, tangential homoclinic orbit from a homoclinic orbit of the vector field. Once this construction is known, our starting procedure will be ready for numerical implementation.

Let $\phi^t(\cdot,\delta)$ be the t-flow of

$$\dot{u}(t) = g(u(t),\delta), \tag{2.23}$$

where g is the vector field given by Lemma 1.4. Then, according to this lemma, the discrete system

$$u \mapsto \psi(u,\delta) := \phi^1(u,\delta) \tag{2.24}$$

is an approximation of the normal form of the $1:1$ resonance. Suppose that system (2.23) has a homoclinic orbit at $\delta = \delta_0 \in \mathbb{R}^2$, and let $u_0 \in \mathbb{R}^2$ be a point on this homoclinic orbit, so that u_0 is not an equilibrium. Let $u_{\mathbb{Z}} \in S^2_{\mathbb{Z}}$ be given by

$$u_i := \phi^i(u_0,\delta_0), \quad i \in \mathbb{Z}\,.$$

Then, it immediately follows that $u_{\mathbb{Z}}$ is a homoclinic orbit of system (2.24), and consequently, by Lemma 1.4, $u_{\mathbb{Z}}$ is an approximation of a homoclinic tangency of the normal form. Thus, it is left to construct a solution of the variational equation of (2.24) along the orbit $u_{\mathbb{Z}}$. Let $U_{\mathbb{Z}} \in S^2_{\mathbb{Z}}$ be given by

$$U_i := g(u_i,\delta_0), \quad i \in \mathbb{Z}\,.$$

Choose an arbitrary $n \in \mathbb{Z}$. Then, it follows that:

$$\begin{aligned}
U_{n+1} &= g(u_{n+1},\delta_0),\\
&= g(\phi^{n+1}(u_0,\delta_0),\delta_0),\\
&= \frac{d}{dt}\left(\phi^{t+1}(u_0,\delta_0)\right)_{t=n},\\
&= \frac{d}{dt}\left(\psi(\phi^t(u_0,\delta_0),\delta_0)\right)_{t=n},\\
&= \psi_u(u_n,\delta_0)\frac{d}{dt}\left(\phi^t(u_0,\delta_0)\right)_{t=n},\\
&= \psi_u(u_n,\delta_0)g(\phi^n(u_0,\delta_0),\delta_0),\\
&= \psi_u(u_n,\delta_0)U_n.
\end{aligned}$$

Therefore, we have that $U_{\mathbb{Z}}$ is indeed a solution of the variational equation of (2.24) along the homoclinic orbit $u_{\mathbb{Z}}$. With these computations we are ready to implement the starting procedure for the continuation of homoclinic tangencies near an R1$_2$ point. The precise implementation of the starting method is summarized in Algorithm B.2.

2.3 Numerical examples

We conclude this chapter with some numerical experiments that illustrate the use of Algorithm B.2. These experiments will also constitute the numerical evidence of the effectiveness of our starting procedure, since we do not present any rigorous analysis that guarantees convergence under Newton iterations.

In what follows, after applying the starting procedure to the systems, we employ the so obtained approximations for initializing (damped) Newton iterations of the defining systems given in terms of $\hat{\Upsilon}^T$, $\hat{\Upsilon}^P$ (cf. Section 2.1). Therefore, it is worth showing how the underlying matrices look like in order to implement the Newton iterations. These matrices will be denoted by A_T, A_P, respectively. Under notation of Section 2.1, let $M := |N_-| + N_+ + 1$. The matrix A_T evaluated at $(x_J, u_J, \alpha) \in S_J^N \times S_J^N \times \mathbb{R}^2$ presents the following sparse structure

$$A_T := (a_{ij})_{i,j=1,\ldots,2NM+1} := \begin{pmatrix} & A_1 & & 0 & A_3 \\ & & & 0 & 0 \\ A_2 & 0 & & A_1 & A_4 \\ 0 & 0 & & & 0 \\ 0 & 0 & & A_5 & 0 \end{pmatrix}, \tag{2.25}$$

with:

$$\begin{aligned} (a_{ij})_{i=1,\ldots,NM,j=1,\ldots,NM} &:= A_1 \in \mathbb{R}^{NM,NM}, \\ (a_{ij})_{i=NM+1,\ldots,2NM,j=NM+1,\ldots,2NM} &:= A_1, \\ (a_{ij})_{i=NM+1,\ldots,N(2M-1),j=1,\ldots,N(M-1)} &:= A_2 \in \mathbb{R}^{N(M-1),N(M-1)}, \\ (a_{ij})_{i=1,\ldots,N(M-1),j=2NM+1} &:= A_3 \in \mathbb{R}^{N(M-1)}, \\ (a_{ij})_{i=NM+1,\ldots,N(2M-1),j=2NM+1} &:= A_4 \in \mathbb{R}^{N(M-1)}, \\ (a_{ij})_{i=2NM+1,j=NM+1,\ldots,2NM} &:= A_5 \in \mathbb{R}^{1,NM}, \end{aligned}$$

and

$$A_1 := \begin{pmatrix} -f_x(x_{N_-},\alpha) & I_N & & 0 \\ & \ddots & \ddots & \\ 0 & & \ddots & \ddots \\ & & -f_x(x_{N_+-1},\alpha) & I_N \\ I_N & & 0 & -I_N \end{pmatrix},$$

$$A_2 := \begin{pmatrix} -f_{xx}(x_{N_-},\alpha)[u_{x_{N_-}}] & & & 0 \\ & \ddots & & \\ & & \ddots & \\ 0 & & & -f_{xx}(x_{N_+-1},\alpha)[u_{x_{N_+-1}}] \end{pmatrix},$$

$$A_3 := \begin{pmatrix} -f_{\alpha_1}(x_{N_-},\alpha) \\ \vdots \\ -f_{\alpha_1}(x_{N_+-1},\alpha) \end{pmatrix},$$

$$A_4 := \begin{pmatrix} -f_{x\alpha_1}(x_{N_-},\alpha)u_{x_{N_-}} \\ \vdots \\ -f_{x\alpha_1}(x_{N_+-1},\alpha)u_{x_{N_+-1}} \end{pmatrix},$$

$$A_5^T := 2\begin{pmatrix} u_{x_{N_-}} \\ \vdots \\ u_{x_{N_+}} \end{pmatrix},$$

where $f_{xx}(x,\alpha)[u] := (f_x(x,\alpha)u)_x$, $(x,u,\alpha) \in \mathbb{R}^N \times \mathbb{R}^N \times \mathbb{R}^2$. Moreover, the matrix A_P is computed similarly as A_T. Just the rows of A_p that are related to the boundary conditions differ from those of A_T, for the projection boundary conditions have a different structure and furthermore they depend on the parameter α, in contrast to the periodic ones.

Once we have found a homoclinic tangency, continuation with respect to a second parameter, say α_2, is possible. By doing so, we will obtain an approximation of a first curve of homoclinic tangencies that emanates from the $R1_2$ point. On the other hand, continuation with respect to one parameter, with the other one fixed, will allow us to obtain a closed curve of transversal homoclinic orbits. In this way, a second homoclinic tangency can be found, and thereby a second curve of homoclinic tangencies can be continued. For the purposes above described, we will use the Euler-Newton method (cf. [2, Algorithm 10.2.10]) combined with step-size control as described in [22, Section 2.3].

Although Algorithm B.2 is essentially a theory-based method, there is still a trial and error-component which cannot be avoided. This component

is found in the choice of a "suitable" $\epsilon > 0$ in Step (iii) of Algorithm B.1. It is clear that the smaller ϵ is chosen, the better is the approximation of the homoclinic orbit, however, also the worse is the condition of the defining system whose solution we need to find. Therefore, there exists a compromise between approximation of the homoclinic orbit and conditioning of the underlying system. Roughly speaking, we can visualize this compromise as if there existed an interval $(\epsilon_{min}, \epsilon_{max})$, $0 < \epsilon_{min} < \epsilon_{max}$, in which we should try choosing values of ϵ in order to generate a converging, nontrivial sequence via (damped) Newton iterations. Choosing values of ϵ outside this interval will be likely to produce either diverging sequences or trivial solutions (i.e. sequences of equilibria, or more complicated types of spurious solutions, etc.).

Throughout the numerical applications, $||\cdot||$ will represent the Euclidean norm. Moreover, for the continuation of transversal homoclinic orbits, we use the amplitude function

$$\text{ampl}(x_J, \alpha) := \sqrt{\sum_{i=N_-}^{N_f} ||x_i - \xi(\alpha)||^2},$$

where $N_f := N_+$ (resp. $N_f := N_+ - 1$), when we use projection boundary conditions (resp. periodic boundary conditions), and $\xi(\alpha)$ stands for the parameter-dependent equilibrium which the points of the homoclinic orbit converge to. This function will allow us to plot closed curves of transversal homoclinic orbits.

In all the numerical examples, we will firstly compute a tangential homoclinic orbit x_J^0 with $-N_- = N_+ = 20$. Then, if an orbit with a larger length is desired, we set an initial approximating orbit to

$$(\ldots, \xi, \ldots, \xi, x_J^0, \xi, \ldots, \xi, \ldots),$$

and then we use it for the corresponding Newton iterations.

Finally, all the computations will be performed in MATLAB.

2.3.1 Normal form of the $1:1$ resonance

The importance of quantitatively analyzing the normal form of the $1:1$ resonance was already discussed in the introduction of the chapter. Therefore, we will begin our numerical experiments with this system, and furthermore we will devote special attention to it. Consider then the system

$$\begin{pmatrix} x_1 \\ x_2 \end{pmatrix} \mapsto g(x, \alpha) := \begin{pmatrix} x_1 + x_2 \\ x_2 + \alpha_1 + \alpha_2 x_2 + x_1^2 + x_1 x_2 \end{pmatrix}, \tag{2.26}$$

where $x := (x_1, x_2) \in \mathbb{R}^2$, $\alpha := (\alpha_1, \alpha_2) \in \mathbb{R}^2$. This system was already discussed in Section 2.1. Let us apply Algorithm B.2 to (2.26). The matrix A is given by

$$A := \begin{pmatrix} 0 & 1 & 1 \\ 0 & 0 & 1 \\ 1 & 1 & 0 \end{pmatrix}.$$

By means of this matrix we obtain the linear transformations:

$$\begin{aligned} \tilde{K}(\delta) &:= \begin{pmatrix} 1 & 0 \\ 0 & 1 \end{pmatrix} \delta, \\ \tilde{H}(u, \delta) &:= \begin{pmatrix} 1 & -1 \\ 0 & 1 \end{pmatrix} u + \begin{pmatrix} 1 & 0 \\ -1 & 0 \end{pmatrix} \delta. \end{aligned}$$

The computed quadratic coefficients are:

$$\begin{aligned} a &:= 1, \\ b &:= 1. \end{aligned}$$

With these coefficients, we obtain the following ϵ-dependent flow approximation:

$$\begin{aligned} \delta_1 &:= -\frac{1}{4}\epsilon^4, \\ \delta_2 &:= -0.35714285714052\epsilon^2, \\ u_1(t) &:= \frac{\epsilon^2}{2}\left(1 - 3\ \mathrm{sech}^2\left(\frac{\epsilon}{2}t\right)\right), \\ u_2(t) &:= \frac{3\epsilon^3}{2}\ \mathrm{sech}^2\left(\frac{\epsilon}{2}t\right)\tanh\left(\frac{\epsilon}{2}t\right) + \frac{1}{2}\delta_1. \end{aligned}$$

It is important to point out that this step can be easily automatized, for the critical eigenvectors of the approximating vector field do not depend on a, b. Therefore, only the Q's (cf. Step (ii) of Algorithm B.1) must be recomputed in each example.

By choosing $\epsilon := 0.9$, $N_- := -40$, $N_+ := 60$, and after some damped Newton iterations, we find a homoclinic tangency x_J, X_J at

$$(\alpha_1, \alpha_2) = (-0.2135818065347, -0.28928571428382),$$

with

$$||\hat{\Upsilon}^T(x_J, X_J, \alpha)|| \approx 8.33 \times 10^{-12}.$$

In Figure 2.3, we present a phase plot of the homoclinic tangency x_J together with the starting orbit x_J^0 obtained via our initializing procedure.

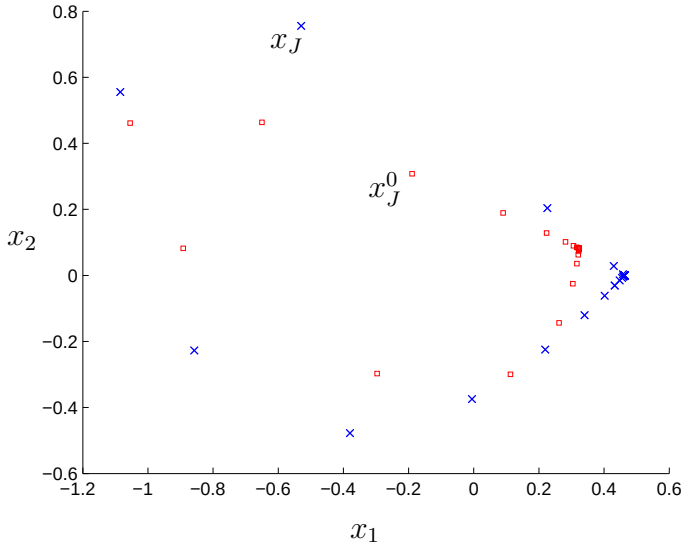

Fig. 2.3: Homoclinic tangency x_J and the starting orbit x_J^0.

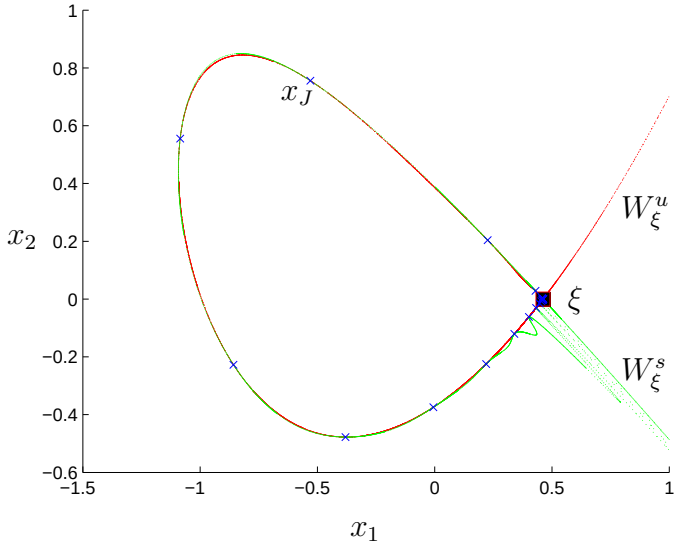

Fig. 2.4: Stable and unstable manifolds along the homoclinic tangency x_J.

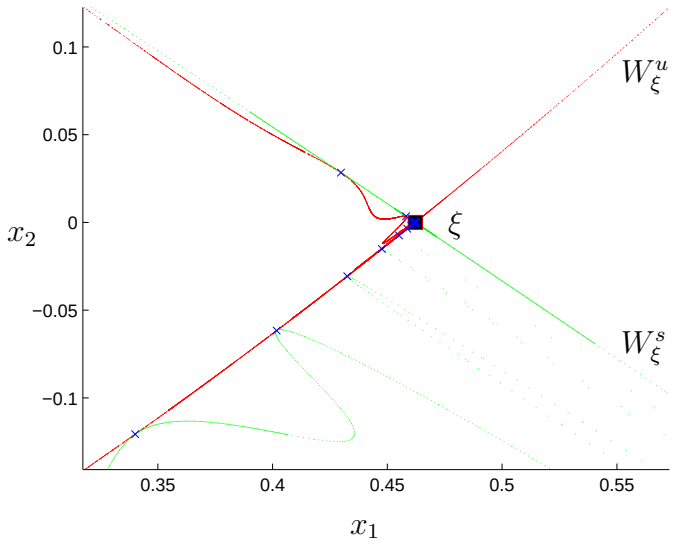

Fig. 2.5: Stable and unstable manifolds around the equilibrium ξ.

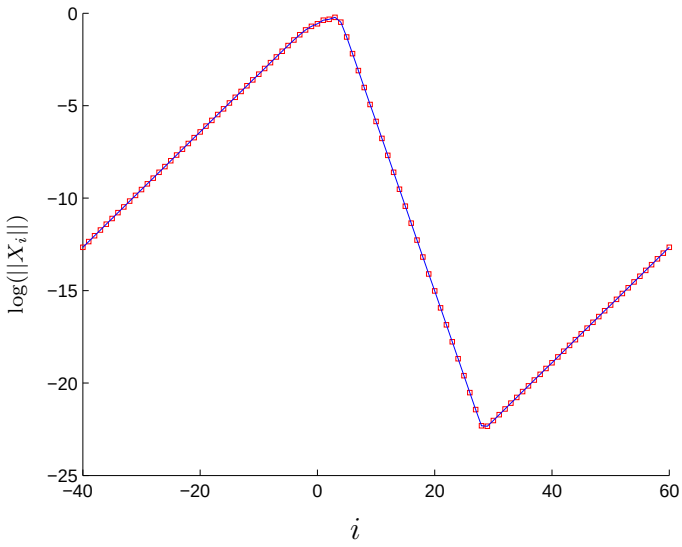

Fig. 2.6: Exponential decay of $||X_i||$ with respect to i.

In this case, the starting orbit lied close enough to the orbit x_J, so that the damped Newton iterations converged to a nontrivial solution. In order to verify that the so obtained orbit x_J is actually a homoclinic tangency, we plot the stable and unstable manifolds of the system. These are shown in Figure 2.4 and 2.5. In these pictures, we can see that the points of x_J indeed correspond to the tangential intersections of W^u_ξ, and W^s_ξ. These manifolds are approximated via forward (resp. backward) iterations of (2.26) starting from points on the tangent space of W^u_ξ (resp. W^s_ξ) at ξ, close enough to the equilibrium. Finally, in Figure 2.6, we plot the logarithm of the norm of X_i, $i \in J$, with respect to the time i. In this picture, we can observe the exponential decay of $||X_i||$, $i \in J$, with i, which is consistent with the theory of exponential dichotomies related to homoclinic tangencies (cf. [41]). In fact, valuable information about dichotomies rates can be numerically obtained by means of the solution X_J of the variational equation of (2.26) along the homoclinic tangency x_J (cf. [38]). On the other hand, note that after attaining $||X_i||$ its minimum value at $i = 29$, $||X_i||$ grows again with exponential rate until it reaches the same value as at $i = -40$. This phenomenon occurs due to the periodic boundary conditions, which forces the first and the last point of x_J, X_J to be equal. The situation will be different when we work with projection boundary conditions.

The next experiment will be the continuation of transversal homoclinic orbits with respect to α_1, letting $\alpha_2 = -0.28928571428382$ fixed. The result is shown in Figure 2.7. In this picture, we obtained a closed loop, which is a known phenomenon that is a consequence of the behavior of the perturbed stable and unstable manifolds (cf. [9]). Along this curve, we marked the points P_{T_1}, P_{T_r}, and P_{T_2}, which correspond to the first homoclinic tangency (i.e. the one we have already computed), a transversal homoclinic point, and a second homoclinic tangency, respectively. The transversal homoclinic orbit is located at

$$(\alpha_1, \alpha_2) = (-0.21528196737544, -0.28928571428382).$$

Furthermore, in Figure 2.8, we show the transversal intersections of the manifolds along the homoclinic orbit. Now, we will switch to the second homoclinic tangency. To achieve this, we firstly use P_{T_2} as a starting point for the Newton iterations. This point is, in parameter space, located at

$$(\alpha_1, \alpha_2) = (-0.21672274959574, -0.28928571428382).$$

In this way, we obtain a very good approximation of both the parameter values, as well as of the second tangential homoclinic orbit, which will be denoted by y^0_J. However, we also need an initial value Y^0_J for the solution of

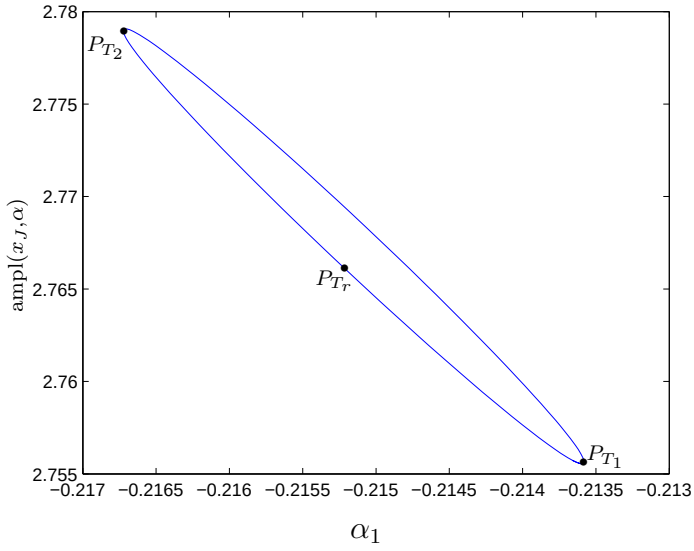

Fig. 2.7: Continuation of transversal homoclinic orbits with respect to α_1, with α_2 fixed.

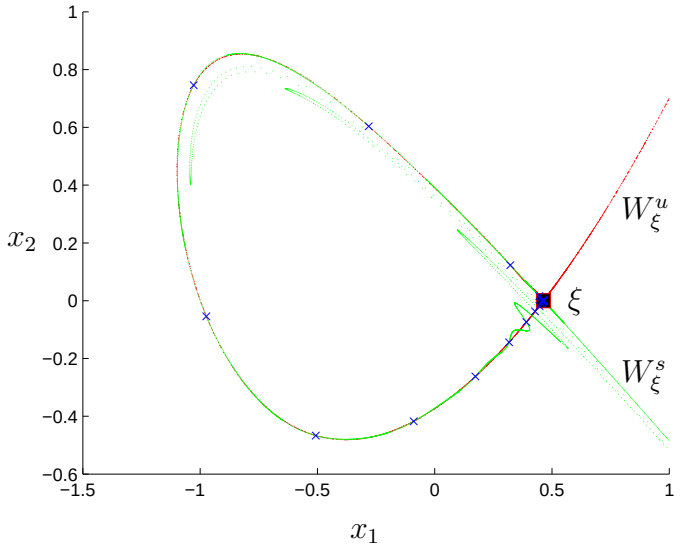

Fig. 2.8: Stable, and unstable manifolds along a transversal homoclinic orbit.

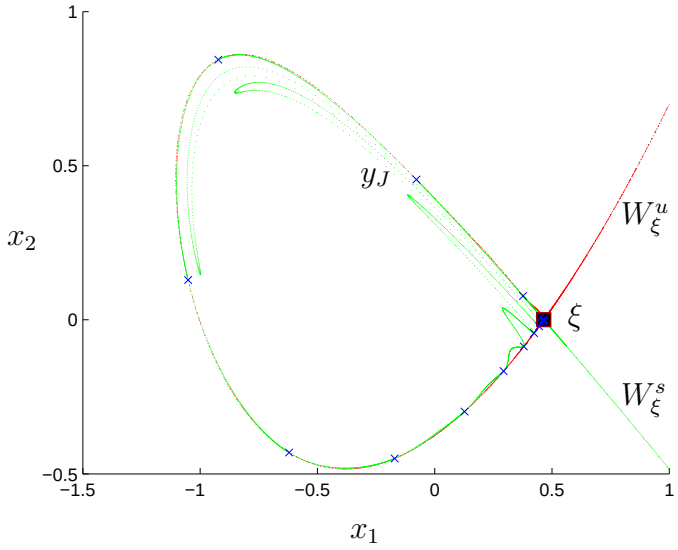

Fig. 2.9: Stable, and unstable manifolds along the second homoclinic tangency y_J.

the variational equation of (2.26) along y_J^0. In order to construct Y_J^0, we use the fact that the matrix

$$\hat{\Gamma}^T_{x_J}(y_J^0, \alpha)$$

is almost singular, which allows us to find a vector Y_J^0, such that

$$\hat{\Gamma}^T_{x_J}(y_J^0, \alpha) Y_J^0 \approx 0.$$

This can be easily implemented by a single command in MATLAB. Thus, after some few Newton iterations, we found a second homoclinic tangency y_J, Y_J at

$$(\alpha_1, \alpha_2) = (-0.2167231774074, -0.28928571428382),$$

with

$$||\hat{\Upsilon}^T(y_J, Y_J, \alpha)|| \approx 5.93 \times 10^{-12}.$$

In Figure 2.9, we show the tangential intersections of the manifolds along the homoclinic orbit y_J.

Up to this point, we have numerically illustrated some aspects about the homoclinic structure of the normal form of the 1 : 1 resonance, which were introduced in Section 2.1. In particular, Figures 2.4, 2.8, and 2.9 illustrate, in a more precise manner, what we just schematically showed in Figure 2.2.

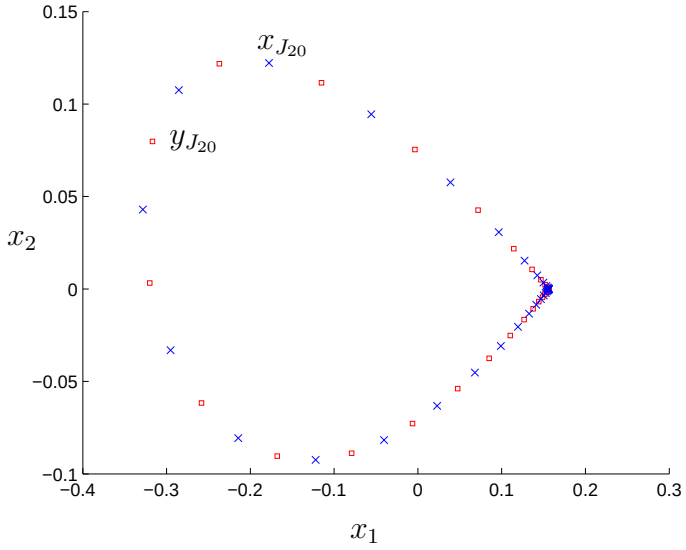

Fig. 2.10: Homoclinic tangencies $x_{J_{20}}$, and $y_{J_{20}}$.

Our next goal in this experiment is to numerically compute the "horn" of homoclinic tangencies that emanate from the $\mathrm{R1}_2$ point. This horn consists of two branches of tangential homoclinic orbits, which are schematically shown in Figure 2.1. Note that in the above performed computations, we already obtained two points of the horn, namely, P_{T_1} and P_{T_2} (see Figure 2.7).

Choose $\epsilon := 0.55$, $N_- := -20$, $N_+ := 20$ with the corresponding discrete interval J_{20}. By doing so, we obtain two homoclinic tangencies $x_{J_{20}}, X_{J_{20}}$, and $y_{J_{20}}, Y_{J_{20}}$, located at

$$\alpha_x = (-0.02442993556905, -0.10803571428571),$$

and

$$\alpha_y = (-0.02442993416031, -0.10803571428571),$$

respectively, with

$$||\hat{\Upsilon}^T(x_{J_{20}}, X_{J_{20}}, \alpha_x)|| \approx 2 \times 10^{-13}, \quad ||\hat{\Upsilon}^T(y_{J_{20}}, Y_{J_{20}}, \alpha_y)|| \approx 6.01 \times 10^{-12}.$$

The so obtained orbits are plotted in Figure 2.10.

With this information, we are ready to perform the continuation of the horn. The result of the continuation is shown in Figure 2.11 and 2.12. The tangential homoclinic branches are labeled by $T_1^{T_{20}}$, $T_2^{T_{20}}$. The superscript T_{20} denotes the use of periodic boundary conditions within the interval J_{20}

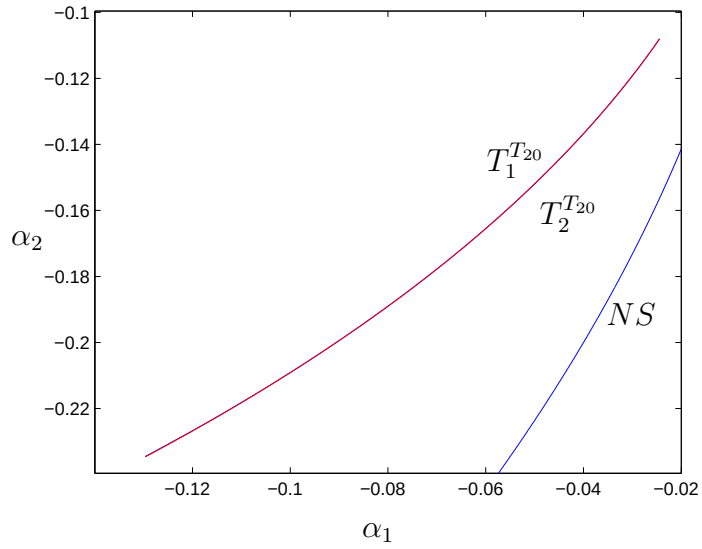

Fig. 2.11: Tangential homoclinic branches.

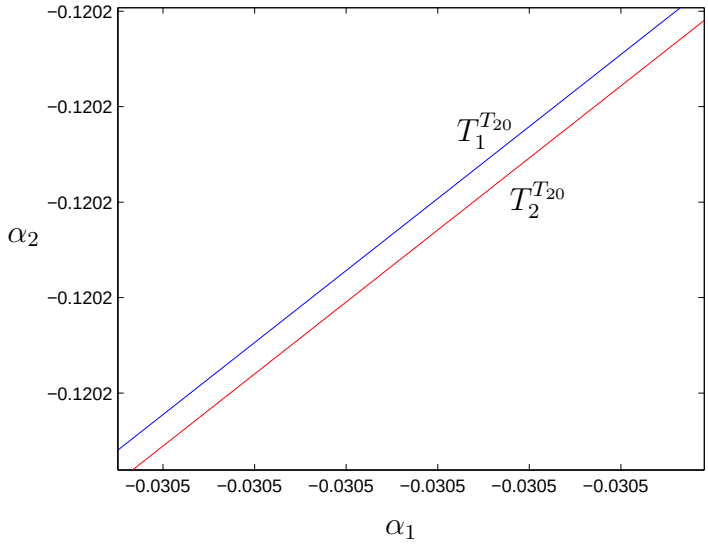

Fig. 2.12: Tangential homoclinic branches in a small region of the parameter space.

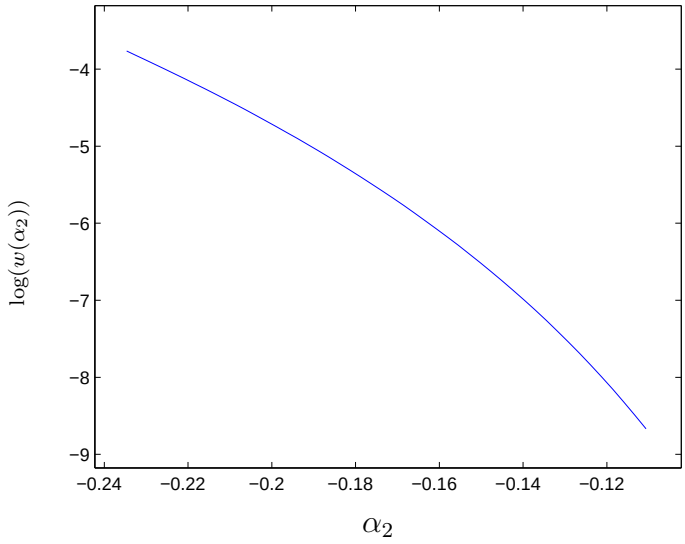

Fig. 2.13: Width of the homoclinic horn.

above defined. The label NS denotes the Neimark-Sacker curve. In Figure 2.11, we can observe that the position of the curves in the parameter space is consistent with Figure 2.1, however, the width of the horn is actually much smaller (see Figure 2.12). In fact, we will next see how small this width really is. To achieve this, we perform the continuation of $T_1^{T_{20}}$, and then, for some α_2's fixed, we continue transversal homoclinic orbits with respect to α_1 (see Figure 2.7). The width of the horn is then obtained by measuring the distance between the maximum and minimum values that α_1 attains along the closed curve of transversal homoclinic orbits. Of course, this procedure is not performed for every point of $T_1^{T_{20}}$, otherwise the numerical and time cost would have been unnecessarily high. The result of this process is shown in Figure 2.13. In this picture, $w(\alpha_2)$ stands for the width of the horn with respect to α_2. It draws our attention how small the region between $T_1^{T_{20}}$ and $T_2^{T_{20}}$ really is, and furthermore, we can also observe that the width increases as the parameters move away from the $\mathrm{R1}_1$ point along $T_1^{T_{20}}$, which is consistent with the theory (cf. [13], [44, Section 9.5.2]).

Along the curve of homoclinic tangencies, several interesting quantities can be computed. For example, in Figure 2.14, we plotted the norm of the tangential homoclinic orbits (as defined in Section 2.1, considering the Euclidean norm) with respect to the parameter α_1. As expected, the norm of the homoclinic tangencies decreases as the parameters move toward the $\mathrm{R1}_2$ point along $T_1^{T_{20}}$. This is consistent with the fact that at the origin the

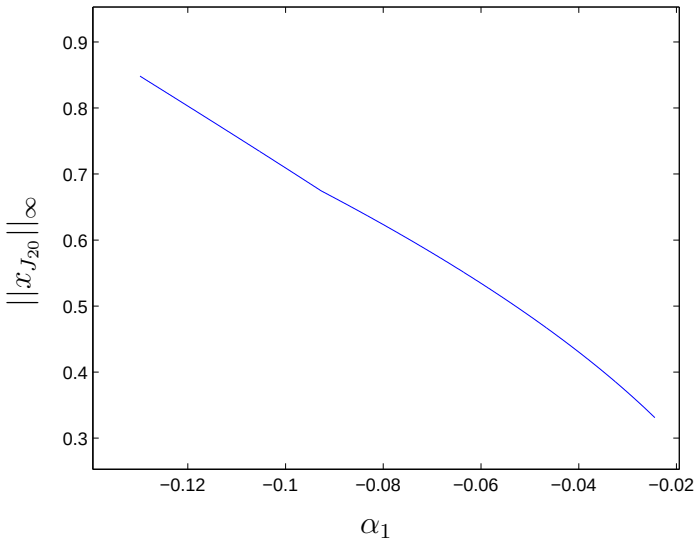

Fig. 2.14: Norm of the homoclinic tangency $x_{J_{20}}$ along the curve $T_1^{T_{20}}$.

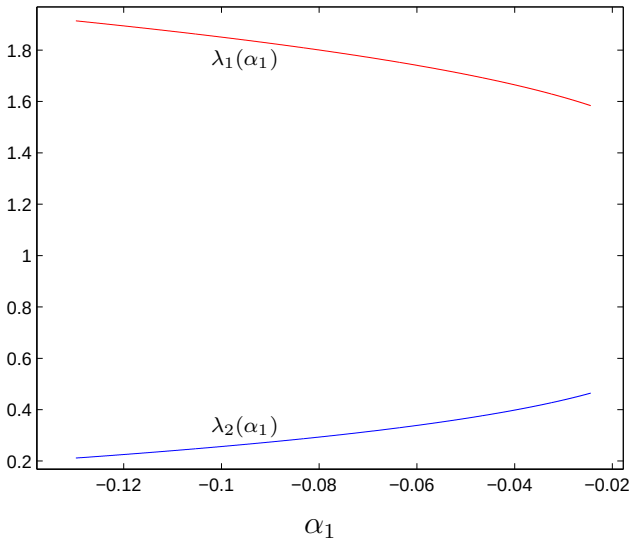

Fig. 2.15: Behavior of the eigenvalues of the system along the curve $T_1^{T_{20}}$.

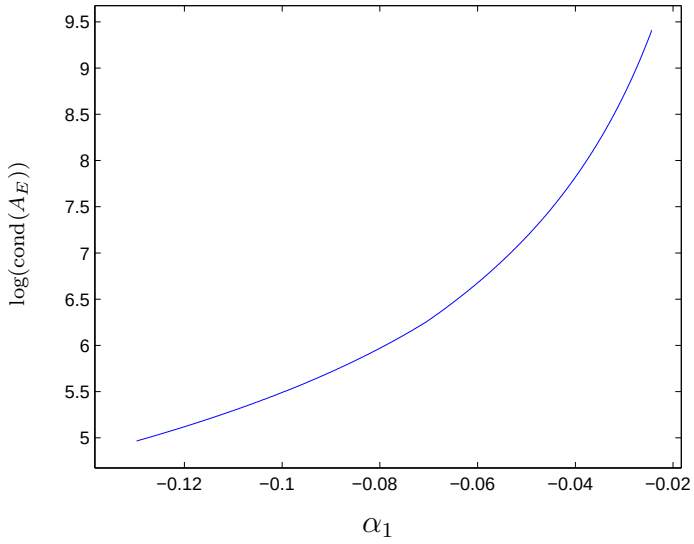

Fig. 2.16: Behavior of the matrix condition along the curve $T_1^{T_{20}}$.

homoclinic tangencies disappear. Next, we have in Figure 2.15 the behavior of the eigenvalues $\lambda_{1,2}$ of the matrix $g_x(\xi(\alpha), \alpha)$ along $T_1^{T_{20}}$. In this picture, we can observe that the equilibrium $\xi(\alpha)$ is actually a hyperbolic saddle along the piece of $T_1^{T_{20}}$ we continued, however, it is also seen that the eigenvalue λ_2 moves toward zero as the parameters move away from the $\mathrm{R1}_2$ point. In fact, λ_2 becomes zero when $T_1^{T_{20}}$ collides with the curve

$$C := \left\{(\alpha_1, \alpha_2) \in \mathbb{R}^2 : \alpha_1 = -(1+\alpha_2)^2\right\}.$$

This causes that $g_x(\xi(\alpha), \alpha)$ becomes singular, giving rise to a further degeneracy, which is referred to as connecting orbits of nondiffeomorphisms (cf. [10]). This prevents us from continuing $T_1^{T_{20}}$ in the left direction. Finally, in Figure 2.16, we show the behavior of the condition number of the matrix A_E with respect to α_1. A_E denotes the matrix used for the Euler-Newton continuation (cf. [2, Algorithm 10.2.10]). The structure of A_E is very similar to that of A_T (see (2.25)). In Figure 2.16, we can see that the continuation problem is highly badly conditioned. Note that the condition number practically "explodes" as we approach the $\mathrm{R1}_2$ point. This is of course not surprising, for the defining system of homoclinic tangencies is singular at the bifurcation point. The bad condition of the continuation problem prevents us from continuing $T_1^{T_{20}}$ in the right direction.

To finish this experiment, we will compare some of the already obtained results via periodic boundary conditions, with projection boundary condi-

tions. In particular, we are interested to know how the computed horn of homoclinic tangencies (cf. Figure 2.11) is affected, if we use different boundary conditions. For this purpose, we need firstly to compute a homoclinic tangency via projection boundary conditions. By choosing $\epsilon := 0.55$, $N_- := -20$, $N_+ := 20$ with the corresponding discrete interval J_{20}, we find a homoclinic tangency $z_{J_{20}}, Z_{J_{20}}$, located at

$$\alpha_z = (-0.02442999356054, -0.10803571428571),$$

with

$$||\hat{\Upsilon}^P(z_{J_{20}}, Z_{J_{20}}, \alpha_z)|| \approx 2.18 \times 10^{-13}.$$

At this very first point, we can already detect a difference with the homoclinic tangency $x_{J_{20}}, X_{J_{20}}$ obtained before, namely

$$||\alpha_x - \alpha_z|| \approx 5.79 \times 10^{-8},$$

however, we cannot tell which approximation is better yet. In Figure 2.17, we plotted the homoclinic tangencies $x_{J_{20}}$ and $z_{J_{20}}$ for comparison. At first glance, both orbits seem to be quite close to each other, however, if we look carefully in a small neighborhood of the equilibrium ξ, we do encounter an important difference (see Figure 2.18). In this picture, we can observe that both orbits deviate from each other as they approach the equilibrium. The orbit obtained via projection boundary conditions comes closer to ξ, which shows that $z_{J_{20}}$ is a better approximation of the homoclinic tangency. This is of course consistent with the theory, since the error that occurs in the approximation of homoclinic tangencies is of the form of (2.3) (cf. [41, Corollary 4.1.3]), which clearly shows that projection boundary conditions yield better approximations than the periodic ones, considering of course the same discrete interval. Another visible difference can be noted when plotting the norm of $||Z_i||$, $i \in J_{20}$. In Figure 2.19, we can observe the exponential decay of $||Z_i||$ with respect to $i \in J_{20}$. It does not occur a "turning back" of the norm of the Z_i's, which did happen when using periodic boundary conditions, see e.g. Figure 2.6. Nevertheless, this is actually not an important drawback of the periodic boundary conditions. For instance, it can be solved by suitably shifting the elements of the computed orbit and then performing again the Newton iterations.

With these previous observations, it becomes clear that the homoclinic horns (computed with projection and periodic conditions) are likely to differ from each other. In order to verify which boundary conditions provide the better approximation of the homoclinic horn, we will also use a homoclinic tangency obtained via periodic conditions over a bigger interval, i.e. $N_- :=$

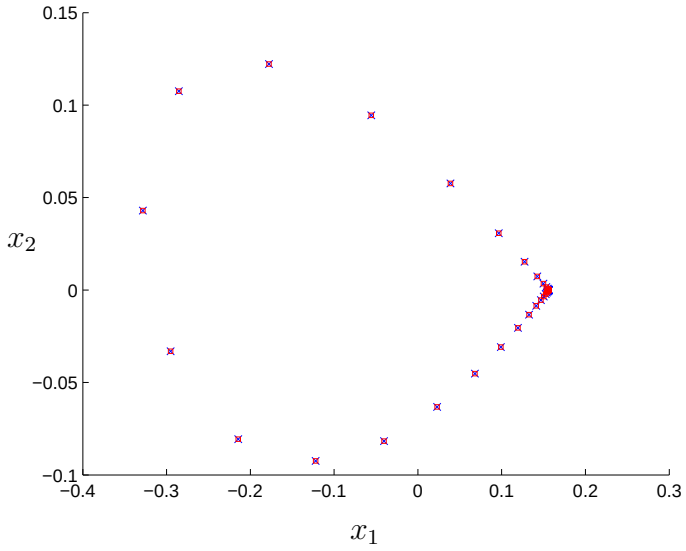

Fig. 2.17: Homoclinic tangencies $x_{J_{20}}$ and $z_{J_{20}}$.

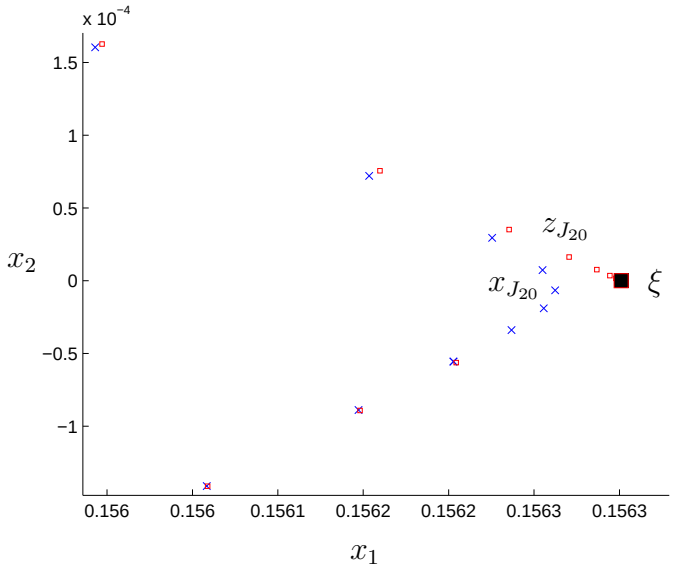

Fig. 2.18: Homoclinic tangencies $x_{J_{20}}$ and $z_{J_{20}}$ in a small neighborhood of the equilibrium ξ.

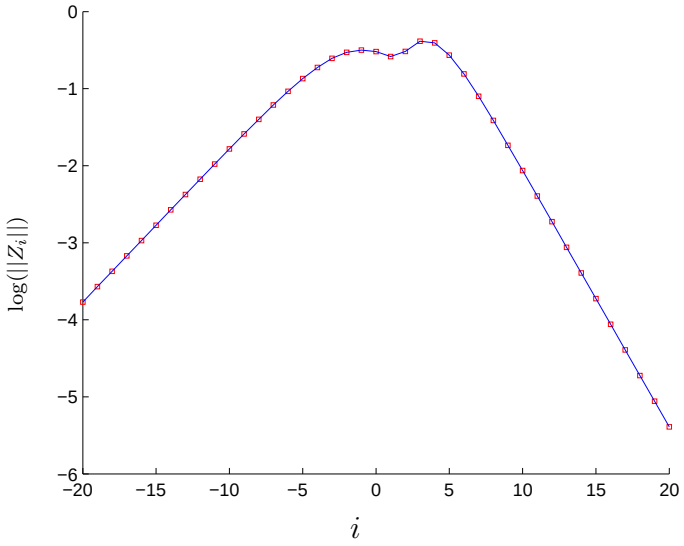

Fig. 2.19: Exponential decay of $||Z_i||$ with respect to i.

-30, $N_+ := 30$ with the corresponding discrete interval J_{30}. By doing so, we obtained six curves corresponding to the horns $T_{1,2}^{T_{20}}$, $T_{1,2}^{P_{20}}$, and $T_{1,2}^{T_{30}}$, which are plotted in Figure 2.20. In this picture, we noted that the so obtained horns are very close to each other. The six curves are grouped in the same line. Nevertheless, if we look carefully in a small region of the parameter space, we can observe an interesting fact (see Figure 2.21). As we pointed out before, the horns $T_{1,2}^{T_{20}}$ and $T_{1,2}^{P_{20}}$ are actually different. The horn $T_{1,2}^{T_{30}}$, which yields a better approximation than $T_{1,2}^{T_{20}}$ does, lies close to the horn obtained via projection conditions, which, however, was computed in the interval J_{20} (as $T_{1,2}^{T_{20}}$ was). Therefore, we can conclude that $T_{1,2}^{P_{20}}$ provides a better approximation of the horn than $T_{1,2}^{T_{20}}$. This is also a consequence of the behavior of the error that occurs in the approximation of homoclinic tangencies. Another question that may arise is whether the width of the horns significantly differ. In Figure 2.22, we plotted the width of the horns $T_{1,2}^{T_{20}}$, $T_{1,2}^{P_{20}}$, and $T_{1,2}^{T_{30}}$, however, no important difference was noted.

Finally, from a numerical viewpoint, it is interesting to compare the condition of the continuation problem. As we did before, we will compare the condition number of the matrix used for the Euler-Newton continuation. The behavior of the condition is shown in Figure 2.23 and 2.24. As it was expected, the continuation problem is also very badly conditioned if we use projection boundary conditions, however, it can be noted that when using pe-

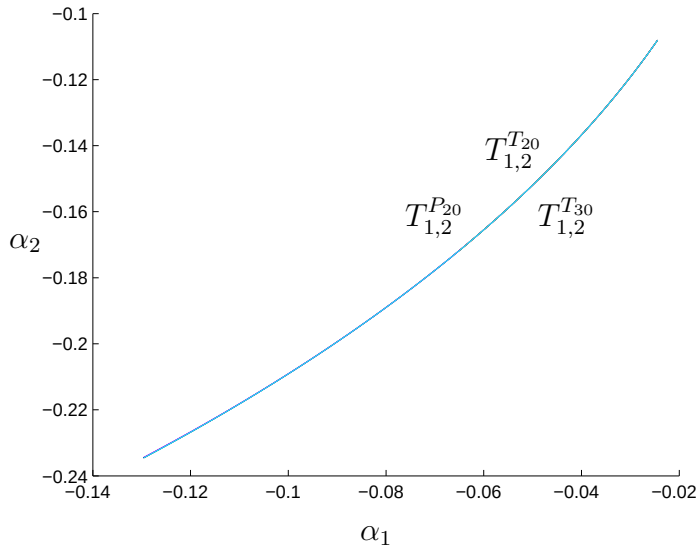

Fig. 2.20: Homoclinic horns.

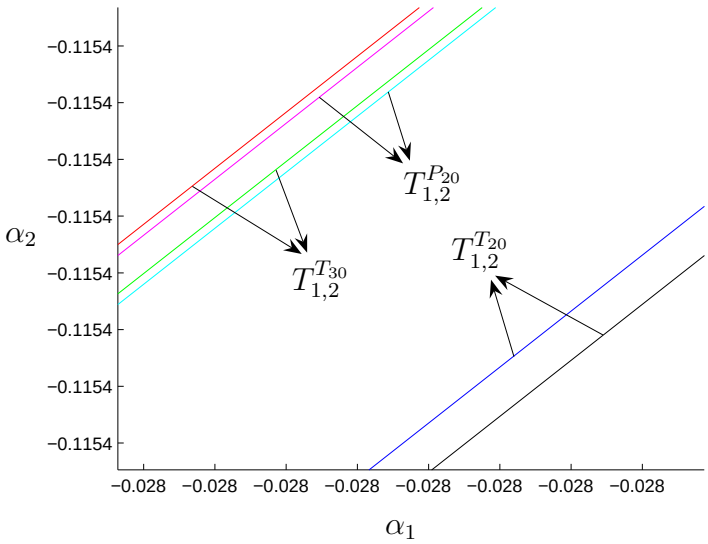

Fig. 2.21: Homoclinic horns in a small region of the parameter space.

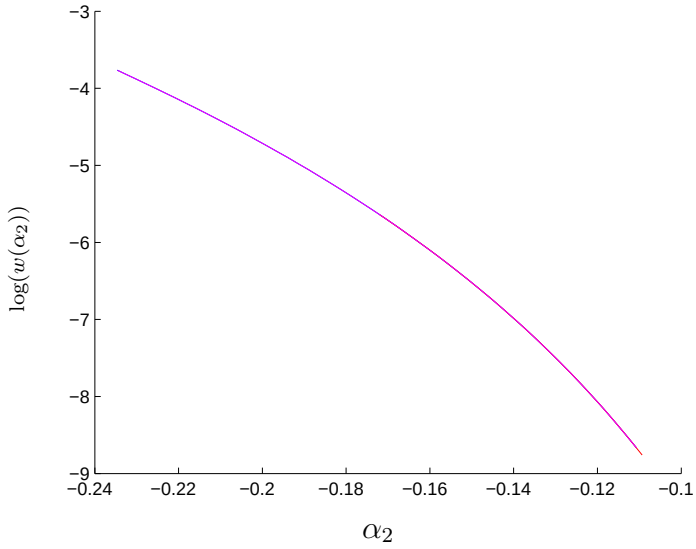

Fig. 2.22: Widths of the homoclinic horns.

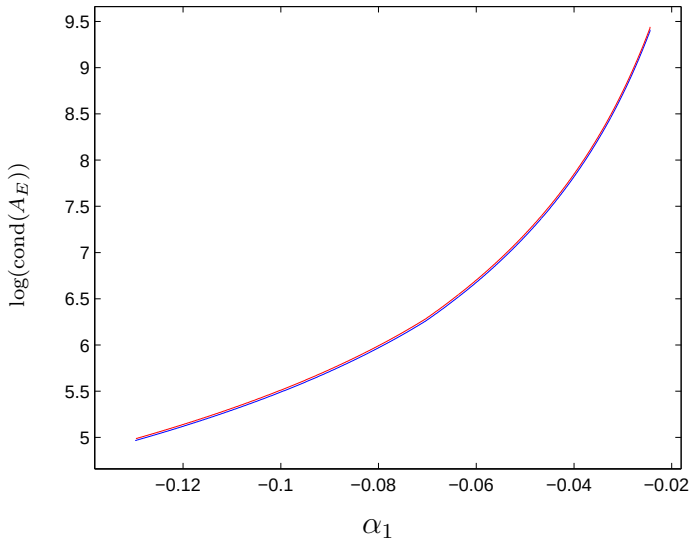

Fig. 2.23: Behavior of the matrix condition along the curves $T_1^{T_{20}}$ and $T_1^{P_{20}}$.

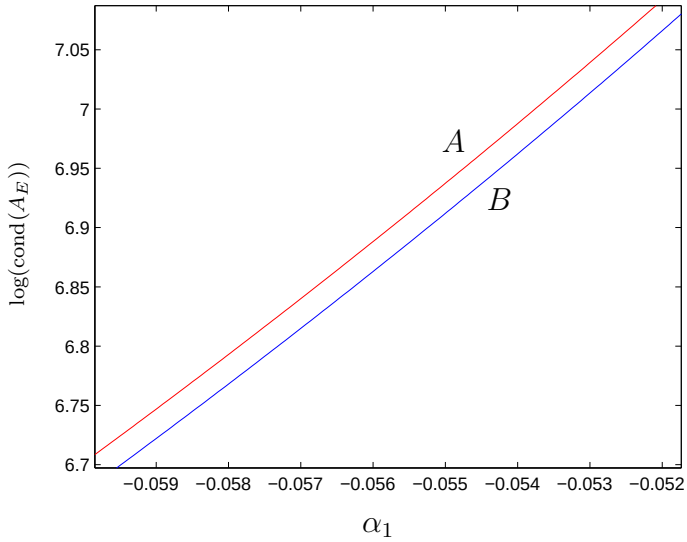

Fig. 2.24: Behavior of the matrix condition along a small piece of the curves $T_1^{T_{20}}$ (labeled by B) and $T_1^{P_{20}}$ (labeled by A).

riodic conditions, the continuation problem is somewhat better conditioned.

2.3.2 Normal form of the Bogdanov-Takens bifurcation

Consider the system

$$\begin{cases} \dot{x}_1 = x_2, \\ \dot{x}_2 = \alpha_1 + \alpha_2 x_1 + x_1^2 + x_1 x_2, \end{cases}$$

which is a particular, truncated version of the normal form of the Bogdanov-Takens bifurcation (cf. Section 1.1.1). In this example, we discretize the above continuous-time system via the classical Runge-Kutta method of fourth order. Denote the so obtained discrete system by

$$x \mapsto g(h, x, \alpha). \tag{2.27}$$

It is clear that the above normal form undergoes a BT_2 bifurcation at the origin, therefore, by Theorem 1.6, system (2.27) undergoes a $1:1$ resonance at the origin for all sufficiently small step-size. Thus, choose $h := 0.1$, and

$$A := \begin{pmatrix} 0 & 0.1 & 1 \\ 0 & 0 & 1 \\ 1 & 1 & 0 \end{pmatrix}.$$

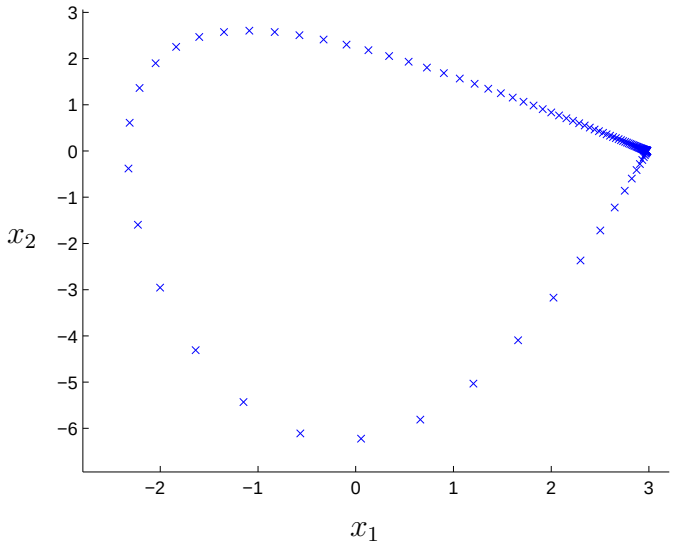

Fig. 2.25: Homoclinic orbit x_J.

By applying Algorithm B.2 to (2.27), with $\epsilon := 0.085$, $N_- := -70$, $N_+ := 70$, and after some few Newton iterations, we find a homoclinic tangency x_J, X_J at

$$(\alpha_1, \alpha_2) = (-1.1989445988353, -2.58035714230002),$$

with

$$||\hat{\Upsilon}^T(x_J, X_J, \alpha)|| \approx 4.16 \times 10^{-11}.$$

In Figure 2.25 and 2.26, we show the phase plot of the computed orbit x_J and the exponential decay of $||X_i||$, $i \in J$, respectively. In this experiment, we computed all the required derivatives numerically.

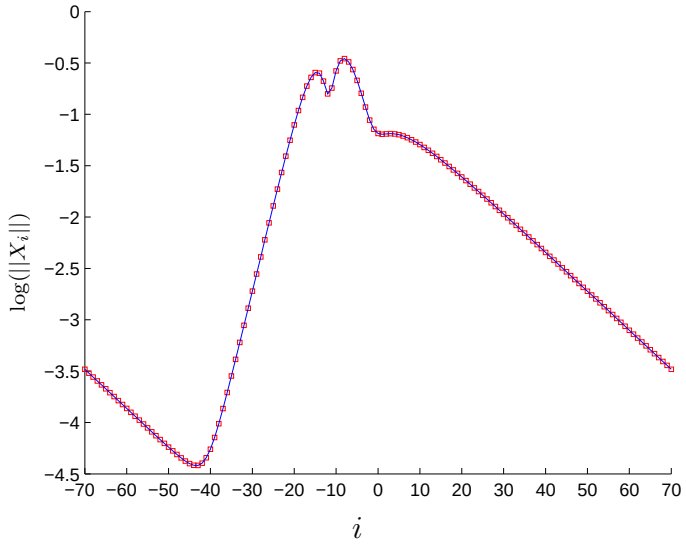

Fig. 2.26: Exponential decay of $||X_i||$ with respect to i.

2.3.3 Hénon 3D map

The Hénon map has proven to be very rich in terms of its bifurcation diagram and fascinating global phenomena that this system exhibits (cf. [44], [50]). In this experiment, we consider the following three-dimensional version of the Hénon map

$$\begin{pmatrix} x \\ y \\ z \end{pmatrix} \mapsto \begin{pmatrix} \alpha_2 + \alpha_1 z - x^2 \\ x \\ y \end{pmatrix}.$$

This system undergoes an $\mathrm{R1}_2$ singularity at $(x, y, z) = (-0.75, -0.75, -0.75)$, $(\alpha_1, \alpha_2) = (-0.5, -0.5625)$. Next, we apply Algorithm B.2 to the Hénon system, with $\epsilon := 0.9$, $N_- := -50$, $N_+ := 50$, and

$$A := \begin{pmatrix} 0.5 & 0 & -0.5 & 0.8 \\ 1 & -1 & 0 & -0.4 \\ 0 & 1 & -1 & -0.4 \\ 0.5 & 0.5 & 0.5 & 0 \end{pmatrix}.$$

After some few Newton iterations, we find a homoclinic tangency x_J, X_J at

$$(\alpha_1, \alpha_2) = (-1.14448083063938, -0.23373257142857),$$

with

$$||\hat{\Upsilon}^P(x_J, X_J, \alpha)|| \approx 8.12 \times 10^{-12}.$$

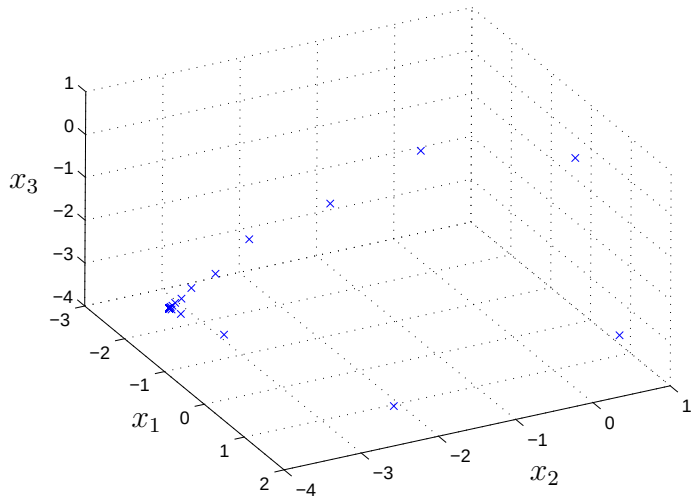

Fig. 2.27: Homoclinic orbit x_J.

In Figure 2.27 and 2.28, we show the phase plot of the computed orbit x_J and the exponential decay of $||X_i||$, $i \in J$, respectively. It is interesting noting that the structure of the computed homoclinic tangency x_J is similar to that of the homoclinic tangencies of the normal form, see e.g. Figure 2.3, however, the very same map may exhibit homoclinic tangencies with a totally different shape if we choose another suitable pair of parameters (cf. [41, Section 7.1.3]).

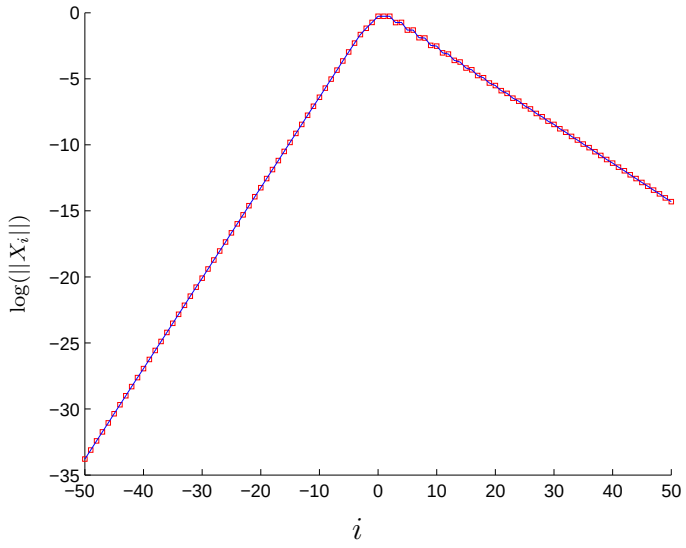

Fig. 2.28: Exponential decay of $||X_i||$ with respect to i.

Chapter 3

Conclusions and perspectives

In this chapter, we want to briefly summarize the results we have obtained and point out some questions and future work based on our analysis.

In the first part of this thesis, we devoted our attention to the local analysis of dynamical systems under discretizations. Theorems 1.6 and 1.13 showed that BT_2 and FH points persist under Runge-Kutta methods and general one-step methods, respectively. Furthermore, we took advantage of the Runge-Kutta structure in order to establish relations between critical coefficients and eigenvectors of a dynamical system and its discretization, in the BT_2 case. This analysis was done in Section 1.3.3. Thus, a natural extension of our analysis would be to obtain persistence results (as that of Theorem 1.13) for the remaining codimension two singularities. More precisely, we want to know whether, and under which assumptions, Bautin and Hopf-Hopf points are turned (and probably $O(h^p)$-shifted) into Chenciner and double Neimark-Sacker points, respectively, under one-step methods of order p.

On the other hand, determining whether or not a codimension two singularity persists under one-step methods can be seen as just the first step of the analysis of the effect of discretization methods on the bifurcation diagram of a dynamical system. The next step is to determine how the emanating curves of codimension one singularities are affected. This problem was tackled in Theorem 1.14, for the Hopf curve. We could conclude that the emanating curve of Hopf points is $O(h^p)$-shifted and turned into a curve of Neimark-Sacker points by discretization methods of order p. This result was established for the BT_2 and FH case. However, the whole discretized bifurcation diagram is not completely understood in either case yet. It is desirable to know what occur with the discretized, emanating path of homoclinic points in the BT_2 case. For an FH point, it remains to understand the effect of one-step methods on the curves of Torus and heteroclinic bi-

furcations. In Section 1.5.2, we analyzed in detail the discretization of the eigenvalues along the Hopf curve that emanates from a BT_2 singularity. We arrived to the conclusion that the eigenvalues of the dynamical system along the Hopf path are followed "correctly" by their discretized counterpart.

In the second part of this thesis, we performed a numerical analysis focused on global phenomena that occur near an $R1_2$ singularity. The homological equation played the central role in Chapter 2, and Theorem 2.6 provided a strong statement which allows us to know in which sense this equation is applicable and also gave us a deep insight into the underlying relations that are embedded in the homological equation. It is well-known that a similar equation can be formulated and exploited for vector fields (cf. [44, Section 8.7.1]). Thus, it is a reasonable aim to perform an analysis similar to that of Theorem 2.6 for vector fields.

The main outcome of Chapter 2 was the Algorithm B.2. This procedure allows us to start the continuation of homoclinic tangencies near an $R1_2$, in a general setting. This method was proven to be effective, and it permitted us to numerically analyze the homoclinic structure of the normal form of the $1:1$ resonance (cf. Section 2.3.1). It was illustrated e.g. how to compute transversal homoclinic orbits, switching between tangencies, and continuation of the homoclinic horn.

Nevertheless, it is worth pointing out some improvements that could be implemented at first glance, if required, in Algorithm B.2:

- Our starting procedure is, loosely speaking, implemented in its simplest form. The center manifold and parameter transformations shown in Section 2.2.2 are just linearly approximated. These Taylor expansions can be, however, improved up to and including quadratic terms, which would yield a reduction of the error introduced by these transformations (see e.g. [6, Section 11.2.1] for the BT_2 case).

- Another improvement may be obtained by computing, via (damped) Newton iterations, a tangential homoclinic orbit for the normal form of the $1:1$ resonance, and just then using the orbit and parameters thus obtained for the center manifold transformation (cf. Step (v) of Algorithm B.2). Recall that we use flow interpolation for approximating a homoclinic tangency of the normal form (cf. Step (iv) of Algorithm B.2).

- Finally, the procedure for the approximation of a homoclinic orbit of the interpolating vector field (cf. (B.1)) can be itself improved. Several methods for this task are available, e.g. [6, Section 11.2.2], [26], and they may be directly used or adapted for Algorithm B.2.

Appendix A

Auxiliary results

Theorem A.1 (Banach)**.** *Let $M \in \mathbb{R}^{N,N}$ and $||\cdot||$ denote any matrix norm in $\mathbb{R}^{N,N}$ for which $||I_N|| = 1$. If $||M|| < 1$, then $(I_N + M)^{-1}$ exists, and it holds*

$$(I_N + M)^{-1} = \sum_{i=0}^{\infty} (-1)^i M^i,$$

and

$$||(I_N + M)^{-1}|| \leq \frac{1}{1 - ||M||}.$$

Proof. See [47]. □

Theorem A.2 (Vainikko's Perturbation Lemma)**.** *Let V, W be Banach spaces, and $H \in C^1(V, W)$. Let $y_0 \in V$, and assume $H'(y_0)$ to be a homeomorphism, and that there exists positive constants δ, κ, σ, such that*

$$||H'(y) - H'(y_0)|| \leq \kappa < \sigma \leq \frac{1}{||(H'(y_0))^{-1}||}, \quad \forall y \in B_\delta(y_0),$$

$$||H(y_0)|| \leq (\sigma - \kappa)\delta,$$

where $B_\delta(y_0)$ denotes the closed ball of radius δ and centered at y_0. Then, H has a unique zero in $B_\delta(y_0)$, and it holds

$$||y_1 - y_2|| \leq \frac{1}{\sigma - \kappa} ||H(y_1) - H(y_2)||, \quad \forall y_1, y_2 \in B_\delta(y_0),$$

and

$$||(H'(y))^{-1}|| \leq \frac{1}{\sigma - \kappa}.$$

Proof. See [40]. □

Theorem A.3 (Parameter-dependent coordinates on manifolds)**.** *Let W_α^C be a parameter-dependent, N_0-dimensional manifold given as in Theorem 2.6. Then, there exists a locally defined, smooth function $\tau : \mathbb{R}^N \times \mathbb{R}^p \to \mathbb{R}^{N_0}$, such that:*

(i) $\forall (u,\alpha) \in \Omega'_{CM} \times \Lambda'_{CM} : \tau(H(u,\alpha),\alpha) = u,$

(ii) $\forall \alpha \in \Lambda'_{CM}, \forall x \in H(\Omega'_{CM},\alpha) : H(\tau(x,\alpha),\alpha) = x,$

where $0 \in \Omega'_{CM} \subset \Omega_{CM}$ and $0 \in \Lambda'_{CM} \subset \Lambda_{CM}$ are open sets.

Proof. Define the function

$$T : \begin{array}{rcl} \Omega_{CM} \times \mathbb{R}^{N-N_0} \times \Lambda_{CM} & \to & \mathbb{R}^N \times \mathbb{R}^p \\ (u,z,\alpha) & \mapsto & \begin{pmatrix} H(u,\alpha) + Pz \\ \alpha \end{pmatrix}, \end{array}$$

where $P \in \mathbb{R}^{N,N-N_0}$ is chosen, so that $\begin{pmatrix} H_u^0 & P \end{pmatrix} \in \mathbb{R}^{N,N}$ is invertible. Therefore, we have that

$$T'(0,0,0) = \begin{pmatrix} H_u^0 & P & H_\alpha^0 \\ 0 & 0 & I_p \end{pmatrix}$$

is invertible. Hence, the Inverse Function Theorem guarantees the existence of a function $Q := (\tau, \varrho, \vartheta) : X_0 \times \Lambda_1 \to U_0 \times Z_0 \times \Lambda_2$, with $0 \in X_0 \subset \mathbb{R}^N$, $0 \in \Lambda_1, \Lambda_2 \subset \Lambda_{CM}$, $0 \in U_0 \subset \Omega_{CM}$, $0 \in Z_0 \subset \mathbb{R}^{N-N_0}$ open sets, such that the following relations holds

$$\begin{array}{rcl} \tau(H(u,\alpha)+Pz,\alpha) & = & u, \\ \varrho(H(u,\alpha)+Pz,\alpha) & = & z, \\ \vartheta(H(u,\alpha)+Pz,\alpha) & = & \alpha, \end{array} \tag{A.1}$$

for all $(u,z,\alpha) \in U_0 \times Z_0 \times \Lambda_2$. Take $\Omega'_{CM} := U_0$ and $\Lambda'_{CM} := \Lambda_2$. Then, by setting $z = 0$ in (A.1), we obtain that

$$\forall (u,\alpha) \in \Omega'_{CM} \times \Lambda'_{CM} : \tau(H(u,\alpha),\alpha) = u. \tag{A.2}$$

Moreover, consider any $\alpha \in \Lambda'_{CM}$. Take an arbitrary $x \in H(\Omega'_{CM},\alpha) \subset W_\alpha^C$. This means that there exists $u \in \Omega'_{CM}$, such that $x = H(u,\alpha)$. Thus, by (A.2), we have

$$\tau(H(u,\alpha),\alpha) = u,$$

which implies that

$$H(\tau(x,\alpha),\alpha) = x. \quad \square$$

Appendix B

Algorithms

B.1 Starting procedure for homoclinic orbits near a BT_2 point

In this section, we present an algorithm for starting the continuation of homoclinic branches near a BT_2 point (cf. [5]). Let system (1.1) have a BT_2 point at the origin. Let

$$A := \begin{pmatrix} f_x^0 & b \\ c^T & 0 \end{pmatrix} \in \mathbb{R}^{N+1,N+1},$$

where $b, c \in \mathbb{R}^N$ are chosen in such a way that A is nonsingular. Compute $v_0, v_1, p_0, p_1 \in \mathbb{R}^N$ from the systems:

$$\begin{aligned} A\begin{pmatrix} v_0 \\ g \end{pmatrix} &= \begin{pmatrix} 0 \\ 1 \end{pmatrix}, & A\begin{pmatrix} v_1 \\ h \end{pmatrix} &= \begin{pmatrix} v_0 \\ 0 \end{pmatrix}, \\ A^T\begin{pmatrix} p_0 \\ g \end{pmatrix} &= \begin{pmatrix} 0 \\ 1 \end{pmatrix}, & A^T\begin{pmatrix} p_1 \\ h \end{pmatrix} &= \begin{pmatrix} p_0 \\ 0 \end{pmatrix}. \end{aligned}$$

Normalize

$$\gamma := p_0^T v_1, \quad p_1 := \frac{1}{\gamma}\left(p_1 - \frac{1}{\gamma}(p_1^T v_1)p_0\right), \quad p_0 := \frac{1}{\gamma}p_0.$$

(i) **Linear transformations**

$$\begin{aligned} \begin{pmatrix} \beta_1 & \beta_2 \end{pmatrix} &:= p_0^T f_\alpha^0, \\ K_1 &:= \frac{1}{\beta_1^2 + \beta_2^2}\begin{pmatrix} \beta_1 & -\beta_2 \\ \beta_2 & \beta_1 \end{pmatrix}, \\ C &:= \begin{pmatrix} v_1 & 0 \end{pmatrix} - f_\alpha^0 K_1 \in \mathbb{R}^{N,2}. \end{aligned}$$

Solve the two linear systems

$$A \begin{pmatrix} D \\ h \end{pmatrix} = \begin{pmatrix} C \\ 0 \end{pmatrix}.$$

Let $d_2 \in \mathbb{R}^{N+2}$ be the second column of $\begin{pmatrix} D \\ K_1 \end{pmatrix}$.

(ii) **Quadratic coefficients of the reduced system**

It is assumed that $f_z = \begin{pmatrix} f_x & f_\alpha \end{pmatrix}$, $z := (x, \alpha)$ can be evaluated explicitly. Furthermore, a suitable $s > 0$ is chosen for numerical differentiation. Compute:

$$\begin{array}{rclcrcl}
w_1 &:=& s^{-1}(f_x(sv_0,0) - f_x^0)v_0, & & Q_{111} &:=& p_1^T w_1, \\
w_4 &:=& s^{-1}(f_z(sv_0,0) - f_z^0)d_2, & & Q_{211} &:=& p_0^T w_1, \\
Q_{212} &:=& s^{-1}p_0^T(f_x(sv_0,0) - f_x^0)v_1, & & Q_{214} &:=& p_0^T w_4, \\
Q_{224} &:=& s^{-1}p_0^T(f_x((0,0) + sd_2) - f_x^0)v_1, & & Q_{114} &:=& p_1^T w_4, \\
Q_{244} &:=& s^{-1}p_0^T(f_z((0,0) + sd_2) - f_z^0)d_2. & & & &
\end{array}$$

(iii) **Approximation of the homoclinic orbit of the reduced system**

$$\begin{aligned}
\Delta &:= Q_{211}(Q_{114} + Q_{224}) - Q_{214}(Q_{111} + Q_{212}), \\
\tau &:= \frac{5}{7\Delta}(Q_{111} + Q_{212}), \\
\sigma &:= \frac{1}{2Q_{211}}((Q_{114}^2 - Q_{211}Q_{244})\tau^2 - 1).
\end{aligned}$$

Choose a suitable $\epsilon > 0$ and let

$$\begin{aligned}
\delta_1 &:= \sigma\epsilon^4, \\
\delta_2 &:= \tau\epsilon^2, \\
u_1(t) &:= \frac{\epsilon^2}{Q_{211}}\left(1 - 3\ \mathrm{sech}^2\left(\frac{\epsilon}{2}t\right) - Q_{214}\tau\right), \\
u_2(t) &:= \frac{3\epsilon^3}{Q_{211}}\ \mathrm{sech}^2\left(\frac{\epsilon}{2}t\right)\tanh\left(\frac{\epsilon}{2}t\right).
\end{aligned}$$

(iv) **Transformation of the homoclinic orbit of the reduced system to the original system**

$$\begin{aligned}
x(t) &:= \begin{pmatrix} v_0 & v_1 \end{pmatrix} u(t) + D\delta, \\
\alpha &:= K_1\delta.
\end{aligned}$$

B.2 Starting procedure for homoclinic tangencies near an $R1_2$ point

In this section, we present an algorithm for starting the continuation of homoclinic tangencies near an $R1_2$ point. This algorithm summarizes the results of Section 2.2. Let system (1.2) have a $R1_2$ point at the origin. Let

$$A := \begin{pmatrix} g_x^0 - I_N & b \\ c^T & 0 \end{pmatrix} \in \mathbb{R}^{N+1,N+1},$$

where $b, c \in \mathbb{R}^N$ are chosen in such a way that A is nonsingular. Compute $v_0, v_1, p_0, p_1 \in \mathbb{R}^N$ from the systems:

$$\begin{aligned} A\begin{pmatrix} v_0 \\ l \end{pmatrix} &= \begin{pmatrix} 0 \\ 1 \end{pmatrix}, & A\begin{pmatrix} v_1 \\ h \end{pmatrix} &= \begin{pmatrix} v_0 \\ 0 \end{pmatrix}, \\ A^T\begin{pmatrix} p_0 \\ l \end{pmatrix} &= \begin{pmatrix} 0 \\ 1 \end{pmatrix}, & A^T\begin{pmatrix} p_1 \\ h \end{pmatrix} &= \begin{pmatrix} p_0 \\ 0 \end{pmatrix}. \end{aligned}$$

Normalize

$$\gamma := p_0^T v_1, \quad p_1 := \frac{1}{\gamma}\left(p_1 - \frac{1}{\gamma}(p_1^T v_1)p_0\right), \quad p_0 := \frac{1}{\gamma}p_0.$$

(i) **Linear transformations**

$$\begin{aligned} \begin{pmatrix} \beta_1 & \beta_2 \end{pmatrix} &:= p_0^T g_\alpha^0, \\ K_1 &:= \frac{1}{\beta_1^2 + \beta_2^2}\begin{pmatrix} \beta_1 & \sigma\beta_2 \\ \beta_2 & -\sigma\beta_1 \end{pmatrix}, \quad \sigma \in \{-1, 1\}, \\ C &:= \begin{pmatrix} v_1 & 0 \end{pmatrix} - g_\alpha^0 K_1 \in \mathbb{R}^{N,2}. \end{aligned}$$

Solve the two linear systems

$$A\begin{pmatrix} D \\ h \end{pmatrix} = \begin{pmatrix} C \\ 0 \end{pmatrix}.$$

Let

$$\begin{aligned} \tilde{K}(\delta) &:= K_1\delta, \\ \tilde{H}(u, \delta) &:= \begin{pmatrix} v_0 & v_1 \end{pmatrix} u + D\delta. \end{aligned}$$

(ii) **Quadratic coefficients of the normal form**

It assumed that g_x can be evaluated explicitly. Furthermore, a suitable $s > 0$ is chosen for numerical differentiation. Compute:

$$\begin{aligned} a &:= \frac{1}{2}s^{-1}p_0^T(g_x(sv_0, 0) - g_x^0)v_0, \\ b &:= s^{-1}p_1^T(g_x(sv_0, 0) - g_x^0)v_0 + s^{-1}p_0^T(g_x(sv_0, 0) - g_x^0)v_1. \end{aligned}$$

(iii) **Flow approximation**

Let

$$\dot{\xi} = F(\xi, \nu), \tag{B.1}$$

with $F(\xi, \nu) := F_0(\nu) + F_1(\xi, \nu) + F_2(\xi)$, where:

$$F_0(\nu) := \begin{pmatrix} -\frac{1}{2}\nu_1 \\ \nu_1 \end{pmatrix},$$

$$F_1(\xi, \nu) := \begin{pmatrix} \xi_2 + \left(\frac{1}{3}b - \frac{1}{2}a\right)\nu_1\xi_1 + \left(\left(\frac{1}{5}a - \frac{5}{12}b\right)\nu_1 - \frac{1}{2}\nu_2\right)\xi_2 \\ \left(\frac{2}{3}a - \frac{1}{2}b\right)\nu_1\xi_1 + \left(\left(\frac{1}{2}b - \frac{1}{6}a\right)\nu_1 + \nu_2\right)\xi_2 \end{pmatrix},$$

and

$$F_2(\xi) := \begin{pmatrix} -\frac{1}{2}a\xi_1^2 + \left(\frac{2}{3}a - \frac{1}{2}b\right)\xi_1\xi_2 + \left(\frac{1}{3}b - \frac{1}{6}a\right)\xi_2^2 \\ a\xi_1^2 + (b-a)\xi_1\xi_2 + \left(\frac{1}{6}a - \frac{1}{2}b\right)\xi_2^2 \end{pmatrix}.$$

Apply Algorithm B.1 to system (B.1). Let $\xi_c(t)$, ν_c be the final approximation obtained in Step (iv) of Algorithm B.1.

(iv) **Approximation of the homoclinic tangency of the normal form**

Choose $N_+, N_- \in \mathbb{Z}$, $N_- < 0 < N_+$, with $|N_-|, N_+$ sufficiently large. Define the discrete interval $J := [N_-, N_+] \cap \mathbb{Z}$. Compute $u_J^d, U_J^d \in S_J^2$:

$$\begin{aligned} u_i^d &:= \xi_c(i), \\ U_i^d &:= F(u_i^d, \nu_c), \end{aligned}$$

$i \in J$.

(v) **Transformation of the homoclinic orbit of the normal form to the original system**

Compute $x_J^d, X_J^d \in S_J^N$, $\alpha_d \in \mathbb{R}^2$:

$$\begin{aligned} x_i^d &:= H(u_i^d, \nu_c), \\ X_i^d &:= H_u(u_i^d, \nu_c)U_i^d, \\ \alpha_d &:= K(\nu_c), \end{aligned}$$

$i \in J$. Normalize

$$X_J^d := \frac{1}{\sqrt{\sum_{i=N_-}^{N_+} ||X_i^d||^2}} X_J^d.$$

Bibliography

[1] Algaba, A., Freire, E., Rodriguez-Luis, A. J., and Gamero, E. Analysis of Hopf and Takens-Bogdanov bifurcations in a modified van der Pol-Duffing oscillator. *Nonlinear Dynamics 16* (1998), 369–404.

[2] Allgower, E., and Georg, K. *Introduction to Numerical Continuation Methods*, vol. 45 of *Classics in Applied Mathematics*. SIAM, New York, 2003.

[3] Beyn, W.-J. On the numerical approximation of phase portraits near stationary points. *SIAM J. Numer. Anal. 24*, 5 (1987), 1095–1113.

[4] Beyn, W.-J. Numerical methods for dynamical systems. In *Advances in Numerical Analysis*, Oxford Sci. Publ., Ed., vol. I. Oxford University Press, New York, 1991, pp. 175–236.

[5] Beyn, W.-J. Numerical analysis of homoclinic orbits emanating from a Takens-Bogdanov point. *IMA Journal of Numerical Analysis 14* (1994), 381–410.

[6] Beyn, W.-J., Champneys, A., Doedel, E., Govaerts, W., Kuznetsov, Y. A., and Sandstede, B. Numerical continuation, and computation of normal forms. In *Handbook of Dynamical Systems*, B. Fiedler, Ed., vol. 2. Elsevier, 2002, pp. 149–219.

[7] Beyn, W.-J., and Kleinkauf, J.-M. The numerical computation of homoclinic orbits for maps. *SIAM J. Numer. Anal. 34*, 3 (1997), 1207–1236.

[8] Beyn, W.-J., and Lorenz, J. Center manifolds of dynamical systems under discretization. *Numer. Funct. Anal. and Optimiz. 9*, 3-4 (1987), 381–414.

[9] Beyn, W.-J., and Zou, J.-K. On manifolds of connecting orbits in discretizations of dynamical systems. *Nonlinear Anal. 52*, 5 (2003), 1499–1520.

[10] Beyn, W.-J., Zou, J.-K., Hüls, T., and Kleinkauf, J.-M. Numerical analysis of degenerate connecting orbits for maps. *Internat. J. of Bif. and Chaos 14*, 10 (2004), 3385–3407.

[11] Bhatia, R. *Matrix Analysis*, vol. 169 of *Graduate Texts in Mathematics*. Springer-Verlag, New York, 1997.

[12] Brezzi, F., Ushiki, S., and Fujii, H. Real and ghost bifurcation dynamics in difference schemes for ordinary differential equations. In *Numerical Methods for Bifurcation Problems*, T. Küpper, H. Mittelmann, and H. Weber, Eds., vol. 70. Birkhäuser-Verlag, Boston, 1984, pp. 79–104.

[13] Broer, H., Simó, C., and Roussarie, R. Invariant circles in the Bogdanov-Takens bifurcation for diffeomorphisms. *Ergod. Th. & Dynam. Sys. 16*, 6 (1996), 1147–1172.

[14] Broer, H., Simó, C., and Vitolo, R. Hopf-saddle-node bifurcation for fixed points of 3D-diffeomorphisms: analysis of a resonance bubble. Preprint, University of Groningen, 2007.

[15] Broer, H., Simó, C., and Vitolo, R. Hopf-saddle-node bifurcation for fixed points of 3D-diffeomorphisms: the arnold resonance web. Preprint, University of Groningen, 2007.

[16] Carr, J. *Applications of Centre Manifold Theory*, vol. 35 of *Applied Mathematical Sciences*. Springer-Verlag, New York, 1981.

[17] Chow, S.-N., Li, C., and Wang, D. *Normal Forms and Bifurcation of Planar Vector Fields*. Cambridge University Press, New York, 1994.

[18] de Dier, B., and Roose, D. Numerical determination of an emamating bracnh of Hopf bifurcation points in a two parameter problem. *SIAM J. Sci. Stat. Comput. 10*, 4 (1989), 671–685.

[19] de Dier, B., Roose, D., and van Rompay, P. Interaction between fold and Hopf curves leads to a new bifurcation phenomena. *J. of Comput. and Applied Mat. 26* (1989), 171–186.

[20] Denker, M. *Einführung in die Analysis dynamischer Systeme*. Springer-Verlag, Berlin, 2005.

[21] Dhooge, A., Govaerts, W., and Kuznetsov, Y. A. MATCONT: a MATLAB package for numerical bifurcation analysis of ODEs. *ACM Trans. Math. Software 29*, 2 (2003), 141–164.

[22] Dhooge, A., Govaerts, W., Kuznetsov, Y. A., Mestrom, W., Riet, A. M., and Sautois, B. *MATCONT and CL_MATCONT: Continuation toolboxes in MATLAB*. University of Gent, Belgium, 2006. Available at `http://www.matcont.ugent.be/manual.pdf`.

[23] Eirola, T. Two concepts for numerical periodic solutions of ODEs. *Appl. Math. Comput. 31* (1989), 121–131.

[24] Fiedler, B., and Scheurle, J. Discretization of homoclinic orbits, rapid forcing and "invisible" chaos. *Mem. Amer. Math. Soc. 570* (1996).

[25] Freire, E., Rodriguez-Luis, A. J., Gamero, E., and Ponce, E. A case study for homoclinic chaos in an autonomous electronic circuit. A trip from Takens-Bogdanov to Hopf-Shil'nikov. *Physica D 62* (1993), 230–253.

[26] Freire, E., Rodriguez-Luis, A. J., and Ponce, E. Un método de continuación de órbitas homoclinas en sistemas autónomos planos biparamétricos. In *Proceedings of the XIVth Spanish-Portuguese Conference on Mathematics* (1990), La Laguna University, pp. 1249–1253.

[27] Garay, B. Discretization and some qualitative properties of ordinary differential equations about equilibria. *Acta Math. Univ. Comenianae LXII*, 2 (1993), 249–275.

[28] Govaerts, W. Computation of Takens-Bogdanov type bifurcations with arbitrary codimension. *SIAM J. Numer. Anal. 30*, 4 (1993), 1121–1133.

[29] Govaerts, W. *Numerical Methods for Bifurcations of Dynamical Equilibria*. SIAM, Philadelphia, 2000.

[30] Govaerts, W., Kuznetsov, Y. A., Khoshsiar Ghaziani, R., and Meijer, H. G. E. Numerical methods for two-parameter local bifurcation analysis of maps. *SIAM J. Sci. Comput. 29*, 6 (2007), 2644–2667.

[31] Govaerts, W., Kuznetsov, Y. A., Khoshsiar Ghaziani, R., and Meijer, H. G. E. *Cl_MatContM: A toolbox for continuation and bifurcation of cycles of maps*. University of Gent, Belgium, 2008. Available at `http://sourceforge.net/projects/matcont/`.

[32] Guckenheimer, J. On a Codimension Two Bifurcation. In *Dynamical systems and turbulence* (1981), vol. 898 of *Lect. Notes Math.*, Springer-Verlag, pp. 99–142.

[33] Guckenheimer, J. Multiple bifurcation problems of codimension two. *SIAM J. Math. Anal. 15*, 1 (1984), 1–49.

[34] Guckenheimer, J., and Holmes, P. *Nonlinear Oscillations, Dynamical Systems, and Bifurcations of Vector Fields*, vol. 42 of *Applied Mathematical Sciences*. Springer-Verlag, New York. Fourth printing, 1993.

[35] Guckenheimer, J., Myers, M., and Sturmfels, B. Computing Hopf bifurcations I. *SIAM J. Numer. Anal. 34*, 1 (1997), 1–21.

[36] Hairer, E., Norsett, S. P., and Wanner, G. *Solving Ordinary Differential Equations I*, second ed. Springer-Verlag, New York, 1993.

[37] Hofbauer, J., and Iooss, G. A Hopf bifurcation theorem for difference equations approximating a differential equation. *Monatsh. Math. 98*, 2 (1984), 99–113.

[38] Hüls, T. Numerical computation of dichotomy rates and projectors in discrete time. Available at `http://www.math.uni-bielefeld.de/~beyn/AG_Numerik/html/de/preprints/index.html`. Preprint sfb701a2 08-081, University of Bielefeld, 2008.

[39] Kleinkauf, J.-M. The numerical computation and geometrical analysis of heteroclinic tangencies. Available at `http://www.mathematik.uni-bielefeld.de/sfb343/`. Preprint 98-48, SFB 343, University of Bielefeld, 1998.

[40] Kleinkauf, J.-M. Numerische Berechnung diskreter homokliner Orbits. Master's thesis, University of Bielefeld, Germany, 1994.

[41] Kleinkauf, J.-M. *Numerische Analyse tangentialer homokliner Orbits*. PhD thesis, University of Bielefeld, Germany, 1997.

[42] Koto, T. Naimark-sacker bifurcations in the euler method for a delay differential equation. *BIT 39*, 1 (1998), 110–115.

[43] Krauskopf, B., Osinga, H., and Galán-Vioque, J., Eds. *Numerical Continuation Methods for Dynamical Systems*. Understanding Complex Systems. Springer-Verlag, Netherlands, 2007.

[44] Kuznetsov, Y. A. *Elements of Applied Bifurcation Theory*, third ed., vol. 112 of *Applied Mathematical Sciences*. Springer-Verlag, New York, 2004.

[45] Kuznetsov, Y. A., and Levitin, V. V. CONTENT: A multiplatform environment for analyzing dynamical systems. Available at `http://www.math.uu.nl/people/kuznet/CONTENT/`. Dynamical Systems Laboratory, Centrum voor Wiskunde en Informatica, Amsterdam, 1997.

[46] Kuznetsov, Y. A., Van Veen, L., and Meijer, H. G. E. The fold-flip bifurcation. *Internat. J. of Bif. and Chaos 14*, 7 (2004), 2253–2282.

[47] Lancaster, P., and Tismenetsky, M. *The Theory of matrices*, second ed. Academic Press, Orlando, 1985.

[48] Lóczi, L. *Discretizing Elementary Bifurcations*. PhD thesis, Budapest University of Technology, 2006.

[49] Lubich, C., and Ostermann, A. Hopf bifurcation of reaction-diffusion and navier-stokes equations under discretization. *Numer. Math. 81* (1998), 53–84.

[50] Meijer, H. G. E. *Codimension 2 Bifurcations of Iterated Maps*. PhD thesis, University of Utrecht, Netherlands, 2006.

[51] Spence, A., Cliffe, K., and Jepson, A. A note on the calculation of paths of Hopf bifurcations. *J. of Comput. and Applied Mat. 26* (1989), 125–131.

[52] Vitolo, R. *Bifurcations of attractors in 3D diffeomorphisms: a study in experimental mathematics*. PhD thesis, University of Groningen, Netherlands, 2003.

[53] Wang, X., Blum, E., and Li, Q. Consistency of local dynamics and bifurcation of continuous-time dynamical systems and their numerical discretizations. *J. Difference Eq. Appl. 4*, 1 (1998), 29–57.

[54] Werner, B. Computation of Hopf bifurcation with bordered matrices. *SIAM J. Numer. Anal. 33*, 2 (1996), 435–455.

[55] Wiggins, S. *Introduction to Applied Nonlinear Dynamical Systems and Chaos*, second ed., vol. 2 of *Texts in Applied Mathematics*. Springer-Verlag, New York, 2003.